

The Official Journal of the Chinese Stomatological Association (CSA)



Chinese Journal of Dental Research

CJDR

V
O
L
U
M
E

27

**2
0
2
4**

N
U
M
B
E
R

3

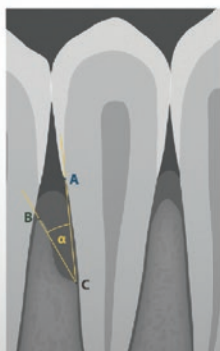
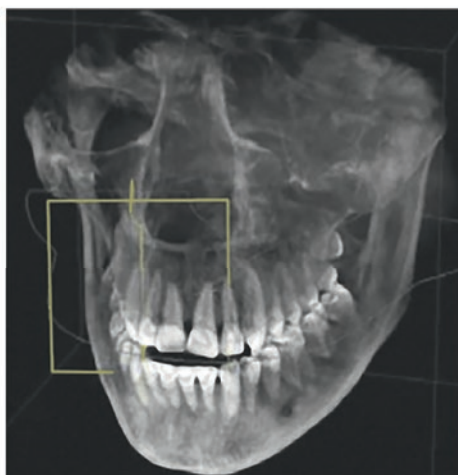
OUTSTANDING SELECTION



QUINTESSENCE INTERNATIONAL

Editorial board's selected articles
Eli Eliav (ed)

Volume 1



Eli Eliav (Ed)

Quintessence International Volume 1

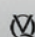
Editorial board's selected articles

216 pages, 100 illus.

ISBN 978-1-78698-143-1, €98

**Special price for subscribers of
Quintessence International: €68**



 QUINTESSENCE PUBLISHING

This Quintessence International (QI) annual yearbook is a compilation of selected articles representing the most significant work from the past year. Through a double-blind process that ensures anonymity and quality, our team of editors and reviewers performed the remarkable and difficult task of reviewing and

evaluating many deserving submissions to present you with this outstanding selection of 20 articles. Organized by disciplines and topics, the articles provide a valuable and user-friendly resource that we hope you find enjoyable and informative. Available at a discounted price for QI subscribers.



www.quint.link/qi-vol1



books@quintessenz.de



+49 (0)30 761 80 667

 QUINTESSENCE PUBLISHING



Chinese Journal of Dental Research

The Official Journal of the Chinese Stomatological Association (CSA)



Chinese Journal of Dental Research

The Official Journal of the Chinese Stomatological Association (CSA)

Review

- 193 Salivary Short-chain Fatty Acids (SCFAs) Are Viable Predictors of Early Changes in Systemic Health
Bina KASHYAP, Eelis HYVÄRINEN, Arja M KULLAA

Original articles

- 203 GREM1 Negatively Regulates Osteo-/Dentinogenic Differentiation of Dental Pulp Stem Cells via Association with YWHAH
Shu DIAO, Xiao HAN, Wei Long YE, Chen ZHANG, Dong Mei YANG, Zhi Peng FAN, Song Lin WANG
- 215 PHD2 shRNA-Modified Bone Marrow Mesenchymal Stem Cells Facilitate Periodontal Bone Repair in Response to Inflammatory Condition
Bin Yan LUO, Shu Yu CHENG, Wen Zheng LIAO, Bao Chun TAN, Di CUI, Min WANG, Jun QIAN, Chang Xing CHEN, Fu Hua YAN
- 225 CB1 Promotes Osteogenic Differentiation Potential of Periodontal Ligament Stem Cells by Enhancing Mitochondrial Transfer of Bone Marrow Mesenchymal Stem Cells
Lan LUO, Wan Hao YAN, Feng Qiu ZHANG, Zhi Peng FAN
- 235 Establishment of an Animal Model of Oral Squamous Cell Carcinoma Invading the Mandible
Xiang Long ZHENG, Kang Wei ZHOU, Wen LI, Ya Qi CHEN, Cheng Hui LU, Li Song LIN



-
- 243 Role of Antioxidant Enzymes in Pathogenesis of Oral Squamous Cell Carcinoma: a Systematic Review and Meta-analysis
Zainab NIAZI, Farah FARHAN, Sadia MUNEER, Hasan MUJTABA, Nurul IBRAHIM, Norhayati YUSOP
- 253 Application of Chairside CAD/CAM and Its Influencing Factors among Chinese Dental Practitioners: a Cross-sectional Study
Aihemaiti MUHETAER, Hong Ye YANG, Cui HUANG

Chinese Journal of Dental Research

CN 10-1194/R • ISSN 1462-6446 • eISSN 1867-5646 • Quarterly

The Official Journal of the Chinese Stomatological Association

Co-sponsor: Peking University School of Stomatology, Quintessenz Verlag

Editor-in-Chief

Chuan Bin GUO Beijing, P.R. China

Chief-Editor Emeritus

Zhen Kang ZHANG Beijing, P.R. China
Xing WANG Beijing, P.R. China
Xu Chen MA Beijing, P.R. China
Guang Yan YU Beijing, P.R. China
Xue Dong ZHOU Chengdu, P.R. China

Executive Associate Editor

Qian Ming CHEN Hangzhou, P.R. China

Executive Editors

Ye Hua GAN Beijing, P.R. China
Hong Wei LIU Beijing, P.R. China

Associate Editors

Li Juan BAI Beijing, P.R. China
Zhuan BIAN Wuhan, P.R. China
Fa Ming CHEN Xi'an, P.R. China
Bin CHENG Guangzhou, P.R. China
Xu Liang DENG Beijing, P.R. China
Xin Quan JIANG Shanghai, P.R. China
Tie Jun LI Beijing, P.R. China
Hong Chen SUN Changchun, P.R. China
Song Ling WANG Beijing, P.R. China
Ling YE Chengdu, P.R. China
Zhi Yuan ZHANG Shanghai, P.R. China
Yi Min ZHAO Xi'an, P.R. China
Yong Sheng ZHOU Beijing, P.R. China

Editorial Board

Tomas ALBREKTSSON
Gothenburg, Sweden
Conrado APARICIO
Barcelona, Spain
Daniele BOTTICELLI
Rimini, Italy
Lorenzo BRESCHI
Bologna, Italy
Francesco CAIRO
Florence, Italy
Tong CAO
Singapore
Jack G. CATON
Rochester, USA
Yang CHAI
Los Angeles, USA
Wan Tao CHEN
Shanghai, P.R. China
Zhi CHEN
Wuhan, P.R. China
Bruno CHRCANOVIC
Malmö, Sweden
Kazuhiro ETO
Tokyo, Japan
Bing FAN
Wuhan, P.R. China
Zhi Peng FAN
Beijing, P.R. China
Alfio FERLITO
Udine, Italy
Roland FRANKENBERGER
Marburg, Germany

Xue Jun GAO
Beijing, P.R. China
Sufyan GAROUSHI
Turku, Finland
Reinhard GRUBER
Vienna, Austria
Gaetano ISOLA
Catania, Italy
Søren JEPSEN
Bonn, Germany
Li Jian JIN
Hong Kong SAR, P.R. China
Yan JIN
Xi'an, P.R. China
Newell W. JOHNSON
Queensland, Australia
Thomas KOCHER
Greifswald, Germany
Ralf-Joachim KOHAL
Freiburg, Germany
Niklaus P. LANG
Bern, Switzerland
Junying LI
Ann Arbor, USA
Yi Hong LI
New York, USA
Wei LI
Chengdu, P.R. China
Huan Cai LIN
Guangzhou, P.R. China
Yun Feng LIN
Chengdu, P.R. China

Hong Chen LIU
Beijing, P.R. China
Yi LIU
Beijing, P.R. China
Edward Chin-Man LO
Hong Kong SAR, P.R. China
Jeremy MAO
New York, USA
Tatjana MARAVIC
Bologna, Italy
Claudia MAZZITELLI
Bologna, Italy
Mark MCGURK
London, UK
Li Na NIU
Xi'an, P.R. China
Jan OLSSON
Gothenburg, Sweden
Gaetano PAOLONE
Milan, Italy
No-Hee PARK
Los Angeles, USA
Peter POLVERINI
Ann Arbor, USA
Lakshman SAMARANAYAKE
Hong Kong SAR, P.R. China
Keiichi SASAKI
Miyagi, Japan
Zheng Jun SHANG
Wuhan, P.R. China
Song SHEN
Beijing, P.R. China

Song Tao SHI
Guangzhou, P.R. China
Richard J. SIMONSEN
Downers Grove, USA
Manoel Damião de SOUSA-NETO
Ribeirão Preto, Brazil
John STAMM
Chapel Hill, USA
Lin TAO
Chicago, USA
Tiziano TESTORI
Ann Arbor, USA
Cun Yu WANG
Los Angeles, USA
Hom-Lay WANG
Ann Arbor, USA
Zuo Lin WANG
Shanghai, P.R. China
Heiner WEBER
Tuebingen, Germany
Xi WEI
Guangzhou, P.R. China
Yan WEI
Beijing, P.R. China
Ray WILLIAMS
Chapel Hill, USA
Jie YANG
Philadelphia, USA
Quan YUAN
Chengdu, P.R. China
Jia Wei ZHENG
Shanghai, P.R. China

Publication Department

Production Manager: Megan Platt (London, UK)
Managing Editor: Xiao Xia ZHANG (Beijing, P.R. China)

Address: 4F, Tower C, Jia 18#, Zhongguancun South Avenue, HaiDian District, 100081, Beijing, P.R. China.
Tel: 86 10 82195785, **Fax:** 86 10 62173402
Email: editor@cjdrcsa.com

Manuscript submission: Information can be found on the Guidelines for Authors page in this issue. To submit your outstanding research results more quickly, please visit: <http://mc03.manuscriptcentral.com/cjdr>

Administrated by: China Association for Science and Technology

Sponsored by: Chinese Stomatological Association and Popular Science Press

Published by: Popular Science Press

Printed by: Beijing ARTRON Colour Printing Co Ltd

Subscription (domestically) by Post Office

Chinese Journal of Dental Research is indexed in MEDLINE.

For more information and to download the free full text of the issue, please visit www.quint.link/cjdr
<http://www.cjdrcsa.com>

Acknowledgements

We would like to express our gratitude to the peer reviewers for their great support to the journal in 2023.

Afrashtehfar, Kelvin (Switzerland)	Han, Dong (China)	Ren, Yi Jin (Netherlands)
Agudelo-Suárez, Andrés (Colombia)	Hashimoto, Kenji (Japan)	Ritchie, Helena H. (United States)
Aksoy, Merve (Turkey)	He, Miao (China)	Rodrigues, Gabriel (Oman)
Alkan Aygor, Fehime (Turkey)	Hong, Guang (Japan)	Saber, Shehabeldin Mohamed (Egypt)
Al-Nuaimi, Nassr (United States)	Hourfar, Jan (Germany)	Saddki, Norkhafizah (Malaysia)
An, Na (China)	Hu, Wen Jie (China)	Saito, Hanae (United States)
Ananthaswamy, Akanksha (India)	Hua, Fang (China)	Sarialioglu Gungor, Ayça (Turkey)
Arpornmaeklong, Premjit (Thailand)	Huang, Zhen (China)	Sharma, Rajinder K. (India)
Arslan, Merve (Turkey)	Jayasinghe, Ruwan D (Sri Lanka)	Shi, Song Tao (China)
Ateş, Melis Oya (Turkey)	Ji, Yi (China)	Si, Yan (China)
Ayna, Emrah (Turkey)	Jiang, Hong Bing (China)	Song, Jin Lin (China)
Ballal, Nidambur (India)	Jiang, Jiu Hui (China)	Song, Xiao Meng (China)
Banerjee, Santasree (China)	Ju, Xiang Qun (Australia)	Song, Ya Ling (China)
Bayindir, Funda (Turkey)	Kaklamanos, Eleftherios G (Cyprus)	Sousa-Neto, Manoel D. (Brazil)
Bi, Liang Jia (China)	Karadas, Muhammet (Turkey)	Su, Guan Yue (China)
Bilgili, Dilber (Turkey)	Khan, Sher Alam (Pakistan)	Sui, Bing Dong (China)
Brailo, Vlaho (Croatia)	Khijmatgar, Shah Nawaz (India)	Sulaiman, Ghassan M. (Iraq)
Buldur, Burak (Turkey)	Kinzinger, Gero (Germany)	Sun, Qiang (China)
Cao, Zheng Guo (China)	Kurt, Aysegul (Turkey)	Sun, Yu Chun (China)
Chabbra, Ajay (India)	Li, Gang (China)	Sun, Zhi Peng (China)
Chai, Yang (United States)	Li, Yi Hong (United States)	Taneja, Pankaj (Denmark)
Chen, Bin (China)	Li, Yu (China)	Tang, Qing Ming (China)
Chen, Chen (China)	Li, Ze Han (China)	Tao, Ren Chuan (China)
Chen, Fa Ming (China)	Lin, Min Kui (China)	Topsakal, Kubra Gulnur (Turkey)
Chen, Li (China)	Lin, Xiao Ping (China)	Tsoi, James (HK, China)
Chen, Li Li (China)	Liu, Da Wei (China)	Tuovinen, Olli (United States)
Chen, Peng (China)	Liu, Da Yong (China)	Uzun, Ismail (Turkey)
Chen, Tao (China)	Liu, Hai Bo (China)	Wajid Hussain Chan, Malik (Pakistan)
Chen, Zhi (China)	Liu, Hong Wei (China)	Wang, Chun Li (China)
Chu, Chun Hung (HK, China)	Liu, Huan (China)	Wang, Fu (China)
Cui, Li (United States)	Liu, Jian Zhang (China)	Wang, Lin (China)
Dede, Dogu Omur (Turkey)	Liu, Jia Qiang (China)	Wei, Fu Lan (China)
Dehghanian, Danoosh (Iran)	Liu, Min (China)	Wei, Xi (China)
Desai, Rajiv S (India)	Liu, Yao (China)	Wu, Tao (China)
Ding, Ming Chao (China)	Liu, Ya Wei (China)	Wu, Yi Qun (China)
Dong, Yan Mei (China)	Lu, Yan (China)	Xie, Shang (China)
Eaton, Kenneth (United Kingdom)	Lucchese, Alessandra (Italy)	Xu, Kang (China)
El-Bialy, Tarek (Canada)	Mady, Fatma (Egypt)	Xu, Tian Min (China)
Elias, Carlos N (Brazil)	Mahjabeen, Wajiha (Pakistan)	Yu, Jin Hua (China)
Erber, Ralf (Germany)	Mossey, P. A. (United Kingdom)	Yu, Xi Jiao (China)
Esen, Çağrı (Turkey)	Nassani, Mohammad zakaria (Saudi Arabia)	Yuan, Quan (China)
Fan, Yuan (China)	Nayak, Ullal Anand (Saudi Arabia)	Zadeh, Homayoun H. (United States)
Fan, Zhi Peng (China)	Neves, Lucimara Teixeira das (Brazil)	Zeng, Xiao Juan (China)
Fathy Abo-Elmahasen, Mahmoud M (Egypt)	Niu, Li Na (China)	Zhang, Cheng Fei (HK, China)
Feng, Chen (China)	Özdemir, Burcu (Turkey)	Zhang, Hao (China)
Fu, Kai Yuan (China)	Ozturk, Taner (Turkey)	Zhang, Hong Liang (China)
Gallo, Camila (Brazil)	Pan, Shao Xia (China)	Zhang, Lei (China)
Gan, Ye Hua (China)	Pan, Ya Ping (China)	Zhao, Yu Ming (China)
Gao, Xue Jun (China)	Pan, Yong Chu (China)	Zheng, Shu Guo (China)
Garoushi, Sufyan (Finland)	Park, Joo-Cheol (Korea)	Zheng, Yun Fei (China)
Geduk, Gediz (Turkey)	Pei, Dan Dan (China)	Zhou, Hai Hua (China)
Grigorian, Mircea (Romania)	Pereira, Jefferson Ricardo (Brazil)	Zhou, Hong Mei (China)
Gruber, Reinhard (Austria)	Pugazhendhi, Sathish kumaran (India)	Zhou, Ping (United States)
Gu, Yong Chun (China)	Qin, Li Zheng (China)	Zhu, Xiao Fei (China)
Gündoğar, Mustafa (Turkey)	Ren, Xiu Yun (China)	Zong, Chen (Belgium)

Editorial Office

Chinese Journal of Dental Research

Salivary Short-chain Fatty Acids (SCFAs) Are Viable Predictors of Early Changes in Systemic Health

Bina KASHYAP¹, Eelis HYVÄRINEN¹, Arja M KULLAA¹

Short-chain fatty acids (SCFAs) are the metabolites identified in both the oral cavity and the gut. They play an important role in the triggering, development and progression of systemic diseases. SCFAs can alter the gut microbial components, intestinal epithelium and host immune system, and are also associated with cancer incidence. Salivary SCFAs, produced by the oral microbiome, are correlated with some oral diseases. The occurrence of systemic diseases associated with gut SCFAs is more clearly defined than oral SCFAs. Salivary SCFAs can enter the bloodstream directly via inflamed gingiva to cause continuous low-grade systemic inflammation. Hence, salivary SCFAs could be an indicator for the early diagnosis of systemic diseases. Furthermore, they provide a basis for understanding the oral-systemic axis driven through salivary SCFAs in the pathogenesis of several diseases.

Keywords: gut microbiome, oral diseases, oral microbiome, salivary metabolites, SCFAs.
Chin J Dent Res 2024;27(3):193–202; doi: 10.3290/j.cjdr.b5698392

Oral diseases, including caries, periodontal disease, oral precancers and cancers, are a major concern globally and a serious health burden that has a substantially negative effect on society. The oral cavity is a complex with different niches for the colonisation of micro-organisms including bacteria, fungi, eukaryotes and viruses, that can cause several oral diseases.¹ These niches are predominantly exposed to the saliva and gingival crevicular fluid that hydrate bacteria and provide a medium for nutrient transportation.² The oral microbiome maintains a dynamic balance in interbacterial and host-bacterial interactions.³ Oral dysbiosis is the interaction between the pathogens and the host's immune response, resulting in oral diseases. The microbial diversity and shifts in bacterial composition increase the abundance of pathogenic bacteria and decrease commensal health-associated bacteria. The most common consequences of this oral dysbiosis are oral diseases and infections, such as periodontitis, gingivitis, oral ulcers, oral candidiasis

and dental caries.⁴ Changes in the oral microbiome have also been observed in connection with metabolic diseases, autoimmune diseases, immunosuppression and pregnancy.⁵

Oral microbes release salivary metabolites as a product of multifactorial interactions between the host, oral bacteria and altered cellular metabolism of the host. Periodontal diseases are initiated and propagated through oral dysbiosis which interacts with the immune defences of the host, leading to inflammation and disease and even systemic inflammation.⁶ The relationship between periodontitis and systemic diseases such as cardiovascular diseases, diabetes mellitus, problems during pregnancy, rheumatoid arthritis, chronic obstructive pulmonary disease, pneumonia, obesity, chronic kidney disease, metabolic syndrome and cancer has been previously demonstrated.⁷ Furthermore, variation in the oral microbiome is reported to be associated with oral cancer,⁸ pancreatic cancer,⁹ colorectal cancer¹⁰ and neurodegenerative diseases.¹¹ Although some relationships involving oral microbiome variations and different diseases have been confirmed, the exact cause of pathogenesis remains unclear.

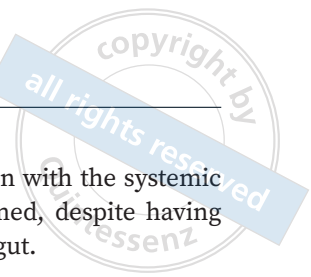
Salivary metabolites

Homeostasis in the oral cavity is maintained primarily by the saliva's multifactorial defence system. Saliva is

¹ Institute of Dentistry, University of Eastern Finland, Kuopio Campus, Kuopio, Finland.

Corresponding author: Dr Bina KASHYAP, Institute of Dentistry, Faculty of Health Sciences, University of Eastern Finland, Kuopio Campus, Kuopio, Finland. Tel: 358-417530854. Email: bkashyap@uef.fi

This study was supported by the Finnish Cultural Foundation.



a complex biofluid consisting of a broad spectrum of components that provides biomarkers of health and disease status. It facilitates diagnosis and prognosis of disease by yielding information on metabolites, proteins, mRNA, DNA, enzymes, hormones, antibodies, antimicrobial constituents and growth factors,¹² and reflects both diseases of the oral cavity and systemic conditions. Salivary metabolites, molecules of a low weight present in the saliva (endogenous or exogenous), often represent a useful tool for the detection of various oral and systemic diseases.¹³

Metabolomic studies have confirmed that micronutrients obtained from dietary sources such as carbohydrates, proteins and lipids are important in regulating energy metabolism and inflammatory responses. The salivary metabolites are studied through different analytical methods such as mass spectroscopy (MS), gas spectroscopy (GS), capillary electrophoresis (CP), high-performance liquid chromatography (HPLC) and nuclear magnetic resonance (NMR) spectroscopy. These technologies have helped to reveal how biochemical reactions and their end-products are involved in the pathogenesis of various diseases. The most common salivary metabolites that are quantitatively analysed are amino acids, carbohydrates and organic acids.¹⁴ NMR spectroscopy is used to detect short-chain fatty acids (SCFAs) such as acetate, butyrate, formate and propionate in human saliva samples.^{15,16}

Of all the metabolites, acetate, propionate and butyrate have shown pathophysiological changes that reflect disturbances in metabolic pathways in different diseases. Acetate, propionate and butyrate are SCFAs that are produced by saccharolytic and proteolytic oral bacteria and correlate with salivary microbial load.¹⁶ Acetate and propionate are mainly produced by gram-negative bacteria (Bacteroidetes), whereas butyrate is the metabolic product of gram-positive bacteria (Firmicutes). Less than 1% of SCFAs are formed as products from peptide and amino acid fermentation.¹⁷ The release of SCFAs as microbial metabolite has contributed to several oral inflammatory diseases. Table 1 presents salivary SCFAs in different oral diseases.¹⁸⁻³³ SCFAs are also produced by some anaerobic periodontal bacteria and are released from infection sites into the microenvironment.³⁴ In addition to oral sources, the main SCFAs including acetate, propionate and butyrate are produced in the large intestine by microbial degradation of undigested carbohydrates.³⁵ Studies from preclinical models have shown that the gut microbiome maintains bidirectional communication with the brain or gut-brain axis via a network of immunological, neuronal and endocrine signalling pathways.³⁶ The presence of SCFAs in the

oral cavity and their communication with the systemic circulations have not been confirmed, despite having overlapping microbiomes with the gut.

SCFAs: a result of oral dysbiosis

Disturbances in the normal symbiotic relationship between the host and its resident microorganisms can increase the risk of disease by changes in the oral environment. Several factors, including smoking, alcohol consumption, socioeconomic status, antibiotic use, diet and pregnancy, can affect the oral microbiome and their metabolites.³⁷ The oral cavity hosts several microbes distributed at different locations. Oral dysbiosis can lead to the loss of beneficial oral species and pathogen colonisation, either directly or indirectly through immunosuppression, oxygen deprivation, biofilm formation or other potential mechanisms.³⁸ SCFAs are produced by oral bacteria, as end-products of their metabolism. These fatty acid-secreting bacteria are present in lesions of both dental caries and periodontitis. It has been speculated that these short-chain organic acids assist in cell-to-cell metabolic communication via bacterial colonisation. The protective or harmful role of dental biofilm in the oral cavity is still unknown, though it is another source of SCFAs.^{39,40}

Salivary lactate, acetate and n-butyrate have been observed in patients with dental caries wherein one or more of the SCFAs reduce the pH and increase the porosity of the dental plaque matrix.⁴¹ In periodontitis, increased salivary metabolites, as acetate, propionate and butyrate are strongly linked to preventing cell division, diminished the ability to repair damage, junctional epithelium degeneration processes and stimulation of inflammatory response with the liberation of cytokines.²³ The presence of these SCFAs is pointed out as a possible indicator of periodontal disease development and progression. In one study, a significant decrease in salivary SCFAs was observed after periodontal treatment.²⁶ The association of salivary SCFAs with periodontal disease requires further investigation, as it is still unclear whether disease susceptibility is based on the local immune-inflammatory reactivity or oral microbiome, or at systemic metabolic level.

Oral dysbiosis with persistent periodontitis contributes to the development and progression of psychiatric and neurodegenerative disorders, as well as autoimmune diseases.⁴² The periodontal pathogens can release or induce pro-inflammatory cytokines such as interleukin-1 (IL-1), IL-6 and tumour necrosis factor (TNF)-alpha that accelerate the neuroinflammation involved with Alzheimer's disease.⁴³ An increased

Table 1 Salivary SCFAs in different oral diseases.

Study	Oral disease	n (C/D)	Saliva	Method	Salivary metabolites (SCFAs)		Oral impact
					Elevated	Decreased	
Fidalgo et al ¹⁸	Dental caries	10/20	USWS	NMR	Butyrate, propionate	NR	Decreased pH and increased porosity of dental plaque matrix
Pereira et al ¹⁹	Dental caries	38/NA	USWS, SWS	NMR	NR	Butyrate	Protein hydrolysis and deglycosylation
Schulz et al ²⁰	Dental caries	36/21	USWS	LC-MS	Acetic acid, propionic acid,	NR	Dietary factors increase organic acids
Aimetti et al ²¹	Periodontitis	22/32	WS	NMR	Acetate, c-aminobutyrate, n- butyrate, propionate	NR	Proteolytic destruction and increased disease severity
Rzeznik et al ²²	Periodontitis	26/26	SWS	NMR	Butyrate	Lactate, acetate	Increased periodontal inflammation and shift in microbial composition
Romano et al ²³	Aggressive and chronic periodontitis	39/61	USWS	NMR	NR	Lactate, acetate, butyrate	Increased prevalence of periodontal bacterial species
García-Villaescusa et al ²⁴	Chronic periodontitis and glioblastoma	120/10	USWS	NMR	Caproate, isocaproate, butyrate, isovalerate, isoleucine, isopropanol	NR	Increased entry of periodontal pathogens and periodontal pocket formation
Liebsch et al ²⁵	Periodontitis	909/NA	SWS	UHPLC-MS/MS	Isovalerate	NR	Increased inflammation, cytokine liberation and periodontal pocket formation
Gawron et al ²⁶	Chronic periodontitis	15/30	USWS	1H-NMR	NR	Propionate, acetate	Shift in microbial colonisation
Citterio et al ²⁷	Periodontitis after therapy	11/12	USWS	NMR	Isovalerate, lactate.	Acetate, propionate, butyrate	Decreased microbial load after treatment
Kim et al ²⁸	Periodontitis	92/129	SWS	NMR	Butyrate, isovalerate	Acetate, propionate	Increased periodontal inflammation and increased recolonisation of periodontal pathogens
Sanches et al ²⁹	TMJ disorder	27/26	USWS	1H-NMR	Acetate, propionate, isovalerate	NR	Increased inflammation and cytokine release
Wei et al ³⁰	OSCC/leukoplakia	34/69	WS	LC-TOF-MS	Lactic acid, 3-indolepropionic acid	γ-aminobutyric acid	Varied metabolic rates, increased glycolysis and increased occurrence of cancer
Wang et al ³¹	OSCC	30/30	USWS	CE-MS	Lactic acid	NR	Altered biochemical process and glycolytic switch
Ishikawa et al ³²	Lichen planus/OSCC	NA/60	USWS	CE-MS	5-aminovalerate, gamma- butyrobetaine	NR	Tumour progression
Yatsuoka et al ³³	HNC with RT	NA/9	USWS	CE-TOFMS	Gamma-aminobutyric acid (GABA), butyrate, 2-aminobutyric acids	NR	Increased severity of disease

C, control; CE-TOF-MS, capillary electrophoresis time-of-flight mass spectrometry; D, disease; GC/MS, gas chromatography/mass spectrometry; HNC, head and neck carcinoma; LC/MS, liquid chromatography/mass spectrometry; NA, not available; NMR, NMR-spectroscopy; NR, not reported; OSCC, oral squamous cell carcinoma; RT, radiotherapy; SWS, stimulated whole saliva; TMJ, temporomandibular joint; UHPLC-MS/MS: ultra-high performance liquid chromatography and tandem mass spectrometry; USWS, unstimulated whole saliva; WS, whole saliva.

Table 2 SCFA function in a healthy oral environment and during oral dysbiosis.

Condition	Source of SCFAs	SCFAs	Oral microbiome	Dental biofilm	Host immune system	CNS
Healthy oral environment				Antibacterial activity, homeostatic balance	Pro-inflammatory, anti-inflammatory, chemo-attractant	Improves synapses, microglial maturation
Oral dysbiosis	Carbohydrate, protein, amino acids	Acetate, butyrate, formate, propionate	<i>Actinomyces spp.</i> , <i>Bacteroides spp.</i> , <i>Corynebacteria spp.</i> , <i>Eubacterium spp.</i> , <i>Fusobacterium spp.</i> , <i>Haemophilus spp.</i> , <i>Megasphaera spp.</i> , <i>Neisseria spp.</i> , <i>Propionibacterium</i> , <i>Prevotella spp.</i> , <i>Porphyromonas spp.</i> , <i>Rothia spp.</i>	Limit commensal microbiota, pathogenic microbiota dominate, homeostatic balance disturbed	Increased inflammation, chronic condition, decrease immunity, increased expression of pro-inflammatory cytokines	Triggers microglia mediated innate immune response, alteration in neurotransmitter production, promotes neuroinflammation, neurodegenerative changes

abundance of *Porphyromonas gingivalis* or *P. gingivalis*, a causative microorganism of periodontitis, was reported in the oral cavity of patients with neurodegenerative diseases.⁴⁴ A study on mice has shown brain colonisation due to *P. gingivalis* infection.⁴⁵ Also, *P. gingivalis* produces proteases that have neurotoxic characteristics. On the other hand, oral species of phylum *Spirochaetes* and genus *Treponema*, have been shown to cause amyloid plaques in Alzheimer's disease.⁴⁵ The pathogenic oral microbes enter the brain tissue through different paths to damage the central nervous system (CNS): haemorrhagic oral treatment, root canal treatment, allows the pathogenic microorganism to cross from periapical lesions into alveolar blood vessels, or via gingival crevices to the capillaries in gingival connective tissues,⁴⁶ or oral microorganisms can gain entry to the brain via the trigeminal nerve.⁴⁷ The presence of oral microorganisms in the bloodstream and the secretion of cytokines and toxic substances can alter blood-brain permeability.⁴⁸ This allows the mobility of microorganisms in the brain to cause damage to the CNS. SCFAs have been shown to have an extensive influence on CNS function, for example causing alterations in neurotransmitter production, mitochondrial function, immune activation, lipid metabolism⁴⁸ and gene expression in animal studies, but these lack human evidence and are contradictory. The potential mechanisms of SCFAs produced by the oral microbiome is another research area for investigation. The potential role of SCFAs in a healthy oral environment and oral dysbiosis is outlined in Table 2.^{42,49-54}

SCFAs and the gut microbiome

The gut microbiome is modulated by food products, dietary habits and geographical origin. The development of certain diseases has been reported to occur

due to alterations in the composition of the intestinal microbiome. Examples of such diseases include heart failure,⁵⁵ colorectal cancer,⁵⁶ obesity, diabetes,⁵⁷ inflammatory bowel disease (IBD)⁵⁸ and neurodegenerative disorders.⁵⁹ Additionally, studies have shown that the intestinal microbiome is an important source of neurotransmitters,⁶⁰ including dopamine, noradrenaline, serotonin, gamma-aminobutyric acid (GABA), acetylcholine and histamine.³⁶ The gut microbiome degrades dietary products to produce organic acids, gases and large amounts of SCFAs. SCFAs have been studied widely in the intestinal-gut microbiome, where they can modulate cellular activity both extra- and intracellularly. The molecular and metabolic activity of SCFAs has been identified as extracellular activity via SCFA-specific G-protein coupled receptors,⁶¹ intracellular inhibition of histone deacetylases (HDACs),⁶² intracellular energy supply for colonic epithelium, substrates for the Krebs cycle,⁶³ and induction of apoptosis.⁶⁴

SCFAs can activate free fatty acid receptors (FFARs) expressed in the colon, kidneys, sympathetic nervous system, blood vessels, enteroendocrine L cells and immune cells, including lymphocytes, neutrophils and monocytes.⁶⁵ In a systematic review of some in vitro studies, the role of SCFAs in human oral epithelial cells via receptor-mediated pathways (FFARs, FFAR3, FFAR2) or inhibition of HDACs by altering DNA transcription was speculated. It was observed that SCFAs can contribute to periodontal destruction and modulation of immune cell migration.⁶⁶ There is evidence showing the presence of SCFA receptors in the CNS and peripheral nervous system, thus allowing communication between the gut and brain.⁶⁷ Gut-brain communication can occur through direct or indirect effects of the gut microbiome. In direct effects, the metabolites can systemically translocate and diffuse or pass through the blood-brain barrier. Alternatively, in indirect effects,

Table 3 Oral microbiome in gut diseases: a possible mechanism of gut pathogenesis induced by oral bacteria.

Oral bacteria	Targeted cells	Cellular pathways involved	Possible pathologic role
<i>Porphyromonas gingivalis</i>	Epithelial cells	Jak1/Akt/Stat3, PI3K/Akt, Cyclin D, β -catenin, NF- κ B, ERK1/2, p38.	Gut dysbiosis, epithelial disruption, anti-apoptotic, cell proliferation, immune evasion, tumour invasion
	Neutrophils	Receptor mediated (Toll-like receptors)	Impair action and decrease antibacterial activity
	Dendritic cells	Metalloproteinase and complement system	Increase tissue destruction and compromise host immune system
<i>Fusobacterium nucleatum</i>	Epithelial cells	Wnt/ β -catenin, receptor mediated (Toll-like receptors)	Cell proliferation and migration, cell adhesion
	Natural killer cells, T cells	T cell immunoreceptor	Immune evasion
<i>Staphylococcus aureus</i>	Epithelial cells, T cells	NR	Epithelial disturbance, immune activation
<i>Klebsiella pneumoniae</i>	Epithelial cells	Cytoplasmic adaptor protein	Generation of Th cells (type1)
<i>K. aerogenes (K. aeromobilis)</i>			
<i>Campylobacter concisus</i>	Epithelial cells	NR	Epithelial disturbance
<i>Fusobacterium varium</i>	Epithelial cells	NR	Inflammatory cytokine production, cell adhesion and invasion
<i>Atopobium parvulum</i>	NR	NR	Affects hydrogen sulfide detoxification, mitochondrial dysfunction

Akt, protein kinase B; ERK1/2, extracellular signal-regulated protein kinases 1 and 2; Jak 1, Janus kinase 1; NF- κ B, nuclear factor kappa-light-chain-enhancer of activated B cells; NR, not reported; PI3K, phosphoinositide 3-kinase; Stat3, signal transducer and activator of transcription 3; Wnt, wingless-related integration site.

the microbes colonise the intestine to release metabolites that are involved in neurological functions. The products generated in the intestine can move via the bloodstream to reach the CNS, where these metabolites act as neurotransmitters or their precursors.⁶⁸

Relations between the oral and gut microbiome

The oral microbiome is the second-largest microbiome in humans after the gut. The gut microbiome shows greater diversity compared to the oral microbiome.⁶⁹ Due to the differences between the two, the oral microorganisms that enter the gut through swallowing saliva could change intestinal microbial colonisation. The release of metabolic end-products by the bacteria can accelerate inflammatory changes and affect various tissues and organs in direct or indirect ways.⁷⁰ It has been shown that periodontal pathogens, mainly *P. gingivalis*, can survive in the gut, change the composition of the intestinal microbiome, and increase intestinal permeability. The survival of *P. gingivalis* in the gut and the release of metabolites can spread through the bloodstream and affect various sites in the human body. Their role in the development of neuropathology has also been documented.⁷¹ The available data suggest that gut-associated systemic pathology is mediated by periodontal microorganisms (Table 3).⁷⁰⁻⁷²

A limited number of shared taxa between the oral cavity and the gut are presented in Fig 1. Recently, a

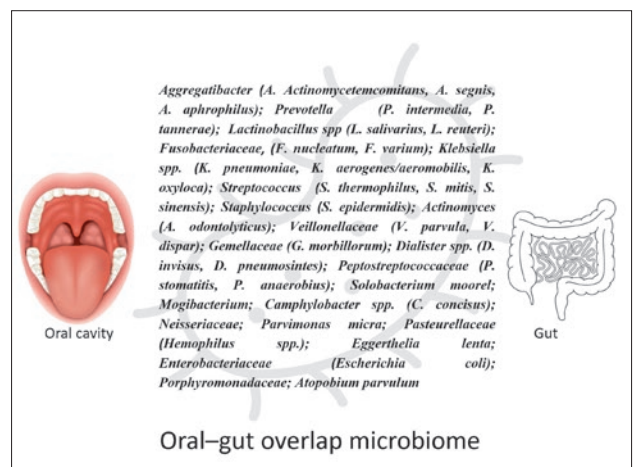


Fig 1 The overlap between the oral and gastrointestinal microbiome, a bridge for the oral-gut axis resulting in several oral and systemic diseases.

subset of 74 species were reported to be transmitted from the mouth to the gut, forming consistent microbiome populations along the gastrointestinal tract.⁷³ The oral mucosa is connected to the gastrointestinal mucosa, and their interrelationships are expected as saliva is ingested every day from the oral cavity to the gut. The oral microbiota affects the gut microbiota through three routes: first, the enteral route, whereby salivary mucins protect the microbiota from gastric acid after swallowing and allow their survival along the gastrointestinal tract; second, the hematogenous route, where-

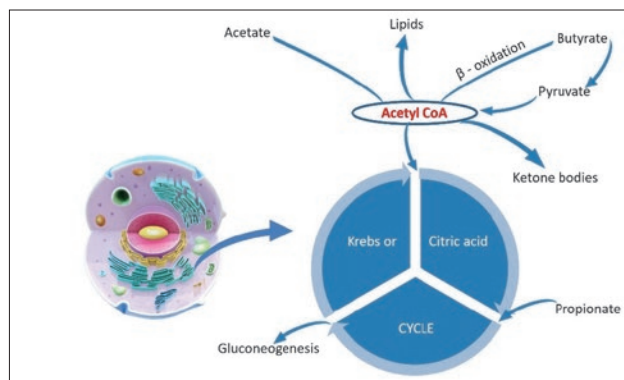


Fig 2 Metabolism of SCFAs. Butyrate absorption negatively regulates pyruvate to produce acetyl-CoA necessary in the Krebs cycle. Butyrate action pushes cell metabolism from glycolysis to β -oxidation. Depending on the metabolic state, acetate and butyrate are converted to acetyl-CoA. SCFAs can enter the citric acid cycle for gluconeogenesis and be utilised to form lipids and ketone bodies.

by oral/dental trauma allows easy penetration of oral microbes through the damaged mucosa and enables oral microbes to spread into the systemic circulation; and third, the immune cell migration route, whereby dendritic cells and macrophages help in the dissemination of oral bacteria from the oral cavity to the gut.⁷⁴

The role of the oral-gut axis in systemic disease has accelerated recently where diabetes and IBD have shown stronger associations between the oral-gut axis and disease progression.⁷⁵ In diabetes, *Streptococcus salivarius* is decreased in the oral cavity as well as in the gut, thereby increasing the abundance of facultative anaerobes including *Enterobacteria*. The increased *Enterobacteria* drives gut inflammation and impacts diabetes progression. *P. gingivalis* or *Fusobacterium nucleatum* from the saliva of periodontitis patients can increase gut permeability by disturbing the intestinal immune system and assisting disease progression.^{75,76} IBD patients have shown oral dysbiosis with different microbial ecotypes exhibiting similar variations as in the gut. Hence, saliva is marked as a convenient tool for risk identification in IBD patients.⁷⁷ There is a bidirectional relationship between the oral and gut microbiota; however, there is limited research on the influence of gut dysbiosis on the oral microbiota and the presence of SCFAs receptors in the oral mucosal epithelium.

Metabolism and action of SCFAs

Both exogenous and endogenous SCFAs may be involved in the pathogenesis of different diseases. SCFA provides approximately 10% of the daily calorie requirement and its receptors are present throughout the human body.⁷⁸

SCFAs may act as ligands to membrane receptors, thus affecting cell metabolism (Fig 2). Acetate, butyrate and propionate are SCFAs with chain lengths of 1 to 6 carbon atoms. These act on many cell types and regulate important biological processes. Catabolism of different bacteria is the main reason for the different proportions of SCFAs in the human colon.⁷⁹ Previous studies on colon epithelium have shown butyrate to be the main substrate, which enhances oxidative phosphorylation within the cell and enhances fatty acid metabolism.^{80,81} Butyrate is produced via glycolysis and with a stepwise reduction of acetoacetyl-CoA to butyryl-CoA. The final step in the formation of butyrate from butyryl-CoA involves either the butyryl-CoA: acetate CoA-transferase route or the phospho-butyrates and butyrate kinase pathways.⁸² Butyrate and acetate are the substrates for lipogenesis. Acetate is metabolised in muscles and is a substrate for cholesterol and fatty acid synthesis. Several anaerobic bacteria, such as *A. muciniphila* and *Bacteroides spp.*, produce acetic acid through fermentation. Acetate is found in a higher concentration in the proximal colon, where it is absorbed by intestinal epithelial cells and later by the liver via the hepatic portal vein. In the blood, acetate exists as a free acid that is metabolized by several tissues and organs.⁸³ Propionate is derived from carbohydrate metabolism during glycolysis, mainly through the succinate pathway, and is a precursor for glucose synthesis in the liver.⁸⁴ A vitro study has shown that increased secretion of propionate by the intestinal epithelium inhibited hepatocyte adipogenesis and reduced fat deposition in chickens.⁸⁵ Several other animal studies have indicated the crucial role played by propionate in lipid metabolism, the nervous system and cardiovascular diseases.^{86,87} Thus, the increase and decrease of SCFAs in the colonic epithelium can impair its structure and function.

The importance of SCFAs has been demonstrated and reported in various animal model studies. SCFA metabolism in the liver can directly affect energy status through an imbalance between lipid formation and breakdown, glucose production and catabolism, and cholesterol synthesis and secretion.⁸⁸ In another study, SCFAs were shown to promote adipogenesis in the rodent cell model.⁸⁹ Acetate or propionate were found to induce significant changes in nuclear receptor expression, leptin secretion and intracellular triglyceride accumulation in the early stage of adipose differentiation.⁸⁹ SCFAs were found to mediate glucose metabolism and fatty acid utilisation in skeletal muscle via stimulation through regulators of skeletal muscle metabolism.⁹⁰ SCFAs play a dual role as a substrate and as a regulatory factor in lipid metabolism.⁹⁰

Hypothesis

Oral diseases, mainly caries and periodontitis, are well known diseases caused by the oral dysbiosis. Microbial metabolites produced in the oral cavity can enhance the prediction of pathogenesis of oral diseases and, furthermore, provide more consolidated information on several systemic diseases. The salivary metabolites produced by the oral microbiome can be helpful in uncovering the causal relationship between the microbiome and disease at earlier stages. In the present article, the authors propose that salivary SCFAs derived from the oral microbiome and oral infectious diseases constitute a key element for driving oral-systemic alterations to cause numerous diseases. Both saccharolytic and proteolytic bacteria are present in the oral cavity that release SCFAs into saliva. These salivary SCFAs can act in two ways: they can be transferred directly from saliva into the bloodstream via inflamed gingiva, or salivary metabolites are swallowed and transferred via the gut to communicate with other organs. SCFAs as immunomodulators cause low-level systemic inflammation. Salivary SCFAs are the key regulators of oral changes that communicate with systemic conditions much earlier than the gut microbiome. Hence, salivary SCFAs can provide possible advantages as an indicator or diagnostic tool for early diagnosis of systemic diseases (Fig 3).

Conclusion

The two largest known microbial habitats in the human body are the gut and oral cavity. There is growing evidence to support the notion that the oral microbiome can change the gut microbiome through direct translocation of oral bacteria and/or indirectly by oral bacterial byproducts. SCFAs are released by both the oral and gut microbiome. Taken together, the oral–systemic microbiome axis is strongly associated with diseases via SCFAs and could be a predictor of early-stage disease development; however, the presence of SCFA receptors in the oral mucosal epithelium is unclear. The present study provides a basis for further research aimed at understanding the oral–systemic axis driven through salivary SCFAs in the pathogenesis of several diseases. Thus, integrative research on salivary SCFAs is needed to control metabolite-associated diseases and develop novel strategies for precise diagnosis, prognosis and treatment.

Conflicts of interest

The authors declare no conflicts of interest related to this study.

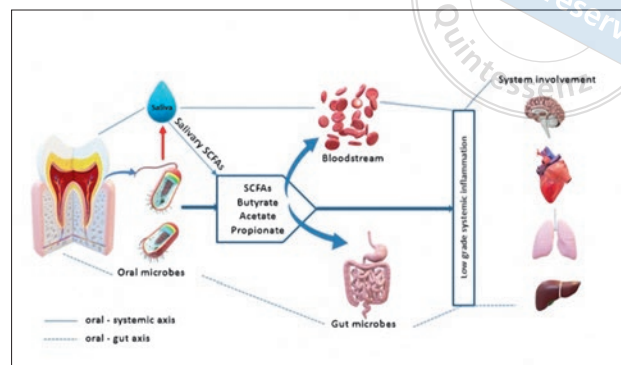


Fig 3 Schematic illustration depicting the paths through which salivary SCFAs produced by the oral microbiome affect systemic health. They are the end-product of oral bacteria and can directly enter the circulating blood and affect systemic health. Salivary SCFAs can be swallowed, which indirectly disturbs the gut microenvironment. The changes in the gut microbiome can further affect systemic health by mediating systemic inflammation. Salivary SCFAs cause low-grade systemic inflammation that can be aggravated via further changes in the oral and gut microbiome.

Author contribution

Dr Bina KASHYAP contributed to the conceptualisation, study design and manuscript draft; Dr Eelis HYVÄRINEN contributed to the data collection and manuscript review; Dr Arja M KULLAA contributed to the manuscript review, editing and finalisation.

(Received Aug 31, 2023; accepted May 16, 2024)

References

1. Sampaio-Maia B, Caldas IM, Pereira ML, Pérez-Mongiovi D, Araujo R. The Oral Microbiome in Health and Its Implication in Oral and Systemic Diseases. *Adv Appl Microbiol* 2016;97:171–210.
2. Faran Ali SM, Tanwir F. Oral microbial habitat a dynamic entity. *J Oral Biol Craniofac Res* 2012;2:181–187.
3. Marsh PD. Are dental diseases examples of ecological catastrophes? *Microbiology (Reading)* 2003;149:279–294.
4. Curtis MA, Zenobia C, Darveau RP. The relationship of the oral microbiota to periodontal health and disease. *Cell Host Microbe* 2011;10:302–306.
5. Georges FM, Do NT, Seleem D. Oral dysbiosis and systemic diseases. *Frontiers in Dental Medicine* 2022:1–7.
6. Kinane DF, Stathopoulou PG, Papapanou PN. Periodontal diseases. *Nat Rev Dis Primers* 2017;3:17038.
7. Linden GJ, Lyons A, Scannapieco FA. Periodontal systemic associations: review of the evidence. *J Periodontol* 2013;84(4, suppl):S8–S19.
8. Tuominen H, Rautava J. Oral Microbiota and Cancer Development. *Pathobiology* 2021;88:116–126.
9. Farrell JJ, Zhang L, Zhou H, et al. Variations of oral microbiota are associated with pancreatic diseases including pancreatic cancer. *Gut* 2012;61:582–588.

10. Koliarakis I, Messaritakis I, Nikolouzakis TK, Hamilos G, Souglakos J, Tsiaoussis J. Oral Bacteria and Intestinal Dysbiosis in Colorectal Cancer. *Int J Mol Sci* 2019;20:4146.
11. Hyvärinen E, Solje E, Vepsäläinen J, Kullaa A, Tynkkynen T. Salivary Metabolomics in the Diagnosis and Monitoring of Neurodegenerative Dementia. *Metabolites* 2023;13:233.
12. Melguizo-Rodríguez L, Costela-Ruiz VJ, Manzano-Moreno FJ, Ruiz C, Illescas-Montes R. Salivary Biomarkers and Their Application in the Diagnosis and Monitoring of the Most Common Oral Pathologies. *Int J Mol Sci* 2020;21:5173.
13. Hyvärinen E, Savolainen M, Mikkonen JJW, Kullaa AM. Salivary Metabolomics for Diagnosis and Monitoring Diseases: Challenges and Possibilities. *Metabolites* 2021;11:587.
14. Meleti M, Quartieri E, Antonelli R, et al. Metabolic Profiles of Whole, Parotid and Submandibular/Sublingual Saliva. *Metabolites* 2020;10:318.
15. Hyvärinen E, Kashyap B, Kullaa AM. Oral Sources of Salivary Metabolites. *Metabolites* 2023;13:498.
16. Gardner A, Parkes HG, So PW, Carpenter GH. Determining bacterial and host contributions to the human salivary metabolome. *J Oral Microbiol* 2019;11:1617014.
17. Smith EA, Macfarlane GT. Enumeration of amino acid fermenting bacteria in the human large intestine: effects of pH and starch on peptide metabolism and dissimilation of amino acids. *FEMS Microbiology Ecology* 1998;25:355–368.
18. Fidalgo TKS, Freitas-Fernandes LB, Angeli R, et al. Salivary metabolite signatures of children with and without dental caries lesions. *Metabolomics* 2013;9:657–666.
19. Pereira JL, Duarte D, Carneiro, TJ, et al. Saliva NMR metabolomics: Analytical issues in pediatric oral health research. *Oral Dis* 2019;25:1545–1554.
20. Schulz A, Lang R, Behr J, et al. Targeted metabolomics of pellicle and saliva in children with different caries activity. *Sci Rep* 2020;10:697.
21. Aimetti M, Cacciatori S, Graziano A, Tenori L. Metabonomic analysis of saliva reveals generalized chronic periodontitis signature. *Metabolomics* 2012;8:465–474.
22. Rzeznik M, Triba MN, Levy P, et al. Identification of a discriminative metabolomic fingerprint of periodontitis using ¹H nuclear magnetic resonance (NMR) spectroscopy. *PLoS One* 2017;12: e0182767.
23. Romano F, Meoni G, Manavella V, et al. Analysis of salivary phenotypes of generalized aggressive and chronic periodontitis through nuclear magnetic resonance-based metabolomics. *J Periodontol* 2018;89:1452–1460.
24. García-Villaescusa A, Morales-Tatay JM, Monleón-Salvadó D, et al. Using NMR in saliva to identify possible biomarkers of glioblastoma and chronic periodontitis. *PLoS One* 2018;13:e0188710.
25. Liebsch C, Pitchika V, Pink C, et al. The Saliva Metabolome in Association to Oral Health Status. *J Dent Res* 2019;98:642–651.
26. Gawron K, Wojtowicz W, Łazarz-Bartyzel K, et al. Metabolomic status of the oral cavity in chronic periodontitis. *In Vivo* 2019;33:1165–1174.
27. Citterio F, Romano F, Meoni G, et al. Changes in the salivary metabolic profile of generalized periodontitis patients after non-surgical periodontal therapy: A metabolomic analysis using nuclear magnetic resonance spectroscopy. *J Clin Med* 2020;9:3977.
28. Kim S, Kim HJ, Song Y, Lee HA, Kim S, Chung J. Metabolic phenotyping of saliva to identify possible biomarkers of periodontitis using proton nuclear magnetic resonance. *J Clin Periodontol* 2021;48:1240–1249.
29. Sanches ML, Sforça ML, Turco EGL, Faber J, Smith RL, Moraes LOC. Women with temporomandibular disorders: Untargeted proton nuclear magnetic resonance spectroscopy-based metabolomics of saliva and psychological instruments dataset. *Data Brief* 2020;34:106677.
30. Wei J, Xie G, Zhou Z, et al. Salivary metabolite signatures of oral cancer and leukoplakia. *Int J Cancer* 2011;129:2207–2217.
31. Wang Q, Gao P, Wang X, Duan Y. The early diagnosis and monitoring of squamous cell carcinoma via saliva metabolomics. *Sci Rep* 2014;4:6802.
32. Ishikawa S, Sugimoto M, Edamatsu K, Sugano A, Kitabatake K, Iino M. Discrimination of oral squamous cell carcinoma from oral lichen planus by salivary metabolomics. *Oral Dis* 2020;26:35–42.
33. Yatsuoka W, Ueno T, Miyano K, et al. Time-Course of Salivary Metabolomic Profiles during Radiation Therapy for Head and Neck Cancer. *J Clin Med* 2021;10:2631.
34. Niederman R, Zhang J, Kashket S. Short-chain carboxylic-acid-stimulated, PMN-mediated gingival inflammation. *Crit Rev Oral Biol Med* 1997;8:269–290.
35. Boets E, Gomand SV, Deroover L, Preston T, Vermeulen K, De Preter V et al. Systemic availability and metabolism of colonic-derived short-chain fatty acids in healthy subjects: a stable isotope study. *J Physiol* 2017;595:541–555.
36. Ahmed H, Leyrolle Q, Koistinen V, et al. Microbiota-derived metabolites as drivers of gut-brain communication. *Gut Microbes* 2022;14:2102878.
37. Huang C, Shi G. Smoking and microbiome in oral, airway, gut and some systemic diseases. *J Transl Med* 2019;17:225.
38. Nociti FH Jr, Casati MZ, Duarte PM. Current perspective of the impact of smoking on the progression and treatment of periodontitis. *Periodontol* 2000 2015;67:187–210.
39. Kolenbrander PE, Andersen RN, Blehert DS, Eglund PG, Foster JS, Palmer RJ Jr. Communication among oral bacteria. *Microbiol Mol Biol Rev* 2002;66:486–505.
40. Tonetti M, Eftimiadi C, Damiani G, Buffa P, Buffa D, Botta GA. Short chain fatty acids present in periodontal pockets may play a role in human periodontal diseases. *J Periodontol Res* 1987;22:190–191.
41. van Houte J. Role of micro-organisms in caries etiology. *J Dent Res* 1994;73:672–681.
42. Hashimoto K. Emerging role of the host microbiome in neuropsychiatric disorders: overview and future directions. *Mol Psychiatry* 2023;28:3625–3637.
43. Sureda A, Daglia M, Castilla SA, et al. Oral microbiota and Alzheimer's disease: Do all roads lead to Rome? *Pharmacol Res* 2020;151:104582.
44. Franciotti R, Pignatelli P, Carrarini C, et al. Exploring the Connection between *Porphyromonas gingivalis* and Neurodegenerative Diseases: A Pilot Quantitative Study on the Bacterium Abundance in Oral Cavity and the Amount of Antibodies in Serum. *Biomolecules* 2021;11:845.
45. Dominy SS, Lynch C, Ermini F, et al. *Porphyromonas gingivalis* in Alzheimer's disease brains: Evidence for disease causation and treatment with small-molecule inhibitors. *Sci Adv* 2019;5:eaa3333.
46. Savarrio L, Mackenzie D, Riggio M, Saunders WP, Bagg J. Detection of bacteraemias during non-surgical root canal treatment. *J Dent* 2005;33:293–303.
47. Teixeira FB, Saito MT, Matheus FC, et al. Periodontitis and Alzheimer's disease: a possible comorbidity between oral chronic inflammatory condition and neuroinflammation. *Front Aging Neurosci* 2017;9:327.

48. Bulgart HR, Neczypor EW, Wold LE, Mackos AR. Microbial involvement in Alzheimer disease development and progression. *Mol Neurodegener* 2020;15:42.
49. Dahlstrand Rudin A, Khamzeh A, Venkatakrishnan V, Basic A, Christenson K, Bylund J. Short chain fatty acids released by *Fusobacterium nucleatum* are neutrophil chemoattractants acting via free fatty acid receptor 2 (FFAR2). *Cell Microbiol* 2021;23:e13348.
50. Dahlstrand Rudin A, Khamzeh A, Venkatakrishnan V, et al. *Porphyromonas gingivalis* Produce Neutrophil Specific Chemoattractants Including Short Chain Fatty Acids. *Front Cell Infect Microbiol* 2021;10:620681.
51. Huang CB, Alimova Y, Myers TM, Ebersole JL. Short- and medium-chain fatty acids exhibit antimicrobial activity for oral microorganisms. *Arch Oral Biol* 2011;56:650–654.
52. Silva YP, Bernardi A, Frozza RL. The Role of Short-Chain Fatty Acids From Gut Microbiota in Gut-Brain Communication. *Front Endocrinol (Lausanne)* 2020;11:25.
53. Nicholson JS, Landry KS. Oral Dysbiosis and Neurodegenerative Diseases: Correlations and Potential Causations. *Microorganisms* 2022;10:1326.
54. Intili G, Paladino L, Rappa F, et al. From Dysbiosis to Neurodegenerative Diseases through Different Communication Pathways: An Overview. *Biology* 2023;12:195.
55. Geleijnse JM, Vermeer C, Grobbee DE, et al. Dietary intake of menaquinone is associated with a reduced risk of coronary heart disease: the Rotterdam Study. *J Nutr* 2004;134:3100–3105.
56. Wang T, Cai G, Qiu Y, et al. Structural segregation of gut microbiota between colorectal cancer patients and healthy volunteers. *ISME J* 2012;6:320–329.
57. Murri M, Leiva I, Gomez-Zumaquero JM, et al. Gut microbiota in children with type 1 diabetes differs from that in healthy children: a case-control study. *BMC Med* 2013;11:46.
58. Machiels K, Joossens M, Sabino J, et al. A decrease of the butyrate-producing species *Roseburia hominis* and *Faecalibacterium prausnitzii* defines dysbiosis in patients with ulcerative colitis. *Gut* 2014;63:1275–1283.
59. Pistollato F, Sumalla Cano S, Elio I, Masias Vergara M, Giampieri F, Battino M. Role of gut microbiota and nutrients in amyloid formation and pathogenesis of Alzheimer disease. *Nutr Rev* 2016;74:624–634.
60. Strandwitz P. Neurotransmitter modulation by the gut microbiota. *Brain Res* 2018;1693 (Pt B):128–133.
61. Brown AJ, Goldsworthy SM, Barnes AA, et al. The Orphan G protein-coupled receptors GPR41 and GPR43 are activated by propionate and other short chain carboxylic acids. *J Biol Chem* 2003;278:11312–11319.
62. Waldecker M, Kautenburger T, Daumann H, Busch C, Schrenk D. Inhibition of histone-deacetylase activity by short-chain fatty acids and some polyphenol metabolites formed in the colon. *J Nutr Biochem* 2008;19:587–593.
63. den Besten G, Lange K, Havinga R, et al. Gut-derived short-chain fatty acids are vividly assimilated into host carbohydrates and lipids. *Am J Physiol Gastrointest Liver Physiol* 2013;305:G900–G910.
64. Sengupta S, Muir JG, Gibson PR. Does butyrate protect from colorectal cancer? *J Gastroenterol Hepatol* 2006;21(1 Pt 2):209–218.
65. Kimura I, Ichimura A, Ohue-Kitano R, Igarashi M. Free Fatty Acid Receptors in Health and Disease. *Physiol Rev* 2020;100:171–210.
66. Magrin GL, Strauss FJ, Benfatti CAM, Maia LC, Gruber R. Effects of Short-Chain Fatty Acids on Human Oral Epithelial Cells and the Potential Impact on Periodontal Disease: A Systematic Review of In Vitro Studies. *Int J Mol Sci* 2020;21:4895.
67. Dalile B, Van Oudenhove L, Vervliet B, Verbeke K. The role of short-chain fatty acids in microbiota-gut-brain communication. *Nat Rev Gastroenterol Hepatol* 2019;16:461–478.
68. Narengaowa, Kong W, Lan F, Awan UF, Qing H, Ni J. The Oral-Gut-Brain AXIS: The Influence of Microbes in Alzheimer's Disease. *Front Cell Neurosci* 2021;15:633735.
69. Li K, Bihan M, Methé BA. Analyses of the stability and core taxonomic memberships of the human microbiome. *PLoS One* 2013;8:e63139.
70. Deo PN, Deshmukh R. Oral microbiome: Unveiling the fundamentals. *J Oral Maxillofac Pathol* 2019;23:122–128.
71. Feng YK, Wu QL, Peng YW, et al. Oral *P. gingivalis* impairs gut permeability and mediates immune responses associated with neurodegeneration in LRRK2 R1441G mice. *J Neuroinflammation* 2020;17:347.
72. Kitamoto S, Nagao-Kitamoto H, Hein R, Schmidt TM, Kamada N. The Bacterial Connection between the Oral Cavity and the Gut Diseases. *J Dent Res* 2020;99:1021–1029.
73. Schmidt TS, Hayward MR, Coelho LP, et al. Extensive transmission of microbes along the gastrointestinal tract. *Elife* 2019;8:e42693.
74. Tan X, Wang Y, Gong T. The interplay between oral microbiota, gut microbiota and systematic diseases. *J Oral Microbiol* 2023;15:2213112.
75. Byrd KM, Gulati AS. The “Gum-Gut” Axis in Inflammatory Bowel Diseases: A Hypothesis-Driven Review of Associations and Advances. *Front Immunol* 2021;12:620124.
76. Vaarala O, Atkinson MA, Neu J. The “perfect storm” for type 1 diabetes: the complex interplay between intestinal microbiota, gut permeability, and mucosal immunity. *Diabetes*. 2008;57:2555–2562.
77. Xun Z, Zhang Q, Xu T, Chen N, Chen F. Dysbiosis and ecotypes of the salivary microbiome associated with inflammatory bowel diseases and the assistance in diagnosis of diseases using oral bacterial profiles. *Front Microbiol* 2018;9:1136.
78. He J, Zhang P, Shen L, et al. Short-Chain Fatty Acids and Their Association with Signalling Pathways in Inflammation, Glucose and Lipid Metabolism. *Int J Mol Sci* 2020;21:6356.
79. Deleu S, Machiels K, Raes J, Verbeke K, Vermeire S. Short chain fatty acids and its producing organisms: An overlooked therapy for IBD? *EBioMedicine* 2021;66:103293.
80. Fogelholm N, Leskelä J, Manzoor M, et al. Subgingival microbiome at different levels of cognition. *J Oral Microbiol* 2023;15:2178765.
81. Kasubuchi M, Hasegawa S, Hiramatsu T, Ichimura A, Kimura I. Dietary gut microbial metabolites, short-chain fatty acids, and host metabolic regulation. *Nutrients* 2015;7:2839–2849.
82. Louis P, Flint HJ. Formation of propionate and butyrate by the human colonic microbiota. *Environ Microbiol* 2017;19:29–41.
83. Zeng H, Umar S, Rust B, Lazarova D, Bordonaro M. Secondary Bile Acids and Short Chain Fatty Acids in the Colon: A Focus on Colonic Microbiome, Cell Proliferation, Inflammation, and Cancer. *Int J Mol Sci* 2019;20:1214.
84. Andriamihaja M, Chaumontet C, Tome D, Blachier F. Butyrate metabolism in human colon carcinoma cells: implications concerning its growth-inhibitory effect. *J Cell Physiol* 2009;218:58–65.
85. Zhang JM, Sun YS, Zhao LQ, et al. SCFAs-Induced GLP-1 Secretion Links the Regulation of Gut Microbiome on Hepatic Lipogenesis in Chickens. *Front Microbiol* 2019;10:2176.



86. Hou YF, Shan C, Zhuang SY, et al. Gut microbiota-derived propionate mediates the neuroprotective effect of osteocalcin in a mouse model of Parkinson's disease. *Microbiome* 2021;9:34.
87. Bartolomaeus H, Balogh A, Yakoub M, et al. Short-Chain Fatty Acid Propionate Protects From Hypertensive Cardiovascular Damage. *Circulation* 2019;139:1407–1421.
88. Donohoe DR, Garge N, Zhang X, et al. The microbiome and butyrate regulate energy metabolism and autophagy in the mammalian colon. *Cell Metab* 2011;13:517–526.
89. Blaak EE, Canfora EE, Theis S, et al. Short chain fatty acids in human gut and metabolic health. *Benef Microbes* 2020;11:411–455.
90. Frost G, Cai Z, Raven M, Otway DT, Mushtaq R, Johnston JD. Effect of short chain fatty acids on the expression of free fatty acid receptor 2 (Ffar2), Ffar3 and early-stage adipogenesis. *Nutr Diabetes* 2014;4:e128.

GREM1 Negatively Regulates Osteo-/Dentinogenic Differentiation of Dental Pulp Stem Cells via Association with YWHAH

Shu DIAO^{1,2}, Xiao HAN¹, Wei Long YE¹, Chen ZHANG¹, Dong Mei YANG², Zhi Peng FAN^{1,3}, Song Lin WANG^{1,3}

Objective: To investigate the biological regulatory function of *Gremlin1* (GREM1) and tyrosine 3-monooxygenase/tryptophan 5-monooxygenase activation protein eta (YWHAH) in dental pulp stem cells (DPSCs), and determine the underlying molecular mechanism involved.

Methods: Alkaline phosphatase (ALP) activity, alizarin red staining, scratch migration assays and in vitro and in vivo osteo-/dentinogenic marker detection of bone-like tissue generation in nude mice were used to assess osteo-/dentinogenic differentiation. Coimmunoprecipitation and polypeptide microarray assays were employed to detect the molecular mechanisms involved.

Results: The data revealed that knockdown of GREM1 promoted ALP activity, mineralisation in vitro and the expression of osteo-/dentinogenic differentiation markers and enhanced osteo-/dentinogenesis of DPSCs in vivo. GREM1 bound to YWHAH in DPSCs, and the binding site was also identified. Knockdown of YWHAH suppressed the osteo-/dentinogenesis of DPSCs in vitro, and overexpression of YWHAH promoted the osteo-/dentinogenesis of DPSCs in vitro and in vivo.

Conclusion: Taken together, the findings highlight the critical roles of GREM1-YWHAH in the osteo-/dentinogenesis of DPSCs.

Keywords: dental pulp stem cells, *Gremlin1*, tooth regeneration, YWHAH
Chin J Dent Res 2024;27(3):203–213; doi: 10.3290/j.cjdr.b5698390

- 1 Salivary Gland Disease Center and Beijing Key Laboratory of Tooth Regeneration and Function Reconstruction, Beijing Laboratory of Oral Health and Beijing Stomatological Hospital, Capital Medical University, Beijing, P.R. China.
- 2 Department of Pediatric Dentistry, Capital Medical University School of Stomatology, Beijing, P.R. China.
- 3 Research Unit of Tooth Development and Regeneration, Chinese Academy of Medical Sciences, Beijing, P.R. China.

Corresponding authors: Prof Zhi Peng FAN, Capital Medical University School of Stomatology, No. 4 Tian Tan Xi Li, DongCheng District, Beijing 100050, P.R. China. Tel: 86-10-57099114. Email: zpfan@ccmu.edu.cn; Prof Song Ling WANG, Capital Medical University, No.10 You An Men Wai Xi Tou Tiao, FengTai District, Beijing 100069, P.R. China. Tel: 86-10-83911708. Email: slwang@ccmu.edu.cn.

This work was supported by grants from the National Natural Science Foundation of China (82130028 to ZPF), the National Natural Science Foundation of China (92049201, 82030031, 81991504, 92149301, L2224038 and 82001067), the Beijing Municipal Government grant (Beijing Laboratory of Oral Health, PXM2021-014226-000041), the Innovation Research Team Project of Beijing Stomatological Hospital, Capital Medical University (CXTD202201), the Beijing Advanced Innovation Center for Big Data-based Precision Medicine (PXM2021_014226_000026), the Beijing Municipal Government (Beijing Scholar Program, PXM2020_014226_000005 and PXM2021_014226_000020), the National Key Research and development Program (2022YFA1104401) and the National Sciences Foundation of China (81800923 to SD).

Stem cell-mediated tooth regeneration is an ideal therapy for tooth loss but still presents many problems, such as limited seed cells and poor efficacy.^{1,2} In tooth tissue, stem cells, growth factors and the extracellular matrix (ECM) in the niche and their multiple interactions determine tooth development, eruption and biological basis for the formation of pulp dentine and so on. However, due to being limited by the current methods, the niche cannot be maintained when mesenchymal stem cells (MSCs) are isolated and cultured in vitro. Disruption of the niche may impede MSC-mediated tooth regeneration.³⁻⁵ The stem cell niche plays a key role in homeostasis and tissue regeneration.

From the perspective of the stem cell microenvironment, previous studies conducted by the present authors^{6,7} revealed that bone morphogenetic proteins (BMPs) are downregulated in stem cells from the apical papilla (SCAPs) compared with the tissues from the apical papilla, but the antagonist of bone morphogenetic protein- *Gremlin1* (GREM1) is upregulated. In vitro experiments showed that BMP6 could significantly enhance the proliferation and differentiation potential

of SCAPs, and that BMP2, BMP6 and BMP7 are negatively regulated by GREM1, suggesting that the GREM1-BMP signalling pathway may play an important role in regulating the function of stem cells.^{6,7}

GREM1 belongs to the DNA family of secreted BMP antagonists. GREM1 is involved in bone development, and *Grem1* mutant mice develop severe limb skeletal deformities.^{8,9} As an endogenous antagonist of BMP, GREM1 not only binds to extracellular BMP but also prevents the secretion of BMP through intracellular BMP and GREM1 interactions and effectively inhibits its activity.¹⁰ Studies have confirmed that *Grem1* blocks the classical BMP signalling pathway by inhibiting the phosphorylation of *smad1/5/8*, but can also directly regulate p38, ERK and JNK.¹¹ However, until recently, the interaction between BMP signalling and GREM1 in MSCs has been unclear. A previous study revealed that GREM1 can bind to tyrosine 3-monooxygenase/tryptophan 5-monooxygenase activation protein eta (YWHAH),¹² a member of the 14-3-3 gene family. The 14-3-3 protein family is a group of highly conserved acidic proteins that are highly expressed in nervous tissues; it interacts with more than 100 proteins that are critical for many cellular physiological processes, such as signalling, cell growth, division, adhesion, derivatives and apoptosis, and thus plays an important role in cell proliferation and transformation.¹³⁻¹⁵ These studies indicated that YWHAH might be a downstream gene of GREM1, and regulate BMP2, BMP6 and BMP7 and stem cell function^{16,17}; however their function and molecular mechanism are not clear. In this study, the present authors investigated the biological regulatory function of GREM1 in DPSCs, and the underlying molecular mechanism to explain how GREM1/YWHAH regulate BMPs in DPSCs.

Materials and methods

Cell culture

With the approval of the Beijing Stomatology Hospital, School of Stomatology, Capital Medical University (CMUSH-IRB-KJ-PJ-2023-28), human impacted third molars were collected from 10 healthy patients. The pulp tissues were treated aseptically and washed with solutions of phosphate-buffered saline (PBS). DPSCs were isolated and cultured as previously described. Briefly cells were grown in a humidified atmosphere of 5% CO₂ at 37°C, and the medium was changed every 3 days.

Plasmids and viruses

Plasmids were produced using standard methods, and enzyme digestion, sequencing or both confirmed the structures of all plasmids. Human full-length YWHAH cDNA with an HA tag was generated via standard gene synthesis. This fragment (HA-YWHAH) was inserted into the PQCXIN plasmid between the AgeI and BamHI restriction sites. GREM1 shRNA, YWHAH shRNA and control shRNA were purchased from Genepharma (Suzhou, China). DPSCs were seeded into plates overnight growth and transfected for 12 hours with the virus using polybrene (Sigma Aldrich, St. Louis, MO, USA). After 48 hours of transfection, the cells were selected in the presence of an appropriate antibiotic. The sequences of the shRNAs used were follows: LV3 shRNA (Consh), 5'-TTCTCCGAACGTGTCACGTTT-3'; GREM1 shRNA (GREM1-sh), 5'-GCAAGCCC AAGAAATTCACCTA-3'. NC shRNA (Consh), 5'-CCATGATTCCTTCATATTTGC-3'; YWHAH shRNA (YWHAH-sh), 5'-GAGCCGACACGGGTTAGGATCC-3'.

Cell ALP activity assay and alizarin red staining

DPSCs were grown in mineralisation-inducing medium using a Stem Pro Osteogenesis Differentiation Kit (Invitrogen, Carlsbad, CA, USA). Cells were cultured for 5 days, and the ALP activity assay was performed with an ALP kit according to the manufacturer's protocol (Sigma Aldrich) and normalised based on protein concentrations. The protein concentration was quantitatively determined using Bio-Rad protein assay solution (Bio-Rad Laboratories, Hercules, CA, USA). To detect mineralisation, the cells were induced for 2 weeks, fixed with 70% ethanol and stained with 2% alizarin red (Sigma Aldrich). To quantitatively determine the calcium mineral content, alizarin red was destained with 10% cetylpyridinium chloride in 10 mM sodium phosphate for 60 minutes at room temperature. The concentration was determined by absorbance measurement at 562 nm on a multiplate reader using a standard calcium curve in the same solution. The final calcium level in each group was normalised to the total protein concentration prepared from a duplicate plate.¹⁸

Reverse transcriptase polymerase chain reaction (RT-PCR) and real-time RT-PCR

Total RNA was isolated from DPSCs with TRIzol reagent (Invitrogen). We synthesised cDNA from 2 µg aliquots of RNA, random hexamers or oligo (dT) and reverse transcriptase, according to the manufacturer's protocol (Invitrogen). Real-time PCR was performed with a Quanti-

Tect SYBR Green PCR Kit (Qiagen, Hilden, Germany) and an Icyler iQ Multicolor Real-time PCR Detection System (Bio-Rad Laboratories). The primers for specific genes are shown in Table S1 and the PCR conditions are presented in Table S2 (both provided on request).

Scratch migration assays

A scratch-simulated wound migration assay was implemented to assess the function of MSC migration. Upon reaching 80% confluence, the cells were digested with 0.25% trypsin-ethylenediaminetetraacetic acid (EDTA) (Gibco, Life Technologies, Carlsbad, CA, USA), seeded onto six-well plates at a density of 2×10^5 cells/well and allowed to grow to close to 95% confluence. The cells were grown in DMEM supplemented with alpha modified Eagle medium (Invitrogen) without foetal bovine serum (FBS; Invitrogen). After culturing for 24 hours, a cross scratch was made in the cell layer along the diameter of the well with a 200- μ l pipette tip (Axygen, Corning, NY, USA), and the cells were grown in fresh culture media. Images from the same view were taken under a microscope at baseline (0 hours), 24 hours and 48 hours after wounding to determine the extent of wound closure. Image-Pro1.49v (National Institutes of Health, Bethesda, MD, USA) was used to measure the void area (VA) and the height and relative width were evaluated ($\text{area}\% = \text{VA}/\text{height}$) in each group.

Western blot

Total proteins were extracted from DPSCs, and SDS polyacrylamide gel electrophoresis was performed as described previously. The primary antibodies used in this study were against GREM1 (cat no. G4672; Sigma Aldrich), YWHAH (cat no. F1804; Sigma Aldrich) and GAPDH (cat. no. G8795, Sigma Aldrich).

Coimmunoprecipitation (Co-IP) assay

DPSCs were lysed with IP lysis buffer (Invitrogen). The cell lysates were incubated with a specific primary antibody and protein A/G Sepharose (Santa Cruz Biotechnology, Dallas, TX, USA) was added overnight at 4°C. After washing, the immunoprecipitated complex was treated with either RNase A or RNase inhibitor (Sigma Aldrich) for 5 minutes at 37°C. The cells were resuspended in SDS-PAGE loading buffer for Western blot analysis using the corresponding antibodies. The primary antibodies used in this study were against GREM1 (cat no. G4672; Sigma Aldrich), YWHAH (cat no. G7633; Sigma Aldrich) and GAPDH (cat. no. G8795, Sigma Aldrich).

Peptide microarray

Polypeptide chip sealing

After the array membrane was activated, sealing solution was added and the membrane was sealed for 4 hours with shaking at room temperature.

Reactive protein labelling

A biotin labelling kit (EZ-LINK™NHS-PEG₄-BIOTIN, PIECE, LOT#tg263646) was used to label the GREM1-isoform1 protein with a biotin reminder. The binding of polypeptide chip was incubated with reactive protein, and the biotin-labelled GREM1-isoform1 protein was diluted with sealing solution and incubated with the array. The experimental group was incubated with 10 ml reaction solution at a concentration of 4 μ g/ml, and the control group chip was incubated with sealing fluid. The membrane was shaken overnight at 4°C, the diaphragm was removed, and the membrane was washed with TBST five times.

Polypeptide chip and HRP-labelled secondary antibody incubation

The membrane was washed with high-sensitivity streptavidin-HRP (Pierce CA#:21130) and diluted with sealing solution. After 1:8,000, the membranes in the experimental group and control group were incubated with 5 ml each, shaken at room temperature for 2 hours, and then washed five times.

Colour development

TotalLab image analysis software (TotalLab, Gosforth, UK) was used to analyse the optical density values of colour rendering points for imaging images. The "Spot Edge Average" algorithm reads the colour rendering values of all peptide segments and sets the colour point light on the film. The highest density value is 100%, with reference to the surrounding background values of each colour developing point, and the optical density values of other points are calculated as the percentage values of the optical density values of the point. The possible binding sites and fragment sequences of GREM1 and YWHAH were obtained through bioinformatics comparative analysis.

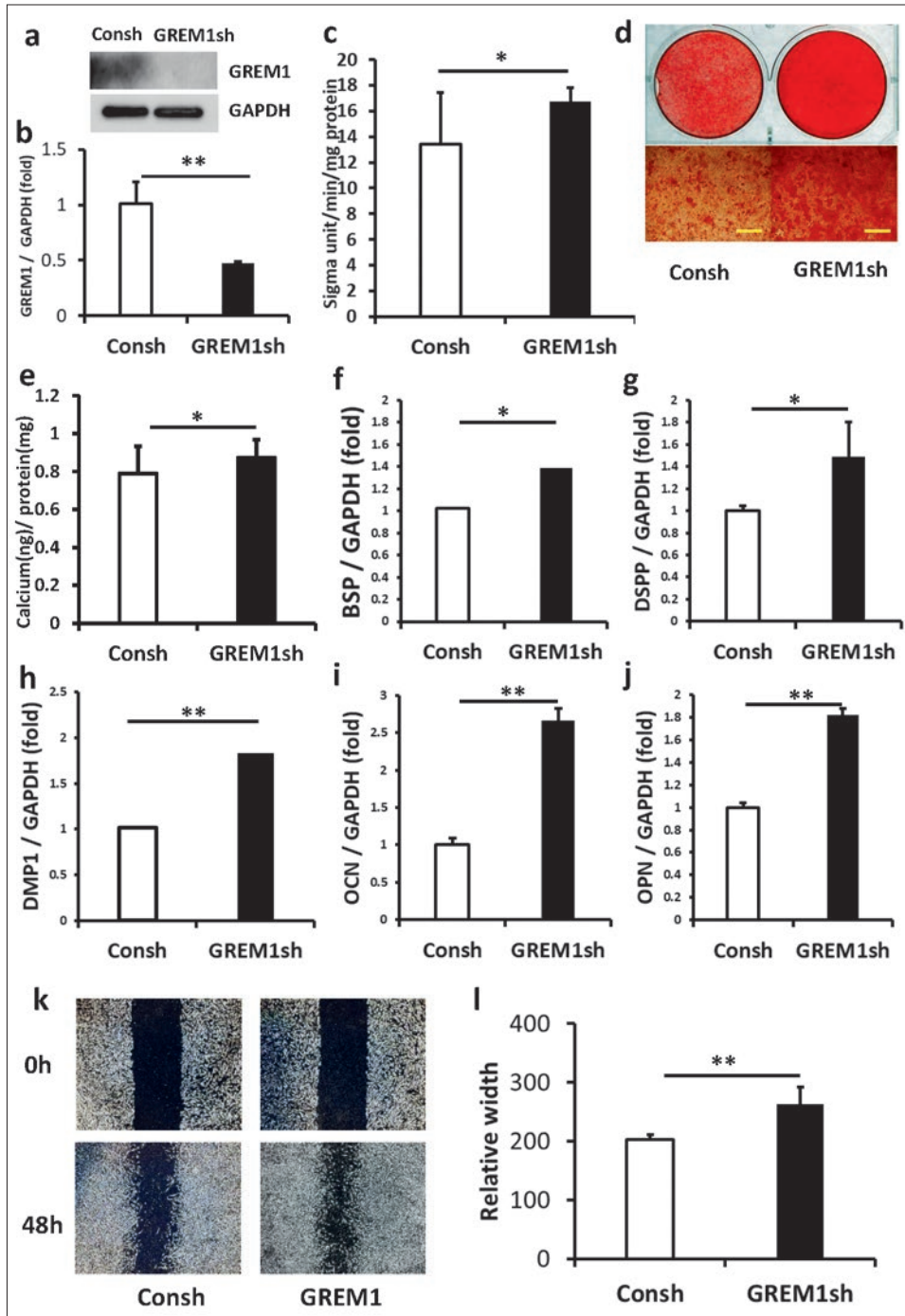


Fig 1a to l Knockdown of GREM1 promoted the osteo/dentinogenic differentiation of DPSCs in vitro. Western blot analysis of GREM1 expression (a). Real-time RT-PCR showed the knockdown efficiency of GREM1 in DPSCs (b). ALP activity assay (c). Alizarin red staining (d). Quantitative calcium analysis (e). The expression of DSPG (f), DMP1 (g), BSP (h), OPN (i) and OCN (j) was detected by real-time RT-PCR at 14 days after induction. The results of the scratch-simulated wound migration assay (k and l). GAPDH was used as an internal control. A Student *t* test was performed to determine statistical significance. All error bars represent the standard deviation (n = 6). **P* ≤ 0.05, ***P* ≤ 0.01.

Nude mouse transplantation with haematoxylin-eosin (HE) staining and immunohistochemical staining

A total of 2.0×10^6 DPSCs were mixed with MC (Engineering Research Center for Biomaterials, Tsinghua University, Beijing, China) at 37°C for 2 hours, and then the mixture was subcutaneously transplanted into the

backs of nude mice (10-week-old females, nu/nu). After 8 weeks, the subcutaneous transplanted tissues were collected, fixed with 10% formalin and decalcified in 10% EDTA. The tissues were stained with haematoxylin-eosin (HE). Image-Pro Plus software (Media Cybernetics, Rockville, MD, USA) was used to calculate the area of bone/dentine-like tissue. Immunohistochemical

staining was performed as described previously.¹⁸ The primary antibodies used were DSPP (cat no. bs10316R, Bioss, China) and BSP (cat no. bs2668R, Bioss, China). The present research was carried out in accordance with the animal experiment regulations.

Statistical analysis

Statistical calculations were implemented using SPSS 10.0 statistical software (SPSS, Chicago, IL, USA). Statistical significance was analysed using a Student *t* test; *P* ≤ 0.05 was defined as statistically significant.

Results

Knockdown of GREM1 promoted the osteo/dentogenic differentiation of DPSCs in vitro and in vivo

First, we constructed a short hairpin RNA (shRNA) to inhibit GREM1 expression and introduced it into DPSCs via lentiviral infection. Infected cells were selected with 2 µg/ml puromycin for 3 days, and the efficiency of GREM1 knockdown was confirmed by real-time RT-PCR and western blotting (Fig 1a and b). After the cells were cultured in osteogenic induction medium, we evaluated their osteogenic differentiation potential. After osteogenic induction for 5 days, the ALP activity in GREM1 knockdown DPSCs was greater than that in control DPSCs (Fig 1c). Alizarin red staining and quantitative calcium measurements showed that GREM1 depletion in DPSCs promoted mineralisation compared to that in control DPSCs (Fig 1d and e). The real-time RT-PCR results showed that GREM1 depletion in DPSCs enhanced BSP, DSPP, DMP1, OCN and OPN expression on day 14 after induction (Fig 1f to j). Then, the scratch-simulated wound migration assay results showed that GREM1 knockdown promoted the migration of DPSCs at 48 hours (Fig 1k and l). Finally, control DPSCs and GREM1 knockdown DPSCs were transplanted subcutaneously into nude mice. We discovered that GREM1 knockdown DPSCs formed more bone/dentine-like tissues (Fig 2a and b). Moreover, immunohistochemical staining and quantitative analysis revealed that DSPP and BSP expression were greater in GREM1 knockdown DPSCs than in control DPSCs (Fig 2c to f).

GREM1/YWHAH can regulate BMP2, BMP6 and BMP7 expression

We used real-time RT-PCR to detect BMP expression. The results showed that GREM1 depletion in DPSCs

enhanced BMP2, BMP6 and BMP7 expression (Fig 3a to c). Knocking down YWHAH in DPSCs suppressed the expression of BMP2, BMP6 and BMP7 (Fig 3d to f). Overexpression of YWHAH promoted the expression of BMP2, BMP6 and BMP7 (Fig 3g to i).

GREM1 can bind to YWHAH in DPSCs

We examined the association of GREM1 with YWHAH in DPSCs. Co-IP showed that the formation of GREM1-YWHAH protein complexes increased with HA-GREM1 overexpression in DPSCs (Fig 4a). In addition, depletion of GREM1 decreased the formation of GREM1-YWHAH protein complexes in DPSCs (Fig 4b). Co-IP results showed that the overexpression of YWHAH promoted the association of GREM1 and YWHAH in DPSCs (Fig 4c), and knocking down of YWHAH in DPSCs suppressed this association (Fig 4d). Furthermore, polypeptide microarray results showed that the polypeptide array derived from the YWHAH protein sequence can bind to the reactive protein GREM1-isoform1 protein, and the protein binding polypeptide points 29, 46 and 47 have obvious colour rendering effects (Fig 4e). Taken together, these results indicate that GREM1 binds to YWHAH. The effective binding sites were- L R D N L T L W T S D Q Q D E and -T L W T S D Q Q D E E A G E G.

Knockdown of YWHAH suppressed the osteo-/dentogenesis of DPSCs in vitro

To verify the role of YWHAH in DPSCs osteo/dentogenic differentiation, we constructed a short hairpin RNA (shRNA) to inhibit YWHAH expression and introduced it into DPSCs via lentiviral infection. Infected cells were selected with 2 µg/ml puromycin for 3 days, and the efficiency of YWHAH knockdown was confirmed by real-time RT-PCR and western blotting (Fig 5a and b). After osteogenic induction for 5 days, the ALP activity decreased in YWHAH knockdown DPSCs compared to control DPSCs (Fig 5c). Alizarin red staining and quantitative calcium measurements showed that YWHAH depletion in DPSCs suppressed mineralisation compared to that in control DPSCs (Fig 5d and e). The real-time RT-PCR results revealed that YWHAH depletion in DPSCs inhibited BSP, DSPP and DMP1 expression on day 14 after induction. There were no statistical differences in OCN and OPN (Fig 5f to j). Then, the scratch-simulated wound migration assay results showed that YWHAH knockdown repressed the migration ability of DPSCs at 48 hours (Fig 5k and l).

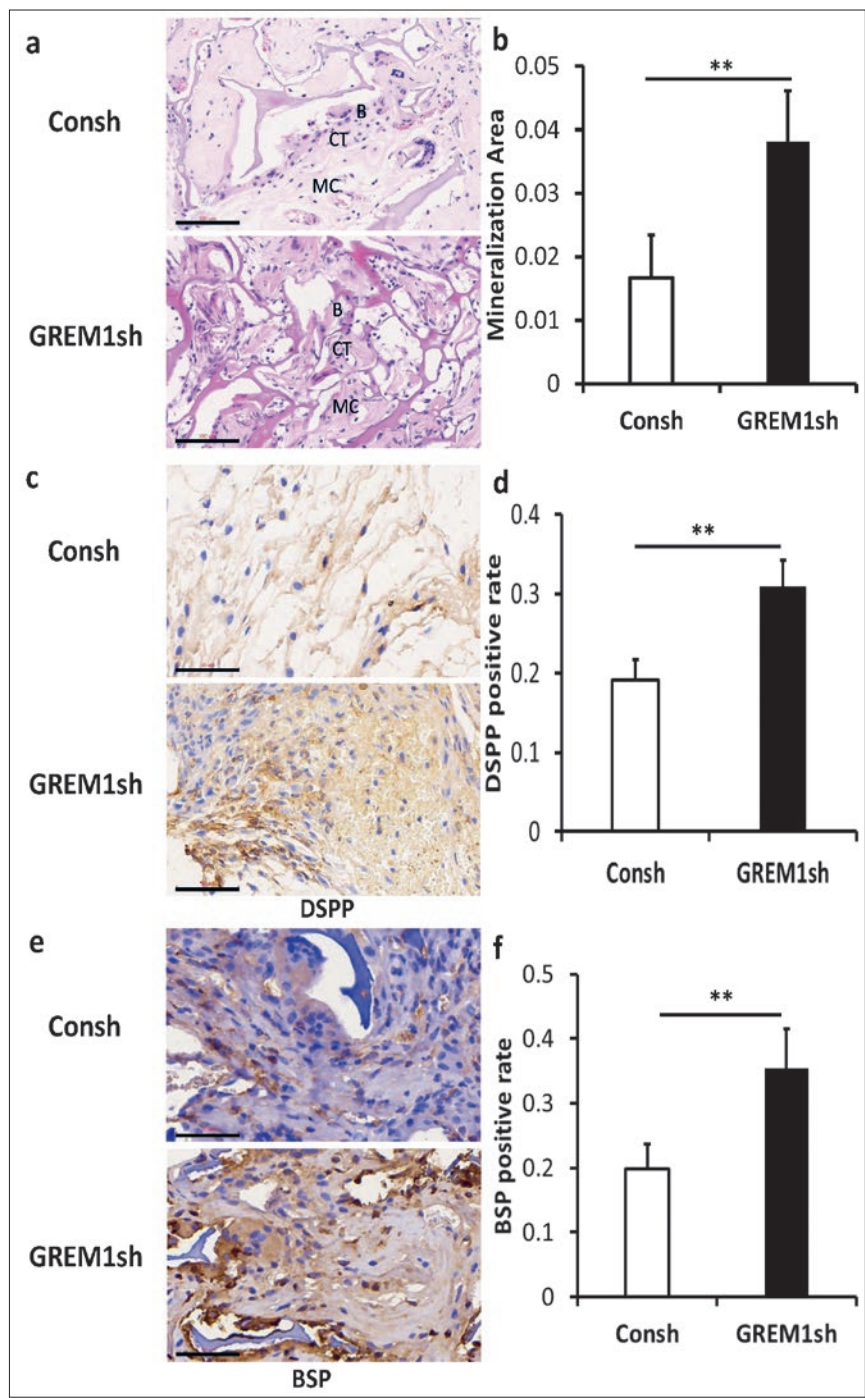


Fig 2a to f Knockdown of GREM1 promoted the osteo/dentinogenic differentiation of DPSCs in vivo. HE staining results showing bone/dentine-like tissue formation. Scale bar 100 μ m. B, bone/dentine-like tissues; CT, connective tissue; MC, mineral collagen (a). Quantitative measurement of the HE staining results (b). Immunohistochemical staining and quantitative analysis of DSPP (c and d). Immunohistochemical staining and quantitative analysis of BSP. Scale bar 50 μ m (e and f). A Student t test was performed to determine statistical significance. All error bars represent the standard deviation (n = 6). *P \leq 0.05, **P \leq 0.01.

Overexpression of YWHAH promoted the osteo/dentinogenesis of DPSCs in vitro and in vivo

The function of YWHAH in DPSCs was investigated by inserting the YWHAH sequence into a retroviral vector. Retroviral infected DPSCs were selected with 600 μ g/ml G418 for 7 days, and western blot and real-time RT-PCR results confirmed the ectopic expression of YWHAH

(Fig 6a and b). After osteogenic induction for 5 days, ALP activity increased in YWHAH overexpressing DPSCs compared to control DPSCs (Fig 6c). Alizarin red staining and quantitative calcium measurements revealed that compared with control DPSCs, YWHAH-overexpressing DPSCs promoted mineralisation (Fig 6d and e). The real-time RT-PCR results showed that YWHAH-overexpressing DPSCs exhibited increased BSP, DSPP, DMP1, OCN

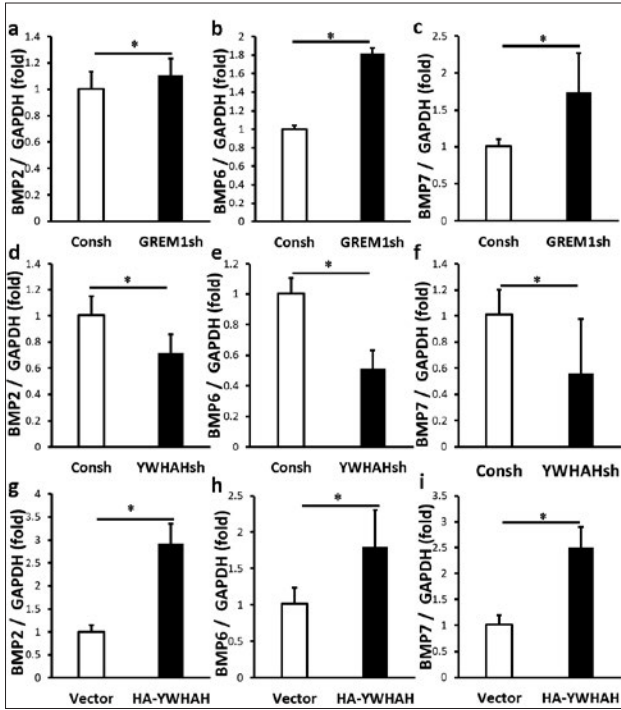


Fig 3a to i GREM1/YWHAH can regulate BMP2, BMP6 and BMP7 expression. The expression of BMP2 (a), BMP6 (b) and BMP7 (c) was detected by real-time RT-PCR after knocking down GREM1 in DPSCs. The expression of BMP2 (d), BMP6 (e) and BMP7 (f) was detected by real-time RT-PCR after YWHAH was knocked down in DPSCs. The expression of BMP2 (g), BMP6 (h) and BMP7 (i) was detected by real-time RT-PCR after YWHAH was overexpressed in DPSCs.

and OPN expression on day 14 after induction (Fig 6f to j). The results of the scratch-simulated wound migration showed that YWHAH knockdown promoted the migration ability of DPSCs at 48 hours (Fig 6k and l). Finally, control DPSCs and YWHAH-overexpressing DPSCs were transplanted subcutaneously into nude mice. The present authors discovered that YWHAH-overexpressing DPSCs formed more bone/dentine-like tissues (Fig 7a and b). Moreover, immunohistochemical staining and quantitative analysis revealed that DSPP and BSP expression were greater in YWHAH-overexpressing DPSCs than in control DPSCs (Fig 7c to f).

Discussion

In tooth tissue engineering, using appropriate stem cells and scaffold materials, the present authors aimed to identify key target genes that affect the function of stem cells in the microenvironment, and apply genes to modify stem cells to improve their differentiation ability and enhance their performance, further improving the success rate of biological tooth root regeneration

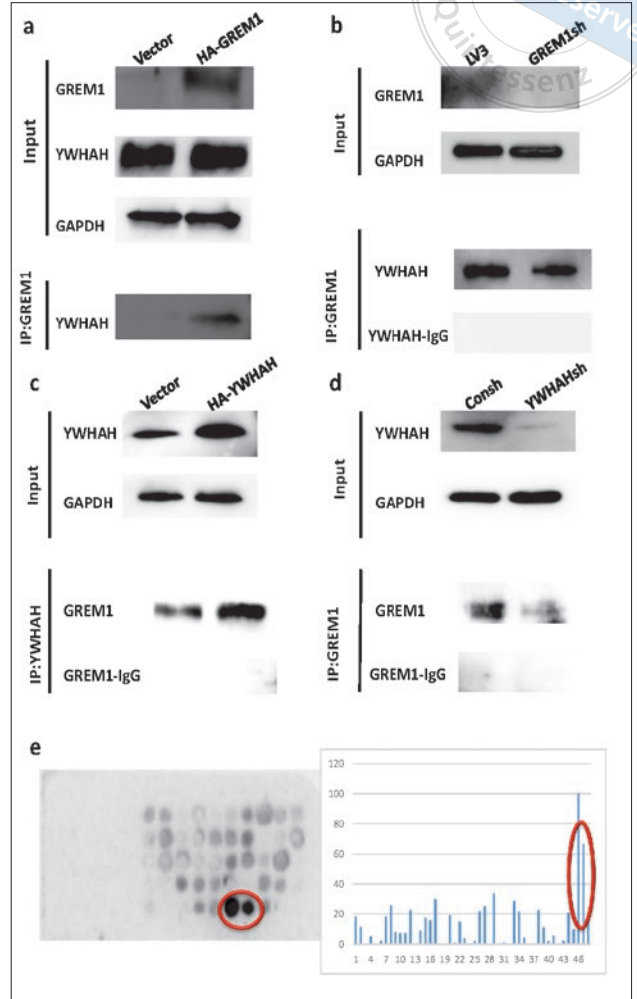


Fig 4a to e GREM1 binds to YWHAH in DPSCs. Western blot showing individual signals (input, 1% lysate) and coimmunoprecipitated protein complexes (IP, 99% lysate). Co-IP results showing more GREM1-YWHAH complexes in GREM1 overexpressing DPSCs (a). Co-IP results showing fewer GREM1-YWHAH complexes in GREM1 silenced DPSCs (b). Co-IP results showing more GREM1-YWHAH complexes in YWHAH overexpressing DPSCs (c). Co-IP results showing fewer GREM1-YWHAH complexes in YWHAH silenced DPSCs (d). There were binding sites in the polypeptide array experimental group. The grey value analysis software Total Lab TL100 showed that protein binding polypeptide points 29, 46 and 47 have obvious colour rendering effects (e). GAPDH was used as an internal control.

and shortening the regeneration cycle. GREM1, a member of the BMP antagonist family, plays an important role in regulating organogenesis, body patterning and tissue differentiation. Like other extracellular BMP antagonists, GREM1 contains a cysteine knot.¹⁹⁻²¹ The role of GREM1 as a BMP antagonist has been identified in the kidney, limb development and lung branching morphogenesis.²²⁻²⁴ A previous study conducted by the present authors found that GREM1 inhibited ADSC

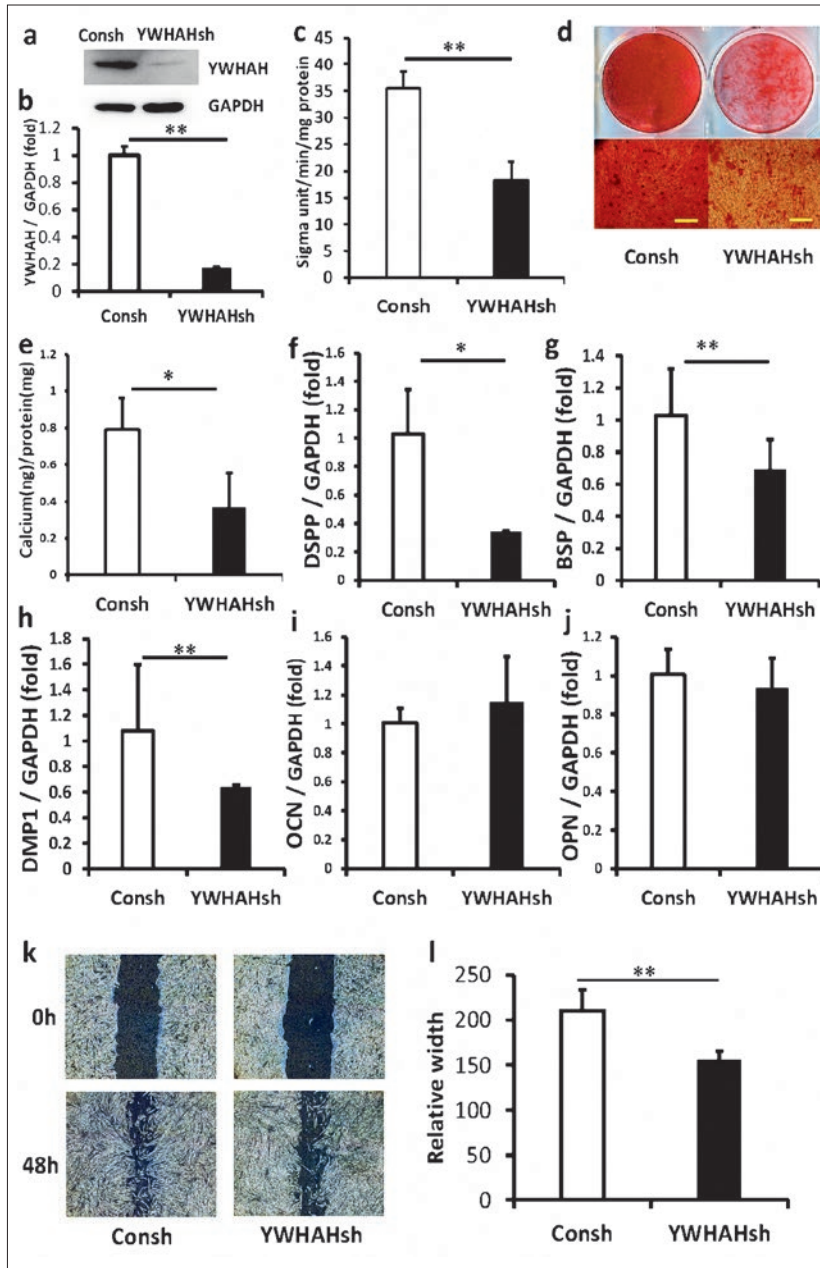


Fig 5a to l Knockdown of YWHAH suppressed the osteo-/dentinogenic differentiation of DPSCs in vitro. Western blot showing YWHAH expression (a). Real-time RT-PCR showed the knockdown efficiency of YWHAH in DPSCs (b). ALP activity assay (c). Alizarin red staining (d). Quantitative calcium analysis (e). The expression of DSPP (f), DMP1 (g) and BSP (h), OPN (i) and OCN (j) was detected by real-time RT-PCR at 14 days after induction. The results of the scratch-simulated wound migration assay (k and l). GAPDH was used as an internal control. A Student t test was performed to determine statistical significance. All error bars represent the standard deviation (n = 6). * $P \leq 0.05$, ** $P \leq 0.01$.

senescence and osteogenic differentiation potential and repressed BMP transcription. The present results provide new insights into the regulation of MSC functions and target the use of MSCs for bone regeneration. Thus, the authors conducted experiments to investigate the role of GREM1 in the osteo-/dentinogenic differentiation and migration of DPSCs in vitro and in vivo. First, alkaline phosphatase (ALP) activity, alizarin red staining and scratch migration assays showed that knockdown of GREM1 promoted osteo-/dentinogenic differentiation and migration of DPSCs in vitro. Our group has

previously conducted in-depth studies on the ability of GREM1 knockdown to promote the osteogenic differentiation of MSCs, and the ability of GREM1 overexpression to inhibit their osteogenic differentiation; however, to date, no experiments have confirmed the regulatory effect of GREM1 on the osteogenic differentiation of DPSCs in vivo. Therefore, we conducted subcutaneous implantation experiments in nude mice, and HE staining and immunohistochemical staining confirmed that knockdown of GREM1 promoted osteo-/dentinogenic differentiation of DPSCs in vivo. To explore the regula-

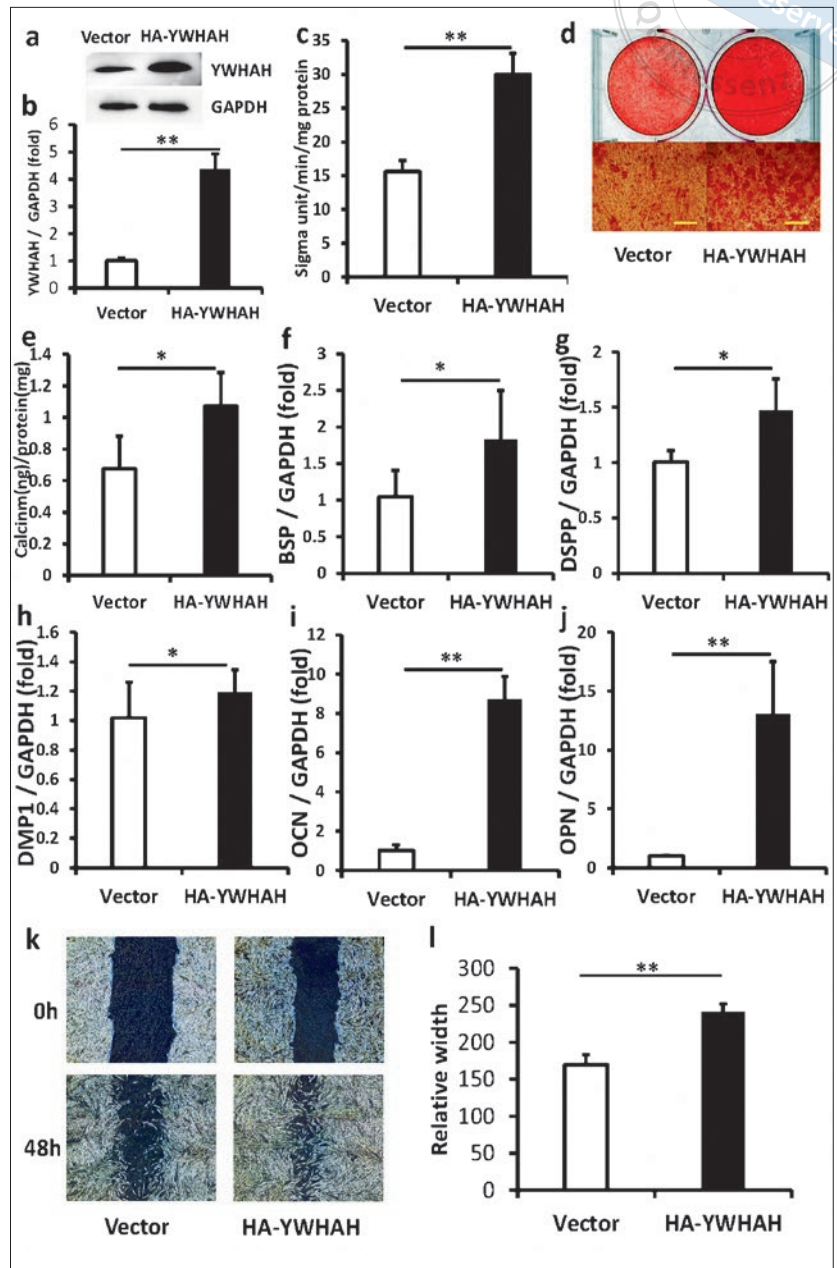


Fig 6a to l Overexpression of YWHAH promoted the osteo-/dentinogenic differentiation of DPSCs in vitro. Western blot showing YWHAH expression (a). Real-time RT-PCR showed the overexpression efficiency of YWHAH in DPSCs (b). ALP activity assay (c). Alizarin red staining (d). Quantitative calcium analysis (e). The expression of DSPP (f), DMP1 (g) and BSP (h), OPN (i) and OCN (j) was detected by real-time RT-PCR at 14 days after induction. The result of scratch-simulated wound migration assay (k and l). GAPDH was used as an internal control. A Student *t* test was performed to determine statistical significance. All error bars represent the standard deviation (*n* = 6). **P* ≤ 0.05, ***P* ≤ 0.01.

tory mechanism of GREM1, we performed a co-IP assay and found that GREM1 can bind to YWHAH in DPSCs. Functional verification revealed that YWHAH knock-down suppressed the osteo-/dentinogenesis of DPSCs in vitro, whereas YWHAH overexpression promoted the osteo-/dentinogenesis of DPSCs in vitro. The product of the YWHAH gene is the 14-3-3 eta protein.²⁵⁻²⁷ The 14-3-3 proteins are a family of conserved regulatory molecules expressed in all eukaryotic cells. A striking feature of these proteins is their ability to bind a multitude of functionally diverse signaling proteins, including kinases,

phosphatases and transmembrane receptors.^{28,29} This plethora of interacting proteins allows 14-3-3 to play important roles in a wide range of vital regulatory processes, such as mitogenic signal transduction, apoptotic cell death and cell cycle control.^{30,31} Acronyms 14-3-3 family proteins interact with many signalling molecules, such as MAPK kinase, Raf-1, Wee1, Cdc25, cyclin B1, protein kinase C, IGF-I receptor, insulin receptor substrate 1, Bad and Bcl, and regulate several signal transduction pathways. Additionally, 14-3-3 proteins help two molecules interact or interrupt the association between

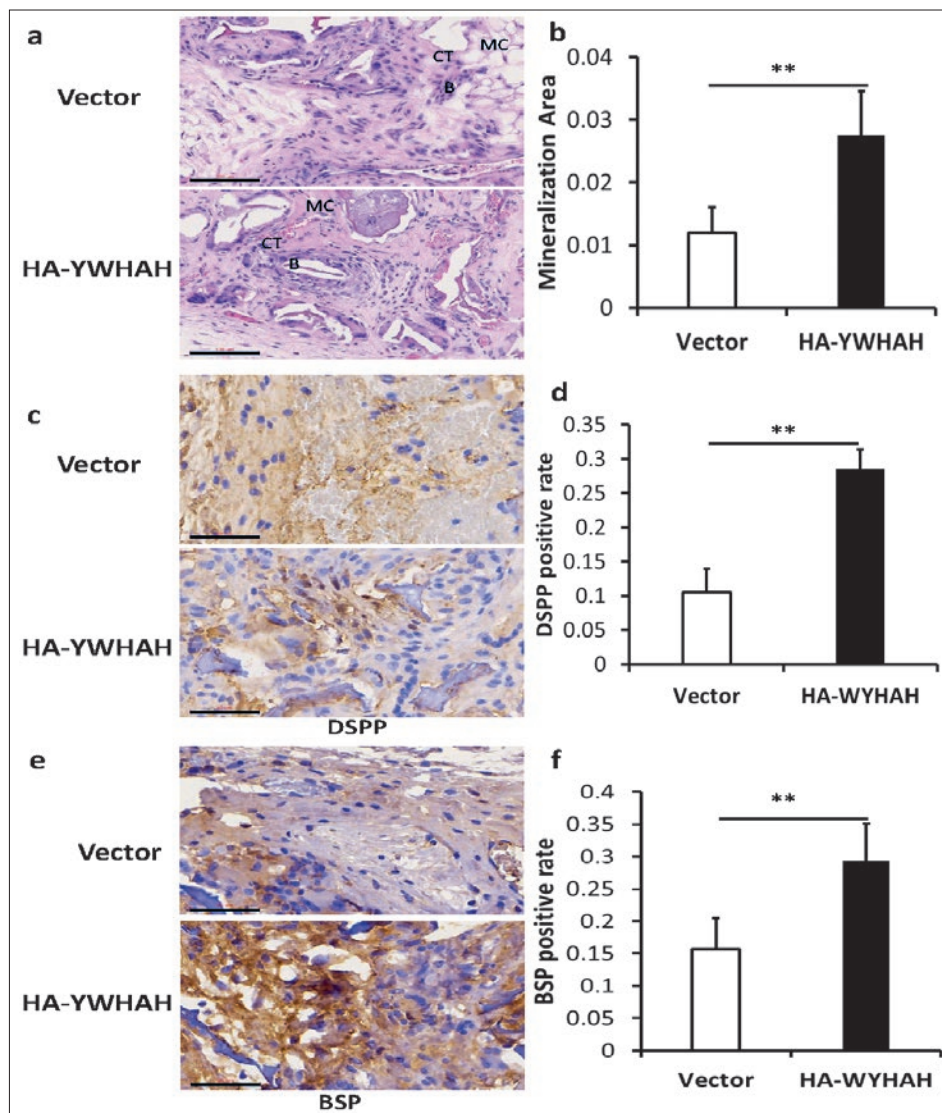


Fig 7a to f Overexpression of YWHAH promoted the osteo/dentinogenic differentiation of DPSCs in vivo. HE staining results showing bone/dentine-like tissue formation. Scale bar 100 μ m. B, bone/dentine-like tissues; CT, connective tissue; MC, mineral collagen (a). Quantitative measurement of the HE staining results (b). Immunohistochemical staining and quantitative analysis of DSPP (c and d). Immunohistochemical staining and quantitative analysis of BSP. Scale bar: 50 μ m (e and f). A Student *t* test was performed to determine statistical significance. All error bars represent the standard deviation (n = 6). **P* \leq 0.05, ***P* \leq 0.01.

them by functioning as molecular scaffolds.³² However, the effect of YWHAH on osteogenic differentiation of dental stem cells is still unclear, and the present study demonstrated for the first time the ability of YWHAH to promote the differentiation of dental pulp stem cells. Through the above experiments, we suggest that YWHAH might be an important downstream gene of GREM1 that regulates BMP expression and stem cell function. In the future, we will conduct further research on the GREM1-YWHAH complex interaction and the effect of small molecule polypeptides on the differentiation of DPSCs to lay a foundation for the application of small molecule preparations in root regeneration and clinical practice.

Conclusion

In conclusion, the present findings highlight the key role played by GREM1 in osteo/dentinogenic differentiation of DPSCs, which may be a potential target gene for promoting MSC osteo/dentinogenic differentiation and tissue regeneration.

Conflicts of interest

The authors declare no conflicts of interest related to this study.

Author contribution

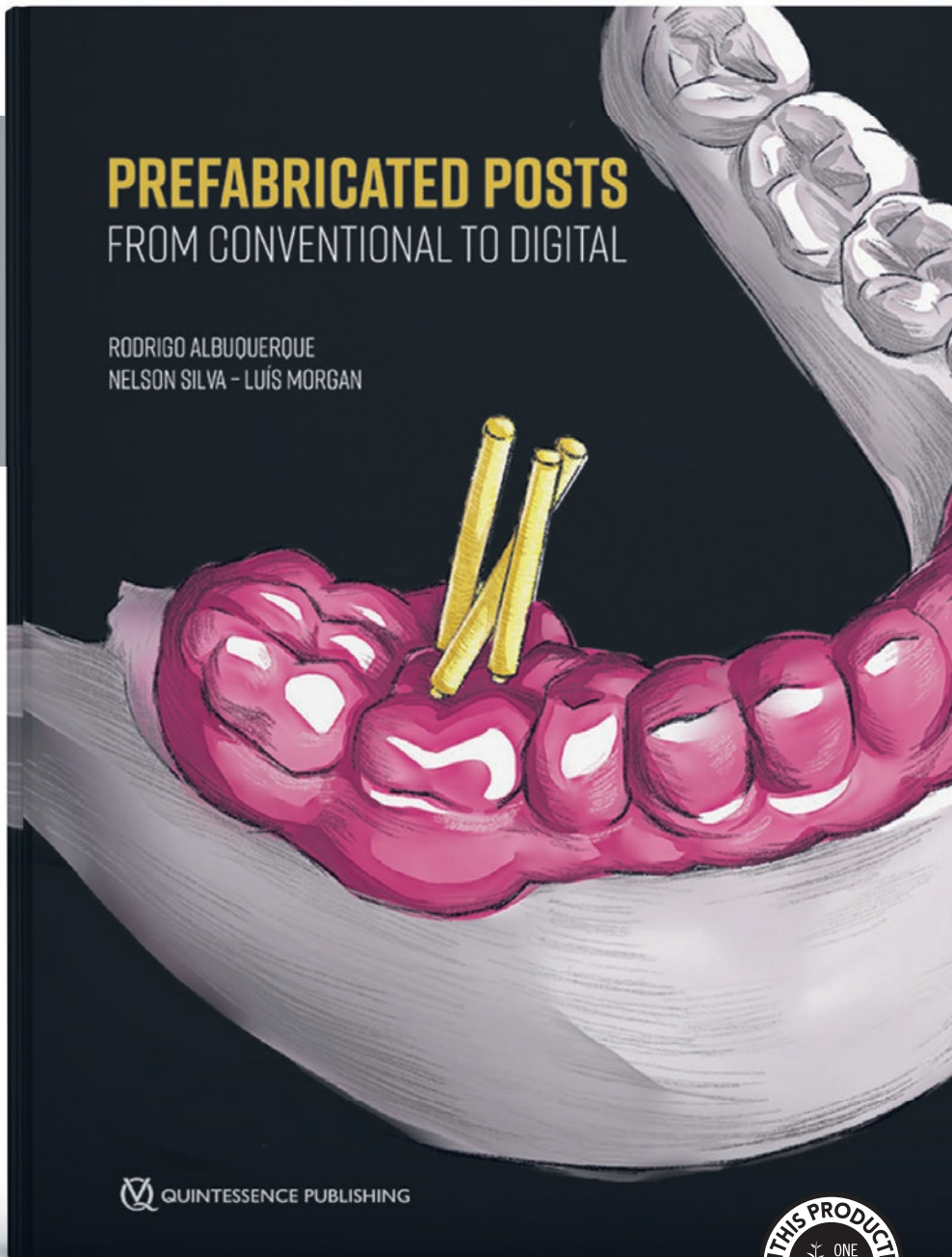
Drs Shu DIAO, Xiao HAN, Wei Long YE, Chen ZHANG and Dong Mei YANG contributed to the material preparation, data collection and analysis; Dr Shu DIAO drafted the manuscript and all authors contributed comments; Profs Zhi Peng FAN and Song Ling WANG contributed to the study conception and design. All authors read and approved the final manuscript.

(Received Nov 18, 2023, accepted April 08, 2024)

References

- Liu Y, Zheng Y, Ding G, et al. Periodontal ligament stem cell-mediated treatment for periodontitis in miniature swine. *Stem Cells* 2008;26:1065–1073.
- Ding G, Liu Y, Wang W, et al. Allogeneic periodontal ligament stem cell therapy for periodontitis in swine. *Stem Cells* 2010;28:1829–1838.
- Li D, Wang X, Yao L, et al. Sox2 controls asymmetric patterning of ameloblast lineage commitment by regulation of FGF signaling in the mouse incisor. *J Mol Histol* 2021;52:1035–1042.
- Nireeksha, Varma SR, Damdoum M, et al. Immunomodulatory Expression of Cathelicidins Peptides in Pulp Inflammation and Regeneration: An Update. *Curr Issues Mol Biol* 2021;43:116–126.
- Cho YD, Kim KH, Lee YM, Ku Y, Seol YJ. Dental-derived cells for regenerative medicine: stem cells, cell reprogramming, and transdifferentiation. *J Periodontal Implant Sci* 2022;52:437–454.
- Diao S, Lin X, Wang L, et al. Analysis of gene expression profiles of apical papilla tissues, stem cells from apical papilla and cell sheet. *Cell Prolif* 2017;50:e12337.
- Diao S, Yang H, Cao Y, Yang D, Fan Z. IGF2 enhanced the osteo-/dentinogenic and neurogenic differentiation potentials of stem cells from apical papilla. *J Oral Rehabil* 2020;47(suppl 1):55–65.
- Canalis E, Parker K, Zanotti S. Gremlin1 is required for skeletal development and postnatal skeletal homeostasis. *J Cell Physiol* 2012;227:269–277.
- Lovely AM, Duerr TJ, Qiu Q, Galvan S, Voss SR, Monaghan JR. Wnt Signaling Coordinates the Expression of Limb Patterning Genes During Axolotl Forelimb Development and Regeneration. *Front Cell Dev Biol* 2022;10:814250.
- Church RH, Krishnakumar A, Urbanek A, et al. Gremlin1 preferentially binds to bone morphogenetic protein-2 (BMP-2) and BMP-4 over BMP-7. *Biochem J* 2015;466:55–68.
- Liu H, Han X, Yang H, et al. GREM1 inhibits osteogenic differentiation, senescence and BMP transcription of adipose-derived stem cells. *Connect Tissue Res* 2021;62:325–336.
- Namkoong H, Shin SM, Kim HK, et al. The bone morphogenetic protein antagonist gremlin 1 is overexpressed in human cancers and interacts with YWHAH protein. *BMC Cancer* 2006;6:74.
- Hein MY, Hubner NC, Poser I, et al. A human interactome in three quantitative dimensions organized by stoichiometries and abundances. *Cell* 2015;163:712–723.
- Liu Z, Hayashi H, Matsumura K, et al. Hyperglycaemia induces metabolic reprogramming into a glycolytic phenotype and promotes epithelial-mesenchymal transitions via YAP/TAZ-Hedgehog signalling axis in pancreatic cancer. *Br J Cancer* 2023;128:844–856.
- Uemura M, Nagasawa A, Terai K. Yap/Taz transcriptional activity in endothelial cells promotes intramembranous ossification via the BMP pathway. *Sci Rep* 2016;6:27473.
- Wang H, Yu H, Huang T, Wang B, Xiang L. Hippo-YAP/TAZ signaling in osteogenesis and macrophage polarization: Therapeutic implications in bone defect repair. *Genes Dis* 2023;10:2528–2539.
- Pan H, Xie Y, Zhang Z, et al. YAP-mediated mechanotransduction regulates osteogenic and adipogenic differentiation of BMSCs on hierarchical structure. *Colloids Surf B Biointerfaces* 2017;152:344–353.
- Yang H, Cao Y, Zhang J, et al. DLX5 and HOXC8 enhance the chondrogenic differentiation potential of stem cells from apical papilla via LINC01013. *Stem Cell Res Ther* 2020;11:271.
- Gu Q, Luo Y, Chen C, Jiang D, Huang Q, Wang X. GREM1 overexpression inhibits proliferation, migration and angiogenesis of osteosarcoma. *Exp Cell Res* 2019;384:111619.
- Guan Y, Cheng W, Zou C, Wang T, Cao Z. Gremlin1 promotes carcinogenesis of glioma in vitro. *Clin Exp Pharmacol Physiol* 2017;44:244–256.
- Pérez-Lozano ML, Sudre L, van Eegher S, et al. Gremlin-1 and BMP-4 Overexpressed in Osteoarthritis Drive an Osteochondral-Remodeling Program in Osteoblasts and Hypertrophic Chondrocytes. *Int J Mol Sci* 2022;23:2084.
- O'Reilly S. Gremlin: a complex molecule regulating wound healing and fibrosis. *Cell Mol Life Sci* 2021;78:7917–7923.
- Jang BG, Kim HS, Chang WY, et al. Prognostic significance of stromal GREM1 expression in colorectal cancer. *Hum Pathol* 2017;62:56–65.
- Kim HS, Shin MS, Cheon MS, et al. GREM1 is expressed in the cancer-associated myofibroblasts of basal cell carcinomas. *PLoS One* 2017;12:e0174565.
- Navarrete M, Zhou Y. The 14-3-3 Protein Family and Schizophrenia. *Front Mol Neurosci* 2022;15:857495.
- Huang X, Zheng Z, Wu Y, Gao M, Su Z, Huang Y. 14-3-3 Proteins are Potential Regulators of Liquid-Liquid Phase Separation. *Cell Biochem Biophys* 2022;80:277–293.
- Guo M, He M, Zhang Y, et al. Nucleo-cytoplasmic shuttling of 14-3-3 epsilon carrying hnRNP C promotes autophagy. *Cancer Biol Ther* 2023;24:2246203.
- Morrison DK. The 14-3-3 proteins: integrators of diverse signaling cues that impact cell fate and cancer development. *Trends in Cell Biol* 2009;19:16–23.
- Lu YC, Cheng AJ, Lee LY, et al. MiR-520b as a novel molecular target for suppressing stemness phenotype of head-neck cancer by inhibiting CD44. *Sci Rep* 2017;7:2042.
- Haonon O, Rucksaken R, Pinlaor P, et al. Upregulation of 14-3-3 eta in chronic liver fluke infection is a potential diagnostic marker of cholangiocarcinoma. *Proteomics Clin Appl* 2016;10:248–256.
- Ren L, Li Y, Zhao Q, et al. miR-519 regulates the proliferation of breast cancer cells via targeting human antigen R. *Oncol Lett* 2020;19:1567–1576.
- Zhou Y, Liu S, Luo Y, Zhang M, Jiang X, Xiong Y. lncRNA MAPKAPK5-AS1 promotes proliferation and migration of thyroid cancer cell lines by targeting miR-519e-5p/YWHAH. *Eur J Histochem* 2020;64:3177.

PRESERVE HEALTHY TOOTH STRUCTURE



Rodrigo Albuquerque | Nelson Silva
Luís Morgan

Prefabricated Posts

From Conventional to Digital

280 pages, 1,023 illus.

ISBN 978-1-78698-144-8

€138

Restoring endodontically treated teeth is undoubtedly a complex procedure. A sound knowledge of biomechanical and clinical principles, careful planning, and the selection of appropriate materials and restorative techniques is essential to achieve the best functional and esthetic outcomes. This concise and exquisitely illustrated book, based on the philosophy and clinical experience of its authors and on sound scientific evidence, is divided into 10 chapters in a didactic sequence to make it easier for dentists to apply the techniques in everyday practice. The focus is on preserving the healthy tooth structure as much as possible using both conventional and digital methodologies.



www.quint.link/posts



books@quintessenz.de



+49 (0)30 761 80 667

 **QUINTESSENZ PUBLISHING**

PHD2 shRNA-Modified Bone Marrow Mesenchymal Stem Cells Facilitate Periodontal Bone Repair in Response to Inflammatory Condition

Bin Yan LUO^{1,#}, Shu Yu CHENG^{1,#}, Wen Zheng LIAO¹, Bao Chun TAN¹, Di CUI¹, Min WANG¹, Jun QIAN¹, Chang Xing CHEN¹, Fu Hua YAN¹

Objective: To investigate whether bone marrow mesenchymal stem cells (BMMSCs) modulate periodontal bone repair through the hydroxylase domain-containing protein 2 (PHD2)/hypoxia-inducible factor-1 (HIF-1) signalling pathway in response to inflammatory conditions.

Methods: Osteogenic differentiation of PHD2 shRNA-modified BMMSCs and the possible mechanism were explored in an inflammatory microenvironment stimulated by porphyromonas gingivalis lipopolysaccharide (Pg-LPS) in vitro. The effect of PHD2 gene-modified BMMSCs on periodontal bone loss was evaluated with experimental periodontitis.

Results: Pg-LPS stimulation greatly impaired the osteogenic differentiation of BMMSCs, whereas the silence of PHD2 significantly enhanced the osteogenesis of BMMSCs. More importantly, increased level of vascular endothelial growth factor (VEGF) was detected under Pg-LPS stimulation, which was verified to be associated with the augmented osteogenesis. In experimental periodontitis, PHD2-modified BMMSCs transplantation elevated osteogenic parameters and the expression of VEGF in periodontal tissue.

Conclusion: This study highlighted that PHD2 gene silencing could be a feasible approach to combat inflammatory bone loss by rescuing the dysfunction of seed cells.

Keywords: BMMSCs, HIF-1, inflammation, PHD2, VEGF

Chin J Dent Res 2024;27(3):215–224; doi: 10.3290/j.cjdr.b5698385

Periodontitis is an inflammatory and destructive disease in periodontal tissue caused by microbial pathogens.^{1,2} Most treatments for periodontitis have limited regeneration effectiveness due to the unpleasant inflammatory microenvironment.^{3,4} Increasing evidence indicates that bone marrow mesenchymal stem cells (BMMSCs) have major advantages, especially immunomodulatory

properties, in promoting new periodontal tissue.⁵⁻⁷ However, patients with periodontitis suffer from an inflammatory environment that not only reduces the number of local mesenchymal stem cells (MSCs), but also impairs the function of autologous MSCs, hindering tissue regeneration.^{8,9} Hence, it is imperative to improve the function and survival of MSCs in the periodontal microenvironment.¹⁰

The $\alpha\beta$ -heterodimeric transcription factor, hypoxia-inducible factor-1 (HIF-1), has been investigated extensively due to its ability to enhance the self-renewal, proliferation and post-homing differentiation of stem cells.^{11,12} The stability of HIF-1 and the alterations in gene expression caused by hypoxia have a significant impact on the microenvironment of inflammatory tissues and the outcomes of diseases.¹³⁻¹⁶ Vascular endothelial growth factor (VEGF), which is regulated by HIF-1, is one of the earliest known angiogenic factors and functions as a pro-survival factor to safeguard cells damaged by inflammation.¹⁷ The overexpression

1 Nanjing Stomatological Hospital, Affiliated Hospital of Medical School, Institute of Stomatology, Nanjing University, Nanjing, P.R. China.

These two authors contributed equally to this work.

Corresponding authors: Dr Chang Xing CHEN and Dr Fu Hua YAN, Nanjing Stomatological Hospital, Affiliated Hospital of Medical School, Institute of Stomatology, Nanjing University, Nanjing 210008, P.R. China. Tel: 86-25-83620362. Email: ccx88202365@126.com; yanfh@nju.edu.cn

This study was supported by National Natural Science Foundation Project of China (no. 81800973), Jiangsu Provincial Medical Key Discipline Cultivation Unit (JSDW202246) and "3456" Cultivation Program for Junior Talents of Nanjing Stomatological School, Medical School of Nanjing University (0222c112).

of VEGF in human MSCs led to an increase in the deposition of mineralised extracellular matrix and the promotion of tissue mineralisation through an autocrine pathway.¹⁸

In normoxia, prolyl hydroxylases (PHDs) induced proteasomal degradation of HIF-1, with PHD2 being the primary enzyme responsible for downregulating HIF-1 α expression.¹¹ Recently, PHD inhibitors have shown promise in cell-based therapy and bone tissue engineering.¹⁹⁻²¹ The use of lentivirus-based vectors has been found to provide stable expression of genes in transplanted cells. Earlier studies by the present authors' team found that PHD2 gene interference in stem cells induced resistance to oxidative stress and enhanced periodontal tissue repair, suggesting potential applications of the PHD2/HIF-1 signalling pathway in periodontal regeneration.^{22,23} Nonetheless, the regulation of the periodontal inflammatory micro-environment and the subsequent effects on periodontal tissue regeneration of PHD2-silenced BMMSCs in periodontitis treatment are unclear. Thus, the present authors hypothesised that the PHD2/HIF-1 signalling pathway might also modulate the osteogenic process of PHD2-silenced BMMSCs in an inflammatory micro-environment.

Porphyromonas gingivalis lipopolysaccharide (*Pg*-LPS) is known to play a significant role in the pathogenesis of periodontitis, exhibiting high toxicity and antigenicity towards periodontal tissue.²⁴⁻²⁶ In the present study, *Pg*-LPS was utilised to induce an inflammatory micro-environment in vitro, with the aim of investigating whether the osteogenic differentiation of PHD2 gene-modified BMMSCs could be enhanced under such conditions. Furthermore, the potential impact of rat BMMSCs with PHD2 gene modification on periodontal regeneration was assessed in ligature-induced experimental periodontitis models. All experimental procedures described were approved by the Animal Ethics Committee of Nanjing University (IACUC-2003053).

Materials and methods

Cell culture

Primary BMMSCs of Sprague-Dawley (SD) rats were isolated and purified by AllCells (Alameda, CA, USA), and their phenotype was identified. The cells were recovered and cultured in low glucose Dulbecco's modified Eagle medium (DMEM; Gibco, Grand Island, NY, USA) containing 10% foetal bovine serum (FBS; Gibco) and 1% penicillin/streptomycin (HyClone, Logan, UT, USA)

at 37°C in 5% CO₂. The cells were used between passages 2 and 4.

Lentiviral vector infection of BMMSCs

Construction and sequencing of plasmids, packaging and purification of lentiviral vectors were performed by a commercial source (GenePharma, Shanghai, China). The short hairpin RNA (shRNA) interference sequence and the method of lentiviral vector infection of BMMSCs are based on a previous report by the present authors.²³ Third-generation BMMSCs were seeded in 6-well plates at a density of 1 \times 10⁵ cells/well and cultured at 37°C and 5% in an incubator. BMMSCs were divided into three groups: the sh-PHD2 group (lentiviral RNA interference vector), the NC group (negative control of the lentiviral vector) and the CON group (no lentiviral vector). Then, the cells were cultured for 48 hours. The infection and status of BMMSCs were observed by routine optical microscopy and inverted fluorescence microscopy. PHD2 gene silencing of BMMSCs was assayed for HIF-1 α and PHD2 expression by western blot (WB).

Osteogenic differentiation

After PHD2 gene silencing, the growth medium was replaced with osteogenic differentiation medium (α -MEM with 10% FBS, 0.1 μ M dexamethasone, 50 μ g/ml L-ascorbic acid and 10 mM β -glycerophosphate). The osteogenic culture medium was replaced every 3 days.

To stimulate the inflammatory microenvironment in vitro, BMMSCs were treated with *Pg*-LPS (1 μ g/ml)²⁴ for 72 hours. The osteogenic culture medium with *Pg*-LPS was replaced every 3 days. On day 4 of osteogenic induction, the mRNA levels of VEGF were assayed by q-PCR. On day 7 of osteogenic induction, the total protein levels of osteogenesis-related parameters were measured by WB.

RNA preparation and q-PCR

Total RNA was extracted by TRIzol Reagent (Thermo Fisher Scientific, Carlsbad, CA, USA), and cDNA was prepared using the PrimeScript RT Reagent kit (TaKaRa Bio, Otsu, Japan). Amplification and detection of cDNA were performed using a ViiA 7 Real-Time PCR System (Thermo Fisher Scientific) with primers (GenScript, Nanjing China) and Maxima SYBR Green/ROX qPCR Master Mix (Thermo Fisher Scientific). The primers used in the experiments are shown in Table 1. The relative gene expression level was normalised to that of the internal control (GAPDH) based on the 2^{- $\Delta\Delta$ Ct} method.

Table 1 Primer sequences.

Primer name	Forward primer sequence (5'-3')	Reverse primer sequence (5'-3')
GAPDH	TGAAGGGTGGAGCCAAAAG	AGTCTTCTGGGTGGCAGTGAT
VEGF	GGCTCTGAAACCATGAACTTTCT	GCAATAGCTGCGCTGGTAGAC

Enzyme-linked immunosorbent assay (ELISA)

BMMSCs from different groups were cultured with Pg-LPS in osteogenic culture media as previously described. The supernatant of cells was collected on day 4 and centrifuged at 3000 rpm/minute for 10 minutes to remove dead cells and debris. A Quantikine ELISA kit was used to detect the concentration of VEGF (Neobioscience, Shenzhen, China).

WB analysis

Total protein was extracted by RIPA lysis Buffer (Beyotime Institute of Biotechnology, Shanghai, China) and the concentration of protein was determined using a BCA protein Assay Kit (Beyotime Institute of Biotechnology). Proteins of the same quantity were separated by SDS-PAGE (Genscript) and transferred to a PVDF membrane, and the membranes were blocked with 5% bovine albumin (Sigma, Louis, MO, USA). Protein expression levels in different groups were measured with PHD2 (Cell Signaling Technology, Danvers, MA, USA), HIF-1 α (Abcam, USA), ALP (Santa Cruz, CA, USA), Runx 2 (Abcam, USA) and COL-I (Proteintech, Rosemont, IL, USA) primary antibodies, and GAPDH (Bioworld Technology, St Louis Park, MN, USA) expression served as an internal control. Membranes were exposed to an ECL reagent (Vazyme Biotech, Nanjing, China), and antibody binding was visualised using a Tanon 5200 Luminescent Imaging Workstation (Tanon, Shanghai, China).

ALP and alizarin red S (ARS) staining

BMMSCs were cultured and treated as described in previous steps at a density of 5×10^4 cells/well in 12-well plates. The cells were washed with PBS and then fixed with 4% paraformaldehyde for 30 minutes. ALP staining was performed on day 7 of osteogenic differentiation, then the plates were stained with a BCIP/NBT alkaline phosphatase staining kit (Beyotime Institute of Biotechnology). Mineral deposition was performed on day 14 of osteogenic differentiation. The cells were examined by ARS staining (Sigma-Aldrich, St. Louis, MO, USA) according to the manufacturer's instructions. The unbound dyes were washed with distilled water. All plates were examined using an inverted optical microscope (Olym-

pus IMT-2, Tokyo, Japan), and digital images were saved. The percentage of mineralized nodules and staining areas were calculated using Image J software (National Institutes of Health, Bethesda, MD, USA).

VEGFR inhibitor treatment

After PHD2 gene silencing, the sh-PHD2+LPS group was treated with 1 μ M of the VEGFR inhibitor tivozanib (Selleck Chemicals, Houston, TX, USA) for 30 minutes²⁷; samples without inhibitor treatment served as controls. The inhibitor treatment continued in subsequent osteogenic induction experiments. WB analysis and mineral deposition were measured to assess osteogenic differentiation.

Ligation-induced experimental periodontitis model

Five-week-old female SD rats (weighing approximately 200 g) were maintained under specific pathogen-free conditions. They were randomly divided into four study groups (n = 5): 1) the Lig group, with ligation alone; 2) the MSC+Lig group, with ligation and 100 μ L of transplanted BMMSCs; 3) the NC+Lig group, with ligation and 100 μ L of BMMSCs infected with negative control of lentiviral vector; and 4) the sh-PHD2+Lig group, with ligation and 100 μ L of BMMSCs infected with lentiviral RNA interference vector. Briefly, 4-0 silk ligatures were ligated firmly and subgingivally around the rats' maxillary left second molars. The ligation process was conducted for up to 14 days in the periodontitis model while pathogenic bacteria of periodontitis were enriched in the ligation silk. Then, the BMMSCs with different treatments were dissociated in 0.9% NaCl (1×10^6 cells/ml), and the cell suspensions were injected into the mesial, middle and distal sites of the palatal gingival tissues around the ligatured molar with a 100 μ L microsyringe (Hamilton, Bonaduz, Switzerland). Stem cell treatment was performed every 2 days. After 2 weeks of cell transplantation, all rats were sacrificed, and the left maxillary bones were collected for further experimental analysis.

Microcomputed tomography (microCT) scanning

After being placed in 4% paraformaldehyde fixative solution for 48 hours, the maxillary bones of the SD rats were scanned with a microCT machine (Bruker, Karlsruhe,

Germany). The scanning parameters were based on an acquisition protocol (70 kV, 353 μ A and 18 μ m voxel size). The data were reconstructed and imported into CTVox and CTAn software to obtain 3D model reconstruction and osteogenic parameters.

Histological examination

After fixation with 4% paraformaldehyde, all specimens were placed in 10% EDTA decalcifying solution (EDTA, Servicebio, Wuhan, China) for 2 months at room temperature. Histological sections (5 μ m) were cut buccolingually for haematoxylin and eosin (HE), Masson trichrome and immunohistochemistry staining (all Servicebio). Sections were scanned with Panoramic MIDI (3DHitech, Budapest, Hungary) and examined with CaseViewer software (3DHitech). For VEGF staining, the positive area of each section was identified and quantified with Image J software.

Statistical analysis

All experimental data are presented as mean \pm standard deviation (SD). After normalisation evaluation, the differences were evaluated by one-way ANOVA. A two-tailed $P < 0.05$ was considered statistically significant. The statistical graphs were produced with GraphPad Prism 8 (GraphPad Software, La Jolla, CA, USA).

Results

Effect of PHD2 silencing on osteogenesis of BMMSCs under inflammatory conditions

After lentiviral infection for 72 hours, the MOI 200 group had obviously higher expression of green fluorescence protein than the MOI 100, MOI 150 and MOI 300 groups, and cells grew well in radial shape (Fig 1a). Hence, MOI 200 was chosen for the following experiments. Under normoxic conditions, WB analysis showed that the constructed lentiviral RNA interference vector could successfully silence the PHD2 gene of BMMSCs and activate the downstream HIF-1 α -related pathway (Fig 1b).

Compared with those of the CON group, sh-PHD2 group and NC group, the total protein expression level, ALP staining and ARS staining were decreased in the CON+LPS, sh-PHD2+LPS and NC+LPS groups; however, these osteogenesis-related parameters in the sh-PHD2+LPS group were higher than those in the CON+LPS and NC+LPS groups under *Pg*-LPS stimulation (Fig 1c to e).

The angiogenic factor VEGF associated with the augmented osteogenesis in an inflammatory environment

In the inflammatory microenvironment, the mRNA levels of VEGF and the concentration of VEGF in the supernatant in the sh-PHD2+LPS group were significantly increased (Fig 2a). To explore the role of VEGF in sh-PHD2-promoted osteogenesis in BMMSCs in an inflammatory environment, the VEGFR inhibitor tivozanib was added during osteogenic induction. On day 7 during osteogenic induction, the osteogenesis-related protein expression in the sh-PHD2+LPS group was increased significantly compared with that of the NC+LPS group but decreased after the addition of VEGFR inhibitors (Fig 2b). ARS also showed deeper staining, more mineralised nodules and a larger staining area in the sh-PHD2+LPS group than in the NC+LPS group on day 14 during osteogenic induction, but this effect disappeared with the addition of the VEGFR inhibitor (Fig 2c).

Effects of the PHD2-silenced BMMSCs on bone repair in the SD rats with periodontitis

The present authors applied a well-established model of chronic periodontitis in rats to examine the effect of PHD2 silencing on its onset, which showed extensive periodontal tissue destruction between the first and second molars, including the proliferation of gingival epithelial spikes and the significantly decreased height of alveolar bone (supplementary material, provided on request). Then, BMMSCs with PHD2 gene silencing were implanted into the gingiva of the experimental periodontitis rats by local injection (Fig 3a). The reconstructed images showed apparent bone resorption and furcation involvement of the second molar in the Lig group. The bone resorption in the sh-PHD2+Lig group exhibited a significant reduction in comparison to that of the Lig group and the remaining ligation groups (Fig 3b). The relative bone volume (BV/TV) in the sh-PHD2+Lig group was notably higher than that of the Lig group and the other ligation groups, with no variance observed between the remaining ligation groups and the Lig group. The results indicated that bone mineral density (BMD) was elevated in the sh-PHD2+Lig, MSC+Lig and NC+Lig groups compared with the Lig group. Specifically, the increase in BMD was most pronounced in the sh-PHD2+Lig group, followed by the MSC+Lig group and then the NC+Lig group (Fig 3c).

HE and Masson trichrome staining showed that periodontal tissue damage was significantly reduced in the sh-PHD2+Lig group, which exhibited only a small amount of inflammatory cell infiltration and minor

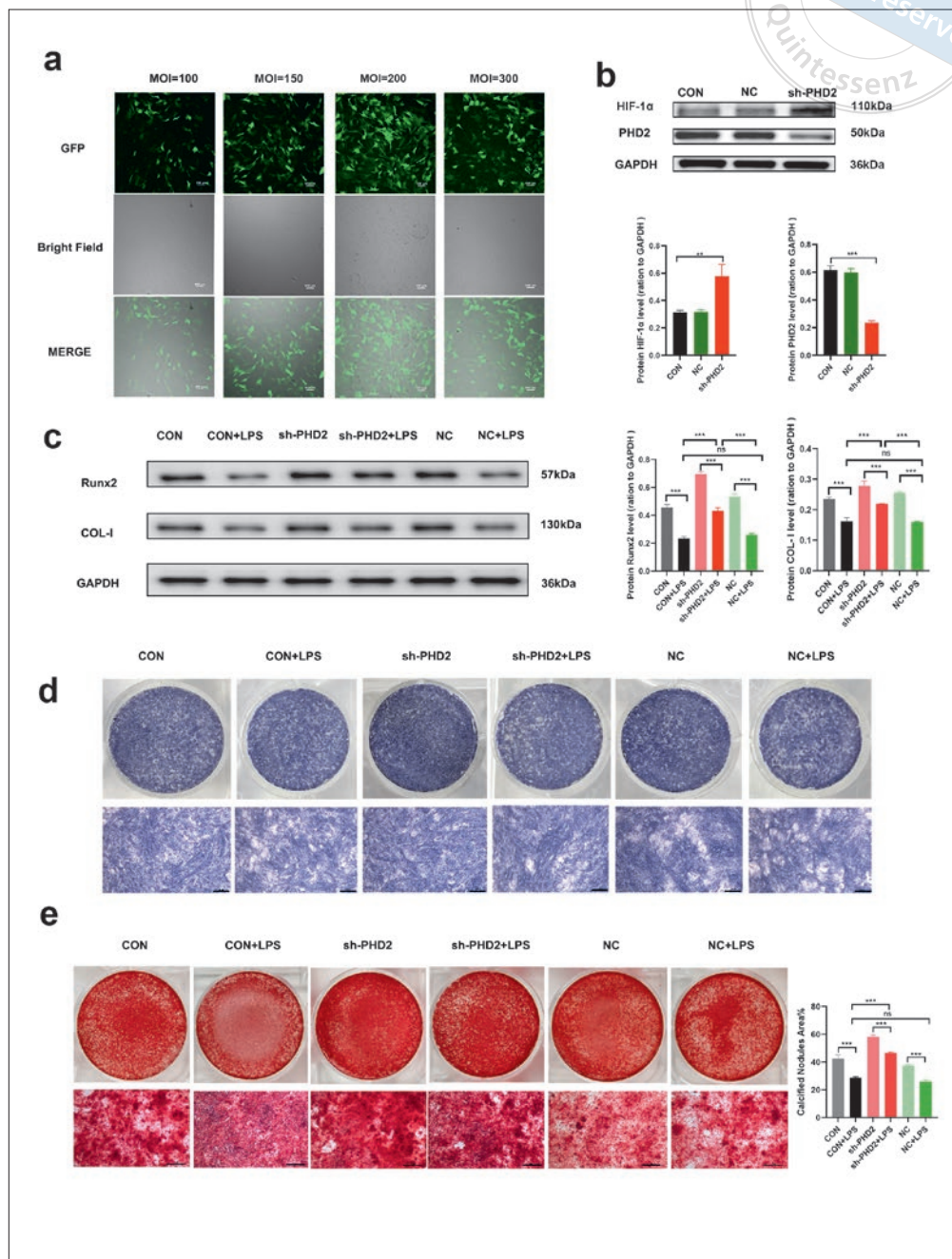


Fig 1a to e PHD2 gene silencing affects the expression of osteogenesis-related parameters in BMMSCs stimulated by *Pg*-LPS. Fluorescence images of BMMSCs transfected with the lentiviral vector at different MOI values ranging from 100 to 300 (scale bar 100 μ m) (a). The protein levels of PHD2 and HIF-1 α after 72 hours of transfection under normoxic conditions (b). On day 7 of osteogenic induction, total protein levels of osteogenesis-related parameters, including COL-1 and Runx 2, in the different groups were determined (c). ALP staining was performed on day 7 (scale bar 200 μ m) (d) and ARS staining was performed on day 14 of osteogenic induction (scale bar 50 μ m) (e). ** $P < 0.01$, *** $P < 0.001$.

changes in the gingival epithelium, periodontal ligament fibres and alveolar bone. In contrast, periodontal damage was more pronounced in the other ligation groups (Fig 4a).

Furthermore, immunohistochemistry indicated that HIF-1 α and VEGF expression in local periodontal tissues changed. The sh-PHD2+Lig group expressed the highest levels of HIF-1 α and VEGF between the first and second molars (Fig 4b and c).

Discussion

BMMSCs are a potential resource for periodontal tissue regeneration due to their multidifferentiation capability, wide spectrum of immunoregulatory effects and ease of expansion.^{6,7} Fair periodontal regeneration in a rat model of periodontitis was observed after local transplantation of allogeneic BMMSCs with tumour necrosis factor- α (TNF- α), interferon-gamma (IFN- γ)

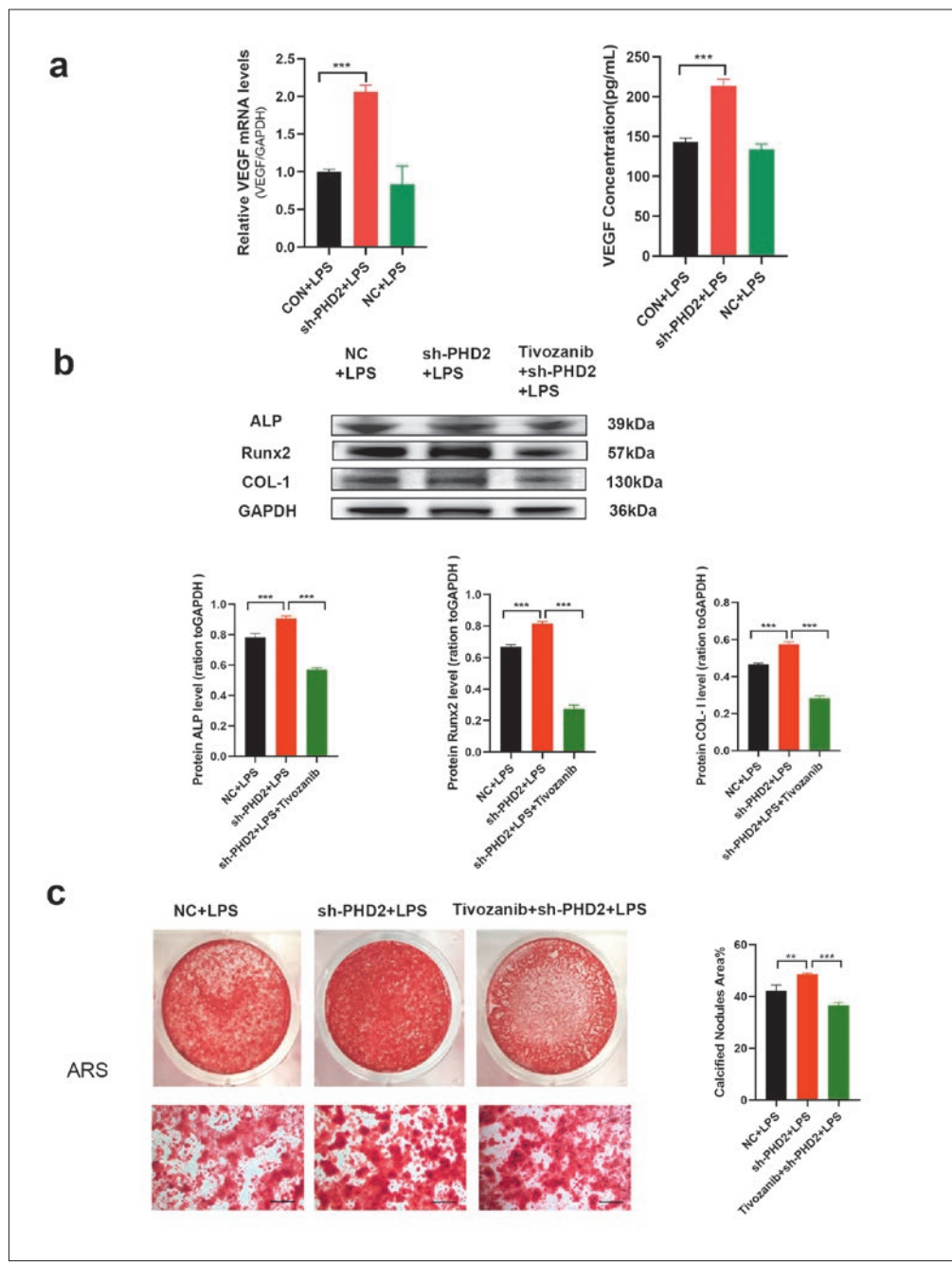


Fig 2a to c Effect of the angiogenic factor VEGF on the osteogenic differentiation potential of PHD2-silenced BMSCs in an inflammatory environment. The mRNA expression levels and secretion of VEGF of different groups: after addition of the VEGF receptor inhibitor (a), the expression of osteogenic proteins was performed on day 7 (b) and ARS staining was performed on day 14 of osteogenic induction (scale bar 50 μm) (c). **P < 0.01, ***P < 0.001.

and interleukin-1beta (IL-1β) expression in periodontal defects.²⁸ However, inflammatory cytokines and mediators released after infection or environmental stress may lead to a decrease in the osteogenic differentiation ability of stem cells.⁹ Pg-LPS is an important pathogenic factor in the occurrence and development of periodontitis.²⁵ Based on the poor osteogenic differentiation and immunomodulatory properties of BMSCs,²⁴ 1 μg/ml Pg-LPS was chosen to create an inflammatory micro-environment in the present study.

Hypoxia is a main component of the cell niche. As a master gene, HIF-1 regulates stem cell features such as multipotency and self-renewal.¹² When PHD activity is suppressed, HIF-1α is stabilised and promotes the transcription of several hypoxia-inducible genes, including VEGF, erythropoietin (EPO) and basic fibroblast growth factor (bFGF).¹¹ As the target gene of HIF-1, VEGF was found to be the most important growth factor coupling angiogenesis and osteogenesis.^{17,18} The vascularisation caused by VEGF can contribute

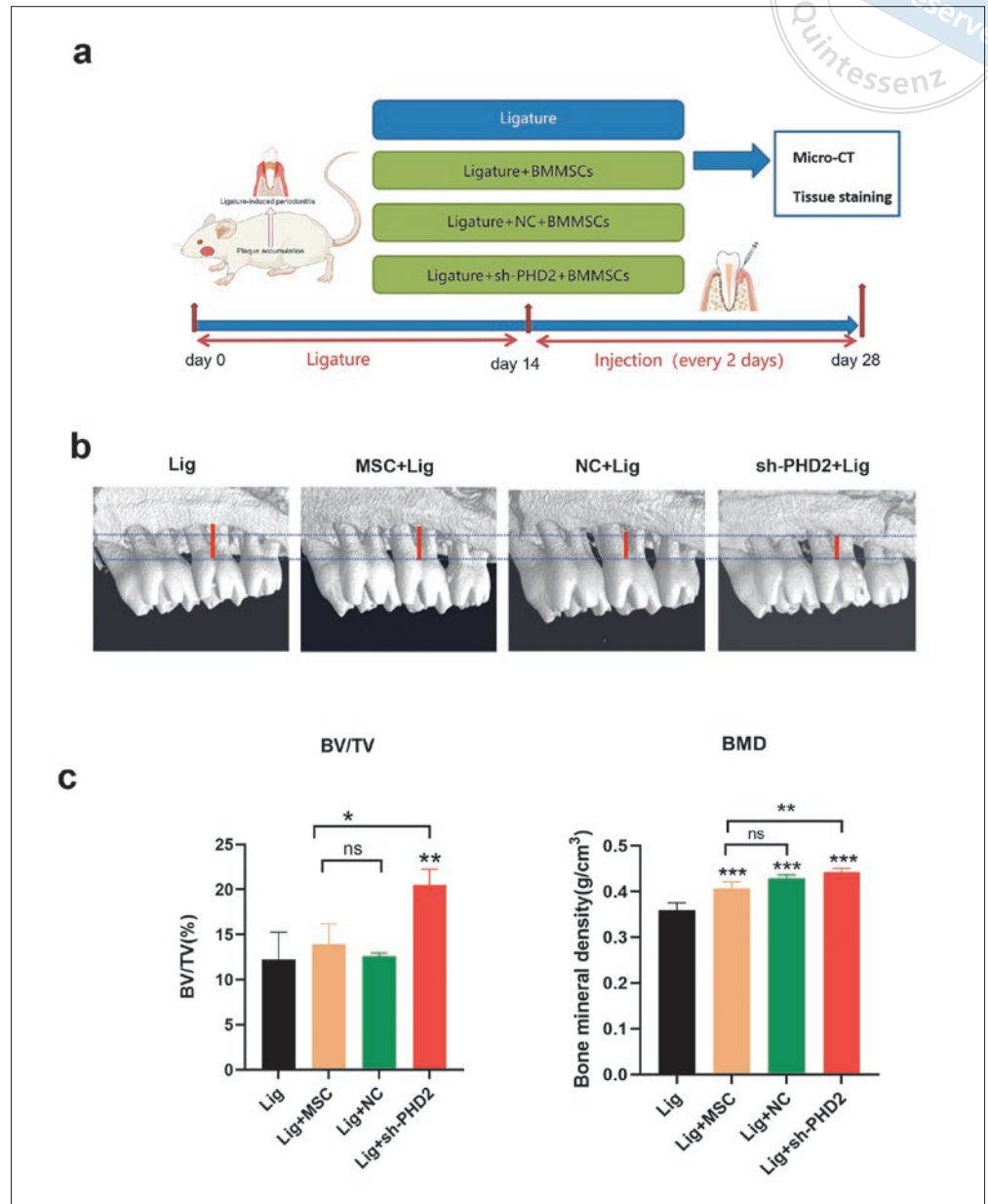


Fig 3a to c Ligature-induced experimental periodontitis and stem cell transplantation. Illustration of the animal experiments. After ligation of the maxillary left second molar in rats to establish the experimental periodontitis model, PHD2-silenced BMMSCs transplantation was performed locally (a). MicroCT reconstruction images showed the alveolar bone loss of the maxillary second molar (red line: the cemento-enamel junction to the alveolar bone crest distance) (b). Parameters to evaluate new bone: BV/TV and BMD (c). * $P < 0.05$, ** $P < 0.01$, *** $P < 0.001$.

to the formation of a neovascularisation network and blood supply for periodontal tissue. More interestingly, osteoblast differentiation is directly affected by VEGF via autocrine and intracrine mechanisms. It was shown that VEGF stimulated osteoblast differentiation through an intracellular mechanism involving the transcription factors Runx 2 and PPARV2, but not through paracrine signalling.²⁹ Subsequent studies reported the effect of VEGF-VEGFR signalling pathways on the recovery from hypoxia-induced tissue damage,³⁰ showing that HIF-1 α has a possible effect on the NF- κ B pathway, thereby connecting natural immunity, inflammation and ischaemia.^{31,32} In the present study, osteogenic

differentiation of BMMSCs in the inflammatory micro-environment was significantly decreased, and was improved after PHD2 gene silencing. Meanwhile VEGF level was increased in BMMSCs after PHD2 silencing, which was confirmed to be associated with enhanced osteogenesis. These results indicate that persistent silencing of the PHD2 gene could enhance the osteogenic differentiation of BMMSCs stimulated by Pg-LPS in vitro. In addition, VEGF plays a crucial role in promoting the osteogenic differentiation of BMMSCs in an inflammatory environment, but further mechanisms of VEGF on stem cells against inflammation remain to be studied.

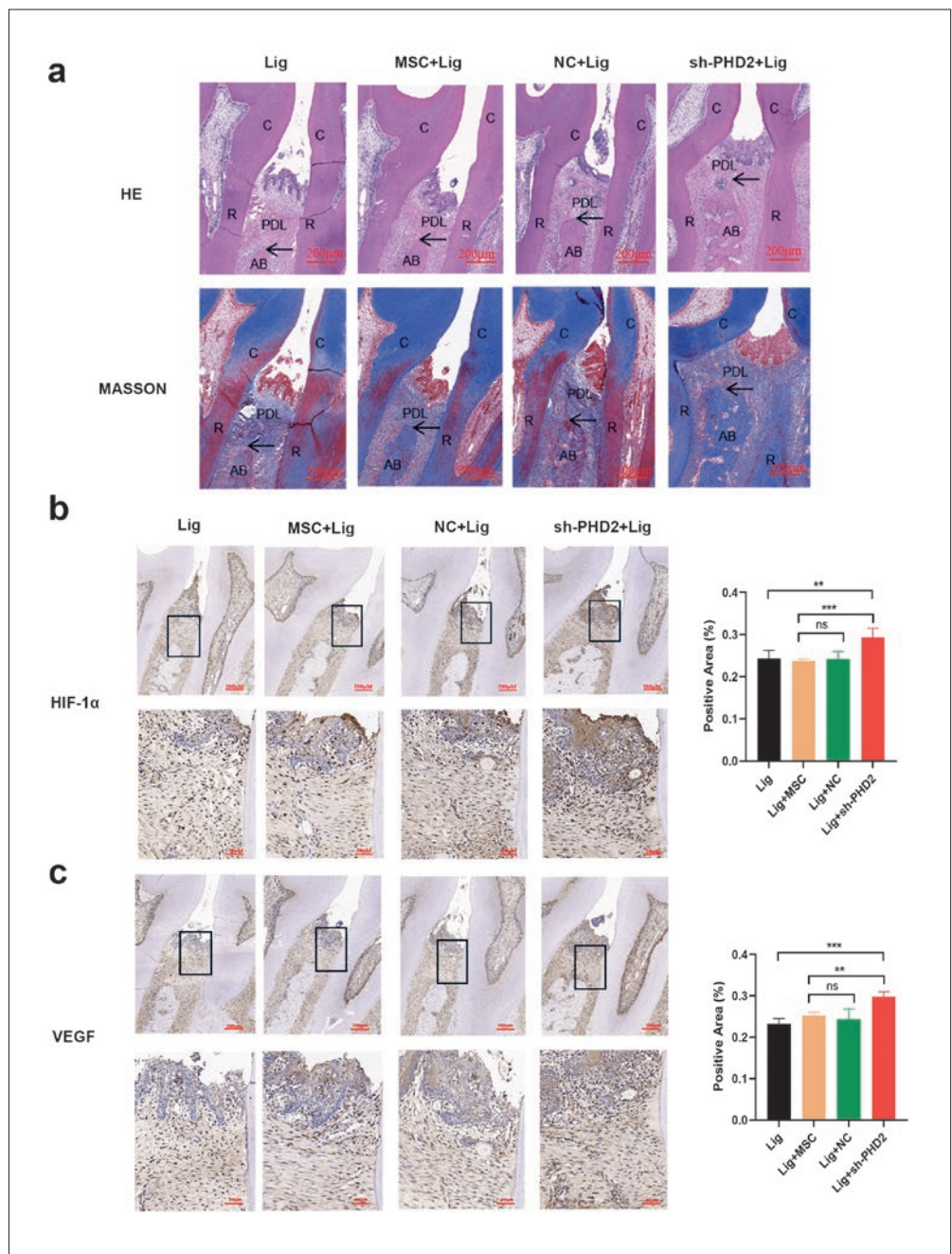


Fig 4a to c Histological observation of the ligatured areas in SD rats. HE and Masson trichrome staining were performed to observe the morphological changes of the periodontal tissues, including gingival tissues, alveolar bone and the periodontal ligament (C, crown; R, root; AB, alveolar bone; PDL, periodontal ligament; black arrow, alveolar ridge crest; scale bar 200 μm) (a). Positive expression of HIF-1α in the different groups and their quantitative analysis (scale bar 200 and 50 μm) (b). Positive expression of VEGF in the different groups and their quantitative analysis (scale bar 200 and 50 μm) (c). ***P* < 0.01, ****P* < 0.001.

Based on previous in vitro results, the present authors further explored the therapeutic effect of PHD2 gene-silenced BMMSCs on periodontal defects in rats. The ligation-induced experimental periodontitis model is a traditional approach to induce periodontitis similar to that in humans caused by microbial plaque accumulation. An experimental periodontitis model established by 2 weeks of silk ligation in rats could simulate periodontal inflammation and bone loss due to microbiome shifts.³³ Cell injection therapy can elim-

inate the adverse effects of degradation scaffolds or complicated manipulation,³⁴ and has been confirmed to effectively promote periodontal tissue regeneration in animal models.^{35,36} With continuous transplantation of the cell suspension for 2 weeks, inflammatory periodontal tissue and bone resorption were significantly reduced, greater BV/TV and BMD values were observed, and higher levels of HIF-1α and VEGF in periodontal tissue were found in the sh-PHD2+Lig group. For BMD, the difference between the sh-PHD2+Lig group and

the NC+Lig group was not significant, probably due to the limited experimental time or the limited effect of PHD2 silencing on the mineralisation degree of the new alveolar bone during inflammation, which still needs further exploration. Moreover, the expression of HIF-1 α in periodontal tissues in the sh-PHD2+Lig group was more obvious than that in the Lig group, as well as the other ligation groups. These results suggest that local injection of the PHD2-silenced BMMSCs can promote the expression of HIF-1 α in periodontal inflammatory tissues in rats. Further exploration revealed that downstream VEGF expression in local periodontal tissues changed after HIF-1 activation. Based on the present study, BMMSCs coupled with PHD2 gene silencing have the potential to generate a better outcome for periodontal repair.

To further develop the application of PHD2 gene silencing in BMMSCs, the present authors note the limitations of this study. Local injection of cell suspension could cause cell loss due to the fluidity of the suspension and requires repeated operation to obtain satisfactory results, which is time-consuming and laborious. Recent studies found that cell sheet tissue engineering can be used to harvest cells together with endogenous extracellular matrix and intact cell–cell interactions, avoiding cell loss and retaining the microenvironment of the cells.^{37,38} In addition, periodontal ligament and cementum regeneration, beyond the alveolar bone, are the two vital and challenging parts of periodontitis therapy that should be explored further.

Conclusion

In summary, the present study demonstrates that lentiviral-mediated RNA interference had the potential to upregulate the expression of VEGF and promote the osteogenic differentiation of BMMSCs in an inflammatory environment. Additionally, PHD2-silenced BMMSCs may effectively inhibit periodontal inflammation and bone resorption. Further studies are needed to clarify the mechanism of PHD2-silenced BMMSCs on periodontal regeneration and immune regulation of the periodontal microenvironment. (This manuscript was preprinted on research square URL <https://doi.org/10.21203/rs.3.rs-1291789/v1>.)

Acknowledgements

The authors thank their colleagues, including Yang Heng ZHANG, Ting ZHANG, Ling Jun LI and Dan QIAO, for their generous assistance.

Conflicts of interest

The authors declare no conflicts of interest related to this study.

Author contribution

Drs Bin Yan LUO and Shu Yu CHENG contributed to the conception, design, data acquisition, analysis and interpretation, drafting and revision of the manuscript; Drs Wen Zheng LIAO, Bao Chun TAN and Di CUI contributed to technical assistance and data analysis; Drs Min WANG and Jun QIAN contributed to the data acquisition and manuscript revision; and Drs Chang Xing CHEN and Fu Hua YAN contributed to the conception, design and manuscript revision. All the authors gave their final approval of the manuscript and agreed to be accountable for all aspects of the work.

(Received Oct 13, 2023; accepted Mar 12, 2024)

References

1. Kinane DF, Stathopoulou PG, Papananou PN. Periodontal diseases. *Nat Rev Dis Primers* 2017;3:17038.
2. Hajishengallis G. Periodontitis: from microbial immune subversion to systemic inflammation. *Nat Rev Immunol* 2015;15:30–44.
3. Tsai SJ, Ding YW, Shih MC, Tu YK. Systematic review and sequential network meta-analysis on the efficacy of periodontal regenerative therapies. *J Clin Periodontol* 2020;47:1108–1120.
4. Liu Y, Guo L, Li X, et al. Challenges and Tissue Engineering Strategies of Periodontal-Guided Tissue Regeneration. *Tissue Eng Part C Methods* 2022;28:405–419.
5. Oryan A, Kamali A, Moshiri A, Baghaban Eslaminejad M. Role of Mesenchymal Stem Cells in Bone Regenerative Medicine: What Is the Evidence? *Cells Tissues Organs* 2017;204:59–83.
6. Xu XY, Li X, Wang J, He XT, Sun HH, Chen FM. Concise Review: Periodontal Tissue Regeneration Using Stem Cells: Strategies and Translational Considerations. *Stem Cells Transl Med* 2019;8:392–403.
7. Andrzejewska A, Lukomska B, Janowski M. Concise Review: Mesenchymal Stem Cells: From Roots to Boost. *Stem Cells* 2019;37:855–864.
8. Chen Y, Wang H, Yang Q, et al. Single-cell RNA landscape of the osteoimmunology microenvironment in periodontitis. *Theranostics* 2022;12:1074–1096.
9. Zhang J, Li ZG, Si YM, Chen B, Meng J. The difference on the osteogenic differentiation between periodontal ligament stem cells and bone marrow mesenchymal stem cells under inflammatory microenvironments. *Differentiation* 2014;88:97–105.
10. Lee CC, Hirasawa N, Garcia KG, Ramanathan D, Kim KD. Stem and progenitor cell microenvironment for bone regeneration and repair. *Regen Med* 2019;14:693–702.
11. Strowitzki MJ, Cummins EP, Taylor CT. Protein Hydroxylation by Hypoxia-Inducible Factor (HIF) Hydroxylases: Unique or Ubiquitous? *Cells* 2019;8:384.



12. Fan L, Li J, Yu Z, Dang X, Wang K. The hypoxia-inducible factor pathway, prolyl hydroxylase domain protein inhibitors, and their roles in bone repair and regeneration. *Biomed Res Int* 2014;2014:239356.
13. Taylor CT, Colgan SP. Regulation of immunity and inflammation by hypoxia in immunological niches. *Nat Rev Immunol* 2017;17:774–785.
14. Lin N, Simon MC. Hypoxia-inducible factors: key regulators of myeloid cells during inflammation. *J Clin Invest* 2016;126:3661–3671.
15. Cramer T, Yamanishi Y, Clausen BE, et al. HIF-1 α is essential for myeloid cell-mediated inflammation. *Cell* 2003;112:645–657.
16. Okumura CY, Hollands A, Tran DN, et al. A new pharmacological agent (AKB-4924) stabilizes hypoxia inducible factor-1 (HIF-1) and increases skin innate defenses against bacterial infection. *J Mol Med (Berl)* 2012;90:1079–1089.
17. Fu L, Zhang L, Zhang X, Chen L, Cai Q, Yang X. Roles of oxygen level and hypoxia-inducible factor signaling pathway in cartilage, bone and osteochondral tissue engineering. *Biomed Mater* 2021;16:022006.
18. Mayer H, Bertram H, Lindenmaier W, Korff T, Weber H, Weich H. Vascular endothelial growth factor (VEGF-A) expression in human mesenchymal stem cells: autocrine and paracrine role on osteoblastic and endothelial differentiation. *J Cell Biochem* 2005;95:827–839.
19. Esfahani M, Karimi F, Afshar S, Niknazar S, Sohrabi S, Najafi R. Prolyl hydroxylase inhibitors act as agents to enhance the efficiency of cell therapy. *Expert Opin Biol Ther* 2015;15:1739–1755.
20. Wu C, Zhou Y, Fan W, et al. Hypoxia-mimicking mesoporous bioactive glass scaffolds with controllable cobalt ion release for bone tissue engineering. *Biomaterials* 2012;33:2076–2085.
21. Ríos CN, Skoracki RJ, Mathur AB. GNAS1 and PHD2 short-interfering RNA support bone regeneration in vitro and in an in vivo sheep model. *Clin Orthop Relat Res* 2012;470:2541–2553.
22. Cui D, Chen C, Luo B, Yan F. Inhibiting PHD2 in human periodontal ligament cells via lentiviral vector-mediated RNA interference facilitates cell osteogenic differentiation and periodontal repair. *J Leukoc Biol* 2021;110:449–459.
23. Chen C, Li H, Jiang J, Zhang Q, Yan F. Inhibiting PHD2 in bone marrow mesenchymal stem cells via lentiviral vector-mediated RNA interference facilitates the repair of periodontal tissue defects in SD rats. *Oncotarget* 2017;8:72676–72699.
24. Tang J, Wu T, Xiong J, et al. Porphyromonas gingivalis lipopolysaccharides regulate functions of bone marrow mesenchymal stem cells. *Cell Prolif* 2015;48:239–248.
25. Bostanci N, Belibasakis GN. Porphyromonas gingivalis: an invasive and evasive opportunistic oral pathogen. *FEMS Microbiol Lett* 2012;333:1–9.
26. Kato H, Taguchi Y, Tominaga K, Umeda M, Tanaka A. Porphyromonas gingivalis LPS inhibits osteoblastic differentiation and promotes pro-inflammatory cytokine production in human periodontal ligament stem cells. *Arch Oral Biol* 2014;59:167–175.
27. Jiang YN, Zhao J, Chu FT, Jiang YY, Tang GH. Tension-loaded bone marrow stromal cells potentiate the paracrine osteogenic signaling of co-cultured vascular endothelial cells. *Biol Open* 2018;7:bio032482.
28. Du J, Shan Z, Ma P, Wang S, Fan Z. Allogeneic bone marrow mesenchymal stem cell transplantation for periodontal regeneration. *J Dent Res* 2014;93:183–188.
29. Berendsen AD, Olsen BR. Regulation of adipogenesis and osteogenesis in mesenchymal stem cells by vascular endothelial growth factor A. *J Intern Med* 2015;277:674–680.
30. Ramakrishnan S, Anand V, Roy S. Vascular endothelial growth factor signaling in hypoxia and inflammation. *J Neuroimmune Pharmacol* 2014;9:142–160.
31. Eltzschig HK, Bratton DL, Colgan SP. Targeting hypoxia signalling for the treatment of ischaemic and inflammatory diseases. *Nat Rev Drug Discov* 2014;13:852–869.
32. Jung YJ, Isaacs JS, Lee S, Trepel J, Neckers L. IL-1 β -mediated up-regulation of HIF-1 α via an NF κ B/COX-2 pathway identifies HIF-1 as a critical link between inflammation and oncogenesis. *FASEB J* 2003;17:2115–2117.
33. de Molon RS, Park CH, Jin Q, Sugai J, Cirelli JA. Characterization of ligature-induced experimental periodontitis. *Microsc Res Tech* 2018;81:1412–1421.
34. Carmagnola D, Tarce M, Dellavia C, Rimondini L, Varoni EM. Engineered scaffolds and cell-based therapy for periodontal regeneration. *J Appl Biomater Funct Mater* 2017;15:e303–e312.
35. Li G, Han N, Zhang X, et al. Local Injection of Allogeneic Stem Cells from Apical Papilla Enhanced Periodontal Tissue Regeneration in Minipig Model of Periodontitis. *Biomed Res Int* 2018;2018:3960798.
36. Lu L, Liu Y, Zhang X, Lin J. The therapeutic role of bone marrow stem cell local injection in rat experimental periodontitis. *J Oral Rehabil* 2020;47(suppl 1):73–82.
37. Chen M, Xu Y, Zhang T, et al. Mesenchymal stem cell sheets: a new cell-based strategy for bone repair and regeneration. *Biotechnol Lett* 2019;41:305–318.
38. Kobayashi J, Kikuchi A, Aoyagi T, Okano T. Cell sheet tissue engineering: Cell sheet preparation, harvesting/manipulation, and transplantation. *J Biomed Mater Res A* 2019;107:955–967.

CB1 Promotes Osteogenic Differentiation Potential of Periodontal Ligament Stem Cells by Enhancing Mitochondrial Transfer of Bone Marrow Mesenchymal Stem Cells

Lan LUO^{1,2}, Wan Hao YAN², Feng Qiu ZHANG¹, Zhi Peng FAN²

Objective: To reveal the role and mechanism of cannabinoid receptor 1 (CB1) and mitochondria in promoting osteogenic differentiation of periodontal ligament stem cells (PDLSCs) in the inflammatory microenvironment.

Methods: Bidirectional mitochondrial transfer was performed in bone mesenchymal stem cells (BMSCs) and PDLSCs. Laser confocal microscopy and quantitative flow cytometry were used to observe the mitochondrial transfer and quantitative mitochondrial transfer efficiency. Real-time reverse transcription polymerase chain reaction (RT-PCR) was employed to detect gene expression. Alkaline phosphatase (ALP) activity, alizarin red staining (ARS) and quantitative calcium ion analysis were used to evaluate the degree of osteogenic differentiation of PDLSCs.

Results: Bidirectional mitochondrial transfer was observed between BMSCs and PDLSCs. The indirect co-culture system could simulate intercellular mitochondrial transfer. Compared with the conditioned medium (CM) for BMSCs, that for HA-CB1 BMSCs could significantly enhance the mineralisation ability of PDLSCs. The mineralisation ability of PDLSCs could not be enhanced after removing the mitochondria in CM for HA-CB1 BMSCs. The expression level of HO-1, PGC-1 α , NRF-1, ND1 and HK2 was significantly increased in HA-CB1 BMSCs.

Conclusion: CM for HA-CB1 BMSCs could significantly enhance the damaged osteogenic differentiation ability of PDLSCs in the inflammatory microenvironment, and the mitochondria of CM played an important role. CB1 was related to the activation of the HO-1/PGC-1 α /NRF-1 mitochondrial biogenesis pathway, and significantly increased the mitochondrial content in BMSCs.

Keywords: bone marrow mesenchymal stem cells, CB1, mitochondrial transfer, osteogenic differentiation, periodontal membrane stem cells,

Chin J Dent Res 2024;27(3):225–234; doi: 10.3290/j.cjdr.b5698381

1 Department of Periodontology, Capital Medical University School of Stomatology, Beijing, P.R. China.

2 Laboratory of Molecular Signaling and Stem Cells Therapy, Beijing Key Research Unit of Tooth Development and Regeneration, Chinese Academy of Medical Sciences Laboratory of Tooth Regeneration and Function Reconstruction, Beijing Laboratory of Oral Health, Capital Medical University School of Stomatology, Beijing, P.R. China.

Corresponding authors: Dr Feng Qiu ZHANG and Dr Zhi Peng FAN, Capital Medical University School of Stomatology, No. 4 Tiantanxili, Dongcheng District, Beijing 100050, P.R. China. Email: zhfangqiu@126.com; zpfan@ccmu.edu.cn

This work was supported by the National Key Research and Development Program of China (no. 2022YFC2504201) and grants from the Innovation Research Team Project of Beijing Stomatological Hospital, Capital Medical University (no. CXTD202204) and grants CAMS Innovation Fund for Medical Sciences (2019-I2M-5-031).

Periodontitis is a multifactorial chronic infectious disease primarily caused by bacteria. The main manifestations are gingival soft tissue inflammation and alveolar bone loss, which can eventually lead to tooth loss. Studies have shown that there is mitochondrial dysfunction in gingival fibroblasts of patients with chronic periodontitis, including increased production of reactive oxygen species (ROS), mitochondrial structure abnormality, mitochondrial DNA (mtDNA) reduction and mutation,^{1,2} decreased mitochondrial membrane potential and increased oxygen consumption,³ of which the latter is pathological. As a result, adenosine triphosphate (ATP) production is abnormally reduced whereas ROS production is increased, leading to a vicious cycle of continuous oxidative stress and aggravated tissue damage.⁴



It is well known that mitochondria produce most of the energy a cell needs through oxidative phosphorylation, and an increasing number of studies have shown that the energy supply conversion from glycolysis to aerobic metabolism is the key to osteogenic differentiation of mesenchymal stem cells.⁵ Optimal periodontal tissue regeneration depends on mesenchymal stem cells, especially PDLSCs; however, inflammatory stimulation leads to decreased function of PDLSCs and impaired mitochondrial function, making it difficult for PDLSCs to meet the requirements of tissue regeneration. The physiological characteristics of healthy mitochondria, including replication, division, fusion, degradation, intracytoplasmic movement and intercellular transfer, make it possible to eliminate and replace damaged mitochondria in cells.^{6,7} Thus, saving the damaged mitochondrial function of cells to promote the proliferation and differentiation of PDLSCs has become the key to periodontal tissue regeneration therapy.

CB1 is an important component of the endocannabinoid system and is involved in regulating the proliferation and differentiation of mesenchymal stem cells and hematopoietic stem cells.⁸ Studies have shown that osteocyte derived 2-arachidonic glycerol (2-AG) activates CB1 receptor of bone sympathetic nerve endings and inhibits norepinephrine (NE) release, thus alleviating tonic inhibition of the sympathetic nervous system on bone formation and promoting bone formation.⁹ In addition, recent studies have found that CB1 exists in the membrane of mouse neuron mitochondria, directly controlling cell respiration and energy production.¹⁰ In addition, the present authors' previous research results also showed that CB1 can improve the oxidative phosphorylation function of mitochondria in BMSCs in the inflammatory environment simulated by tumour necrosis factor alpha (TNF- α), thus preserving the damaged osteogenic differentiation function of BMSCs in the inflammatory state.¹¹ This evidence suggested that CB1 may play an important role in regulating mitochondrial function in inflammatory environments. Thus, the mechanism by which CB1 regulates the osteogenic differentiation ability of mesenchymal stem cells by regulating mitochondrial function deserves further investigation.

In this study, 10 ng/ml TNF- α was used to simulate the inflammatory microenvironment, and conditioned medium (CM) was employed to simulate intercellular mitochondrial transfer in an indirect co-culture system. The mechanism of the effect of HA-CB1 BMSCs on osteoblast differentiation of PDLSCs through mitochondrial transfer was investigated, and the application prospect of mitochondrial transfer replacement therapy in periodontal tissue regeneration was explored.

Materials and methods

Cell culture

PDLSCs were derived from the impacted third molar or teeth that needed to be removed for orthodontic treatment after patients had provided informed consent and following the rules approved by the Beijing Stomatological Hospital, Capital Medical University (Ethics Committee Agreement, Beijing Stomatological Hospital Ethics Review CMUSH-IRB-KJ-PJ-2023-13). BMSCs were purchased from Cyagen Biosciences (Guangzhou, China). PDLSCs and BMSCs were stimulated with 10 ng/ml TNF- α to simulate the inflammatory environment.

Plasmid construction and viral infection

According to previous methods used by the present authors,¹¹ the pQCXIN-HA-CB1 plasmid was constructed and infected with the virus. CB1 shRNA and control shRNA lentiviruses were purchased from GenePharma (Shanghai, China). Stable transfected HA-CB1 BMSCs and CB1sh BMSCs were obtained after transfection. MitoDsRed and mitoEGFP lentiviruses were purchased from Gikat Corporation (Shanghai, China) for localisation of intracellular mitochondria. Control LVCON525 and mitoDsRed and mitoEGFP viruses were transfected with BMSCs and PDLSCs, respectively. The stable transfected cells of mitoDsRed BMSCs, mitoEGFP PDLSCs, mitoEGFP BMSCs and mitoDsRed PDLSCs were confirmed under a fluorescence microscope.

Intracellular mitochondrial staining and cell staining

MitoDeepRed (Invitrogen, Waltham, MA, USA) was used to stain cells to locate intracellular mitochondria. 5(6)-carboxyfluorescein diacetate N-succinimidyl ester (CFSE) (Beyotime Biotechnology, Shanghai, China) was used to label cells. When the cells grew to 80% to 90% confluence, the present authors removed the supernatant and washed the cells twice with phosphate-buffered saline (PBS). The MitoDeepRed working dye or CFSE dye solution was added to the cells at 37°C and in a 5% CO₂ environment for 30 minutes. The efficiency of cell staining was confirmed by quantitative flow cytometry.

Real-time reverse transcription polymerase chain reaction (RT-PCR)

Total RNA extraction, reverse transcription and real-time RT-PCR procedures were described previously.¹²

Table 1 Real-time RT-PCR primer sequence.

Gene	Primer sequence
GAPDH-FORWARD	5'-CGGACCAATACGACCAAATCCG-3'
GAPDH-REVERSE	5'-AGCCACATCGCTCAGACACC-3'
CB1-FORWARD	5'-CGGACCAATACGACCAAATCCG-3'
CB1-REVERSE	5'-AGCCACATCGCTCAGACACC-3'
HO-1-FORWARD	5'-TTCTTCACCTTCCCCAACATTG-3'
HO-1-REVERSE	5'-CAGCTCCTGCAACTCCTCAAA-3'
PGC-1A-FORWARD	5'-AGCCTCTTTGCCAGATCTT-3'
PGC-1A-REVERSE	5'-GCAATCCGTCTTCATCCACC-3'
NRF1-FORWARD	5'-ACATACTCAACTCCACGGCA-3'
NRF1-REVERSE	5'-ATGTGGCTCTGAGTTTCCGA-3'
ND1-FORWARD	5'-CACACTAGCAGAGACCAACCGAAC-3'
ND1-REVERSE	5'-CGGCTATGAAGAATAGGGCGAAGG-3'
HK2-FORWARD	5'-GCCAGCCTCTCCTGATTTAGTGT-3'
HK2-REVERSE	5'-GGGAACACAAAAGACCTCTTCTGG-3'

CB1, cannabinoid receptor I; HK2, hexokinase gene 2; HO-1, heme oxygenase-1; ND1, NADH dehydrogenase 1; NRF-1, nuclear respiratory factor-1; PGC-1 α , PPAR γ co-activator 1 α .

The Icyler iQ multi-color real-time RT-PCR detection system was used, and the QuantiTect SYBR Green PCR kit was employed for real-time RT-PCR reaction. Primer sequences for specific genes are shown in Table 1.

Establishing a cell co-culture system

The direct cell co-culture system was established by mixing cell suspension containing 1×10^5 BMSCs and 1×10^5 PDLSCs evenly and inoculating them in six-well plates or 35-mm laser confocal culture dishes.

The present authors established the indirect cell co-culture system based on the method described in the study by Hayakawa et al.¹³ When BMSCs grew to a confluent degree of 80%, the complete medium was changed into DMEM containing 1% penicillin and streptomycin (P+S). The supernatant was collected 24 hours later, which was the CM containing mitochondria of BMSCs. CM was centrifuged at a high speed of 2000 g for 10 minutes, cell precipitation was removed and supernatant was collected. The mitochondria-depleted CM (mdCM) was obtained by filtering CM through a 0.22- μ m filter. CM or mdCM and adherent PDLSCs were co-cultured for 24 hours. The experimental technique is shown in Fig S1 (provided on request).

Laser scanning confocal microscopy

After direct or indirect co-culture, the supernatant was discarded and washed with PBS three times. The cells were fixed with 4% paraformaldehyde at room temperature for 30 minutes, washed with PBS three times, and

anti-fluorescence quenching sealing tablets (including DAPI) were added. The cells were observed and photographed under a laser confocal microscope.

Flow cytometry

The direction and efficiency of mitochondrial metastasis were analysed by quantitative flow cytometry. Adherent cells after 24 hours of direct or indirect co-culture were washed three times using PBS, followed by cell digestion using 0.25% ethylenediaminetetraacetic acid (EDTA)-free trypsin, and the cell suspension was collected and centrifuged at 1,100 rpm for 5 minutes. After the supernatant was discarded, the cells were resuspended in complete medium and analysed through flow cytometry. In order to perform single positive analysis of samples, the present authors used an FACS dot plot to gate mitoDsRed positive cells on APC channel. To perform double-positive analysis of samples, we gated mitoDsRed positive cells using FACS dot plots on APC channels and analysed mGFP or CFSE signals of cell populations using FACS dot plots on FITC channels.

Alkaline phosphatase (ALP) activity assay and alizarin red detection

The osteogenic induction medium was prepared in a similar way to in the present authors' previous study,¹⁴ which performed osteogenic induction of periodontal ligament stem cells. ALP activity was determined using an ALP activity kit. To detect the mineralisation potential of PDLSCs, the latter were fixed with 70% ethanol and

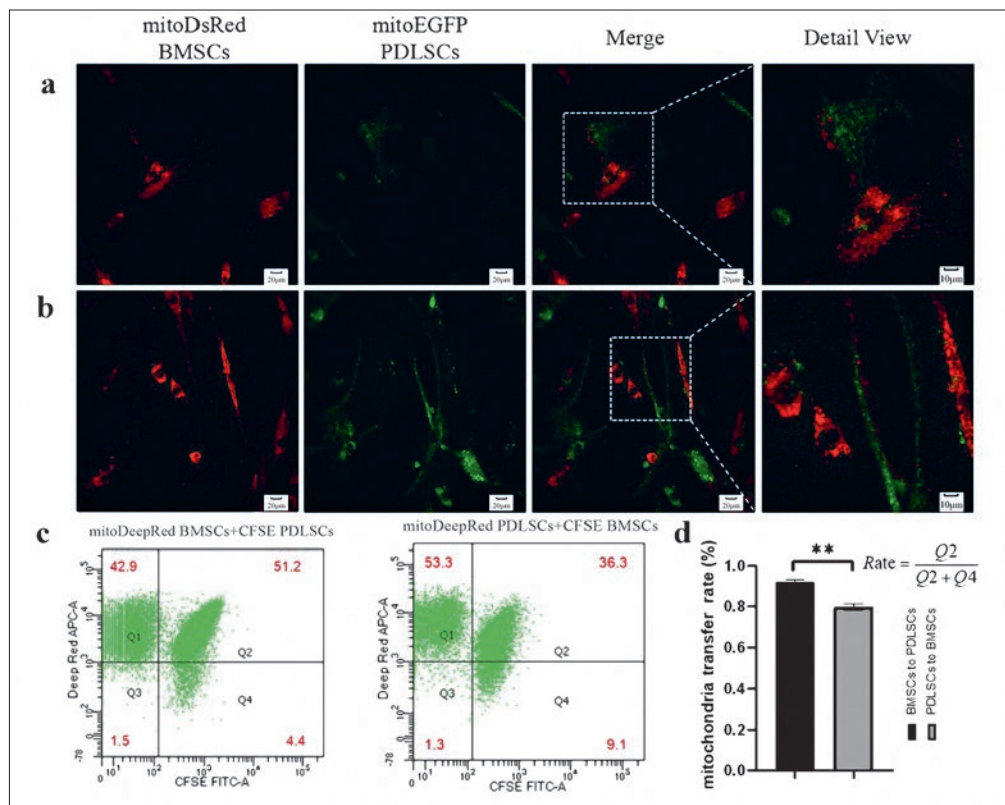


Fig 1a to d Direct co-culture of BMSCs and PDLSCs could induce mitochondrial transfer. Laser confocal microscope observed red and green fluorescence overlap between cells, bar = 20 μm (**a and b**). The staining efficiency of mito-DeepRed and CFSE dyes was determined by quantitative flow cytometry, and the mitochondrial transfer efficiency of BMSCs to PDLSCs and PDLSCs to BMSCs was determined (**c**). There were significant differences between the two groups. Error bars represent standard deviation (SD) (n = 3) (**d**). *P < 0.05; **P < 0.01.

stained with 2% alizarin red 2 weeks after osteogenesis induction. After scanning the staining results, calcium ion levels were measured using 10% w/v O-cresolphthalein complex ketone (CPC) as described above.¹⁴

Statistical analysis

The relative expression content of each index was measured using SPSS 16.0 software (IBM, Chicago, IL, USA). A t test was used to compare the measurement data between the two groups, and a one-way analysis of variance was performed to compare the measurement data between multiple groups. The level of statistical significance was set at P ≤ 0.05.

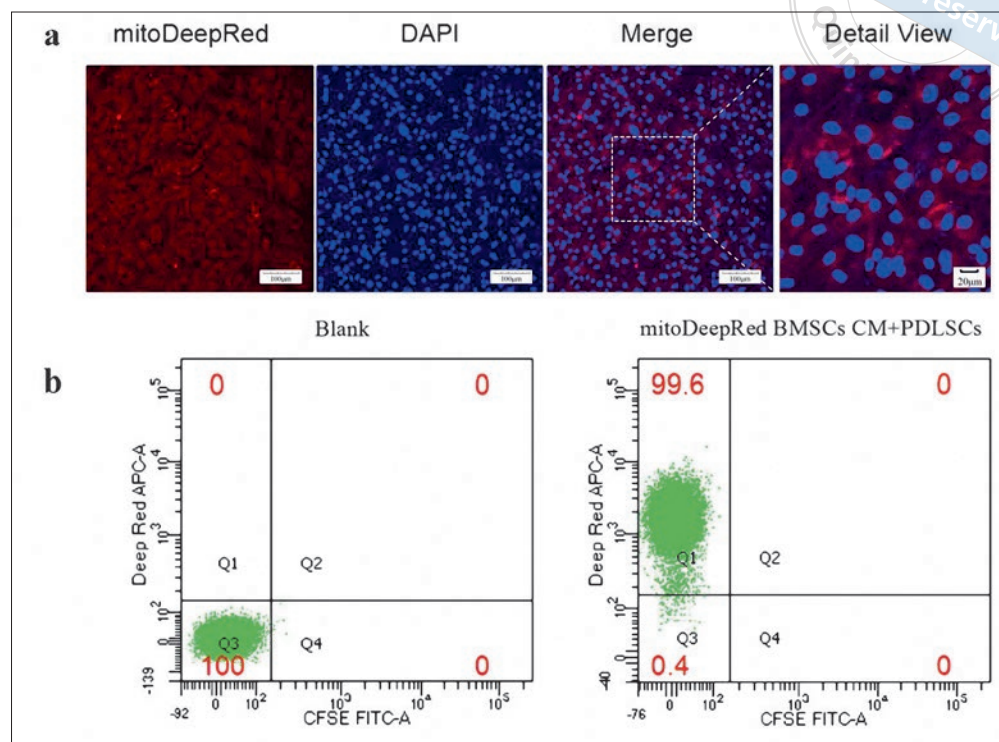
Results

Direct co-culture of BMSCs and PDLSCs could induce mitochondrial transfer

To confirm the presence of mitochondrial transfer between BMSCs and PDLSCs, mitoDsRed and mitoEGFP mitochondrial localisation lentivirus were used to transfect cells to obtain mitoDsRed BMSCs and mitoEGFP

PDLSCs. The two cells were mixed in a ratio of 1:1 and inoculated in a confocal laser culture dish. The mixture was observed under a confocal laser microscope 24 hours later. Red and green fluorescence overlapping regions were observed between red fluorescent cells (mitoDsRed BMSCs) and green fluorescent cells (mitoEGFP PDLSCs), which revealed that mitochondria exchanged between cells (Fig 1a and b). Next, the present authors examined the direction and efficiency of mitochondrial transfer between cells. MitoDeepRed and CFSE dyes were used to label PDLSCs and BMSCs, respectively, to obtain mitoDeepRed PDLSCs, mitoDeepRed BMSCs, CFSE PDLSCs and CFSE BMSCs. MitoDeepRed BMSCs and CFSE PDLSCs, mitoDeepRed PDLSCs and CFSE BMSCs were mixed in a ratio of 1:1, respectively, and inoculated in the six-well plate. 0.25% EDTA free pancreatic enzyme was used to harvest cells 24 hours later, and the double positive cell rate of DeepRed and CFSE was analysed by quantitative flow cytometry. Flow cytometry (Fig 1c) showed that bidirectional mitochondrial transfer could occur between BMSCs and PDLSCs, and the mitochondrial transfer efficiency from BMSCs to PDLSCs (93%) was significantly higher than that from PDLSCs to BMSCs (79%) (Fig 1d). In addition, the present authors measured the rate of mitochondrial transfer

Fig 2a and b Mitochondrial transfer to PDLSCs could be achieved by CM. After MitoDeepRed BMSC CM and PDLSCs were co-cultured for 24 hours, red fluorescence was observed in the cells under laser confocal microscope, bar = 100 μm (a). MitoDeepRed BMSCs CM and PDLSCs were co-cultured for 24 hours. The number of DeepRed-positive cells in the blank control group and indirect co-culture group was determined by quantitative flow cytometry. Error bars represent SD (n = 3) (b). CM, conditioned medium.



between cells at 48 hours by quantitative flow cytometry, which showed that the rate of mitochondrial transfer from BMSCs to PDLSCs could be as high as 99%, and that from PDLSCs to BMSCs could be as high as 82% (Fig S2, provided on request). To test whether 10 ng/ml TNF- α could affect the mitochondrial transfer between cells, quantitative flow cytometry analysis was performed in the direct co-culture system under normal conditions and in the presence of 10 ng/ml TNF- α . The results showed that there was no significant difference in the mitochondrial transfer rate between the two groups, which was higher than 90%. The results are shown in Fig S3 (provided on request). This may be due to the fact that both BMSCs and PDLSCs have high stemness and a high level of mitochondrial transfer can occur under normal conditions.

The indirect co-culture system of CM and PDLSCs could simulate intercellular mitochondrial transfer

MitoDeepRed BMSCs CM was co-cultured with PDLSCs in confocal culture dishes for 24 hours to construct an indirect co-culture system of BMSCs and PDLSCs. Under laser confocal microscopy, adherent PDLSCs were found to capture red fluorescent-labelled BMSC mitochondria in CM (Fig 2a). PDLSCs were inoculated in six-well plates and co-cultured with CM for 24 hours. Cells were har-

vested and analysed by quantitative flow cytometry. The results showed that BMSCs CM could transfer mitochondria to PDLSCs, with an efficiency of up to 99.6% (Fig 2b). Comparing the mitochondrial transfer rate of the direct co-culture system with that of the indirect co-culture system, the present authors found that the indirect co-culture system had a higher mitochondrial transfer rate than the direct system, and there was a significant difference between the two groups, as shown in Fig S4 (provided on request).

Effects of BMSC CM, CB1sh BMSC CM and HA-CB1 BMSC CM on osteogenic differentiation of PDLSCs in the inflammatory microenvironment

After it was confirmed by laser confocal microscopy and quantitative flow cytometry that BMSC CM could transfer mitochondria to PDLSCs through the indirect co-culture system, the present authors began to investigate whether BMSC CM could improve the osteogenic differentiation ability of PDLSCs stimulated by 10 ng/ml TNF- α . First, 5 days after osteogenic induction, ALP activity assay results showed that 10 ng/ml TNF- α decreased the ALP activity in PDLSCs compared with the control group (Fig 3a). ARS and quantitative calcium ion analysis demonstrated that 10 ng/ml TNF- α stimulation significantly inhibited the mineralisation of PDLSCs in vitro compared with the

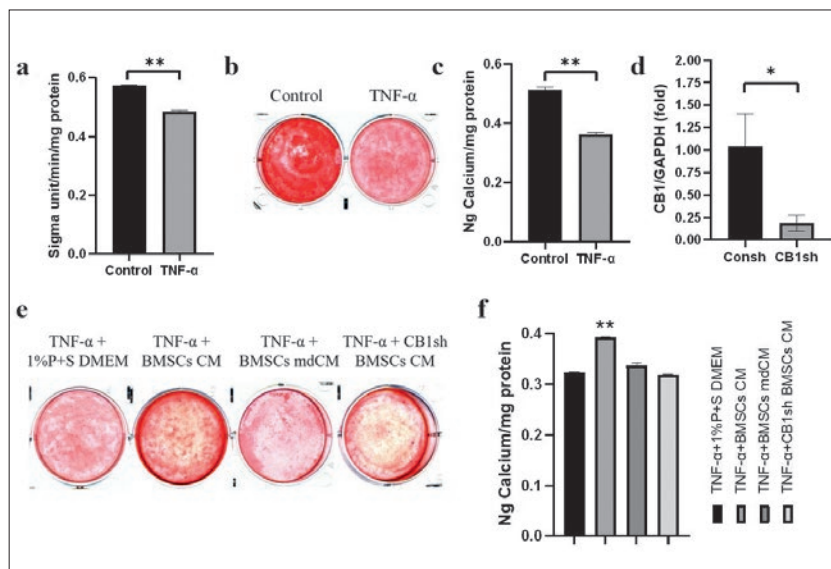


Fig 3a to f BMSCs CM promoted PDLSCs osteogenesis, but CB1 sh BMSCs CM did not. After osteogenic induction, ALP activity (a), ARS (b) and quantitative calcium ion analysis (c) were used to determine the effect of 10 ng/ml TNF-α on the osteogenic differentiation of PDLSCs. Real-time RT-PCR was used to detect the knockdown efficiency of CB1 in BMSCs (d). ARS (e) and quantitative calcium ion analysis (f) were used to determine the effects of BMSC CM, BMSC mdCM and CB1sh BMSC CM on the osteogenic differentiation ability of PDLSCs stimulated by 10 ng/ml TNF-α. Error bars represent SD (n = 3). *P < 0.05; **P < 0.01. ALP, alkaline phosphatase activity; ARS, alizarin red staining; CB1, cannabinoid receptor I; CM, conditioned medium; P+S, penicillin and streptomycin; TNF-α, tumour necrosis factor alpha.

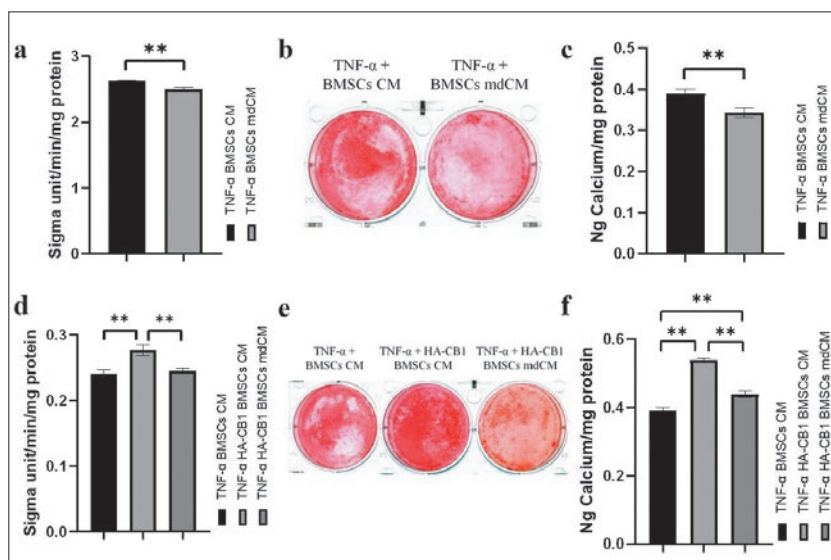


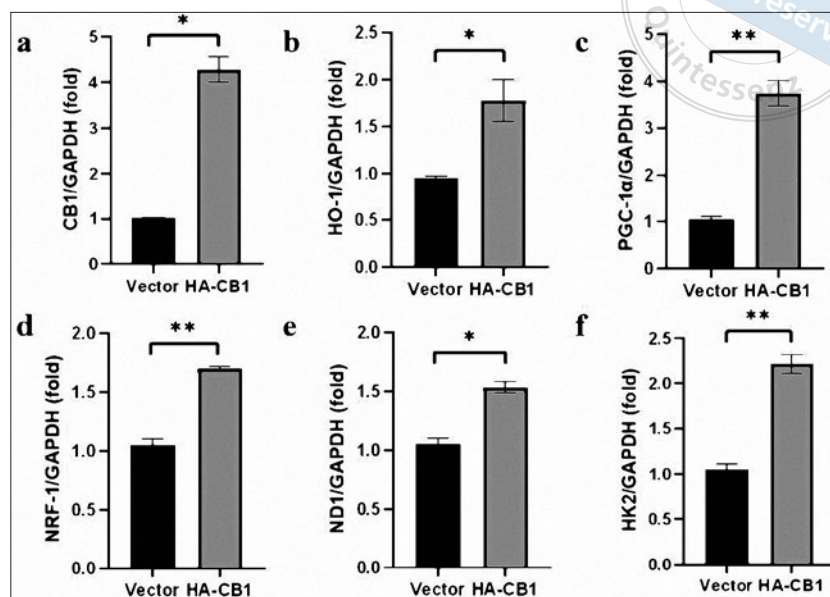
Fig 4a to f HA-CB1 BMSC CM significantly enhanced the osteogenic function of PDLSCs, but could not save the osteogenic ability of PDLSCs after mitochondrial filtration. ALP activity assay (a), ARS (b) and quantitative calcium ion analysis (c) were used to determine the effects of BMSC CM and BMSC mdCM on the osteogenic differentiation ability of PDLSCs stimulated by 10 ng/ml TNF-α. ALP activity assay (d), ARS (e) and quantitative calcium ion analysis (f) were used to detect the effects of BMSC CM, HA-CB1 BMSC CM and HA-CB1 BMSC mdCM on the osteogenic differentiation ability of PDLSCs under 10 ng/ml TNF-α stimulation. Error bars represent SD (n = 3). *P < 0.05; **P < 0.01. ALP, alkaline phosphatase activity; ARS, alizarin red staining; CB1, cannabinoid receptor 1; CM, conditioned medium; mdCM, mitochondria-depleted conditioned medium; TNF-α, tumour necrosis factor alpha.

control group (Fig 3b and c). CB1 expression in BMSCs was knocked down using CB1 shRNA lentivirus, and the expression level of CB1 was detected by real-time RT-PCR, demonstrating decreased expression in BMSCs (Fig 3d). The BMSC and PDLSC CMs obtained were co-cultured under the stimulation of 10 ng/ml TNF-α, and osteogenic induction was performed 24 hours later. The results of ARS and calcium ion quantitative analysis showed that BMSC CM increased the osteogenic differentiation ability of PDLSCs damaged by 10 ng/ml TNF-α compared with the control group (Fig 3e and f), indicating that BMSC CM could save the damaged osteogenic differentiation ability of PDLSCs, but CB1sh BMSC CM could not. These results

suggest that mitochondria might be essential to enhance the osteogenic differentiation of PDLSCs, and CB1 plays a role in this process.

Next, mitochondria in BMSC CM were removed using a 0.22-μm filter to obtain mdCM, which was co-cultured with adherent PDLSCs. ALP, ARS and quantitative calcium ion analysis showed that BMSC mdCM could not save the osteogenic differentiation ability of PDLSCs stimulated by 10 ng/ml TNF-α (Fig 4a to c). In addition, the present authors compared the results of osteogenesis experiments on PDLSCs after co-culturing with mdCM and CB1sh BMSC CM (Fig 3d to f). They found that CB1sh BMSC CM had no significant effect

Fig 5a to f CB1 promoted the expression of mitochondrial biogenesis related factors and mitochondrial content marker genes in BMSCs. The overexpression efficiency of CB1 in BMSCs was detected by real-time RT-PCR (**a**). The expression levels of HO-1, PGC-1 α and NRF-1 in HA-CB1 BMSCs were detected by real-time RT-PCR (**b to d**). The expression levels of ND1 and HK2 encoded by mitochondria in HA-CB1 BMSCs were detected by real-time RT-PCR (**e to f**). Error bars represent SD (n = 3). * $P < 0.05$; ** $P < 0.01$. CB1, cannabinoid receptor 1; HK2, hexokinase gene 2; HO-1, heme oxygenase-1; ND1, NADH dehydrogenase 1; NRF-1, nuclear respiratory factor-1; PGC-1 α , PPAR γ co-activator 1 α .



on osteogenesis of PDLSCs, which was similar to the results of the control group using complete medium. There were no significant differences between the two groups; however, mdCM was least able to promote PDLSC osteogenesis compared with the other two groups, perhaps due to the 0.22- μm filter that can filter out mitochondria and vesicles containing various factors larger than 0.22 μm . To further verify the role and mechanism of HA-CB1 BMSC CM, the present authors formed three groups: BMSC CM and 10 ng/ml TNF- α PDLSCs, HA-CB1 BMSC CM and 10 ng/ml TNF- α PDLSCs, HA-CB1 BMSC mdCM and 10 ng/ml TNF- α PDLSCs. Osteogenesis induction was performed 24 hours after co-culture. ALP activity was performed 7 days later, whereas ARS and quantitative calcium ion analysis were performed 14 days later (Fig 4d to f). The results showed that compared with BMSC CM, HA-CB1 BMSC CM could significantly enhance the mineralisation ability of PDLSCs; however, that of PDLSCs could not be enhanced after removing the mitochondria in HA-CB1 BMSC CM.

CB1 contributed to mitochondrial biogenesis of BMSCs and increased the number of mitochondria in cells

To further explore the mechanism of CB1 affecting intracellular mitochondrial function, the present authors used real-time RT-PCR to detect the expression levels of mitochondrial biogenesis related factors, including heme oxygenase-1 (HO-1), PPAR γ co-activator 1 α (PGC-1 α) and nuclear respiratory factor-1 (NRF-1), and detected the expression levels of mitochondrial coding genes

NADH dehydrogenase 1 (ND1) and hexokinase gene 2 (HK2) to quantitatively determine intracellular mitochondrial content. Real-time RT-PCR results showed that BMSCs with stable overexpression of CB1 were successfully constructed (Fig 5a). Meanwhile, real-time RT-PCR results showed that, compared with the control group, the expression of HO-1, PGC-1 α and NRF-1 in HA-CB1 BMSCs was significantly increased (Fig 5b to d), and the expression of marker genes ND1 and HK2 of mitochondrial content were also increased in the HA-CB1 group (Fig 5e and f). These results suggest that CB1 might promote BMSC mitochondrial biogenesis to increase mitochondrial content.

Discussion

Studies have shown that during bone formation induction of BMSCs, proteins involved in mitochondrial biogenesis are increased, accompanied by the development of mitochondrial ridge, the expression level of constituent subunits and the activity of the respiratory enzyme complex. Mitochondrial membrane potential, cellular respiration rate and intracellular ATP content are also increased. This evidence indicates that mitochondrial oxidative metabolism is upregulated during BMSC differentiation, and biological energy changes occur in cells from glycolysis to aerobic metabolism,⁵ indicating that mitochondria play a vital role in osteogenic differentiation of BMSCs. However, many studies have shown that the periodontal inflammatory microenvironment impels the mitochondrial function of periodontal cells, and some have confirmed that bacterial lipopolysaccha-

rids (LPS)-mediated mitochondrial dysfunction may be the initial cause of oxidative stress in patients with periodontitis. Insufficient energy supply, massive release of ROS and an imbalance of calcium ions lead to mitochondrial damage, and aggravate apoptosis and necrosis of cells around the damaged area.^{15,16} This suggests that mitochondrial dysfunction may be a key factor in the onset and progression of periodontitis.

In the inflammatory microenvironment, the accumulation of TNF- α is involved in the alveolar bone resorption process, which is crucial in the occurrence and development of periodontitis.^{17,18} Studies have shown that the osteogenesis and regeneration abilities of PDLSCs in periodontitis patients are impaired in inflammatory environment, and such impaired characteristics can be simulated *in vitro* by treating healthy PDLSCs with 10 ng/ml TNF- α .¹⁹ In the previous study conducted by the present authors, it was found that 10 ng/ml TNF- α reduced the oxygen consumption rate (OCR) and membrane potential in BMSCs, and inhibited mitochondrial synthesis.¹¹ These results indicated that the mitochondrial function of MSCs was impaired under 10 ng/ml TNF- α stimulation.

Many studies have proved that stem cells can replace damaged mitochondria by transferring mitochondria to recipient cells and restore their oxidative metabolism function,^{12,20} which provides therapeutic ideas for saving mitochondrial dysfunction of damaged cells.²¹ Thus, the present authors hypothesised that BMSCs can also improve the function of PDLSCs in inflammatory injury through mitochondrial transfer, and observed mitochondrial exchange between mitoDsRed BMSCs and mitoEGFP PDLSCs under laser confocal microscopy. In addition, the results of quantitative flow cytometry proved the efficiency of mitochondrial transfer from BMSCs to PDLSCs was up to 93%. In the study by Hayakawa et al,¹³ astrocyte-derived CM was co-cultured with adherent neuron cells to achieve mitochondrial transfer to neurons, improve neuron vitality and promote the repair of the nervous system after stroke. These results indicated that mitochondrial transfer can be carried out by non-cellular contact. Therefore, to examine the effect of mitochondria from BMSCs on PDLSCs, the present authors constructed an indirect co-culture system for experiments, and laser confocal microscopy showed that PDLSCs could obtain free mitochondria from the conditioned medium. Flow cytometry also proved that up to 99.6% of PDLSCs could internalise exogenous mitochondria.

Based on these results, the present authors used the indirect co-culture system to further explore the role of mitochondria in saving the osteogenic differ-

entiation ability of damaged cells in an inflammatory microenvironment. ALP activity results showed that BMSC CM could significantly enhance the osteogenic ability of PDLSCs damaged by 10 ng/ml TNF- α . ARS and quantitative calcium ion analysis results also demonstrated that the mineralisation ability of PDLSCs was significantly enhanced. In the present authors' previous study,¹¹ CB1 was found to promote the mitochondrial energy metabolism of BMSCs, including OCR and MMP, and recover the impaired osteogenic differentiation potential in the case of 10 ng/ml TNF- α stimulation. This suggested that CB1 activation promoted osteogenic differentiation of BMSCs by rescuing mitochondrial metabolism under inflammatory conditions. Therefore, in the present study, the authors continued to explore whether mitochondria are the key to the effect of CB1 on osteogenic differentiation by the indirect co-culture system. ALP, ARS and quantitative calcium analysis showed that BMSC CM could enhance the osteogenic differentiation ability of PDLSCs; however, the effect of CB1-knockdown BMSC-derived CM was significantly reduced. Next, the present authors removed mitochondria from CM for experiments and found that BMSC mdCM did not save the osteogenic differentiation ability of PDLSCs stimulated by 10 ng/ml TNF- α . In order to verify whether CB1 affects the impact of CM on the osteogenic ability of PDLSCs by influencing the mitochondrial function of BMSCs, the authors conducted three osteogenesis experiments. The results of ALP, ARS and quantitative calcium ion analysis showed that CM obtaining from CB1 over-expressed BMSCs had a stronger promoting effect on osteogenic differentiation of PDLSCs than the vector group; however, this effect was cancelled after removing mitochondria from HA-CB1 BMSC CM. This indicated that HA-CB1 BMSC CM can significantly enhance the osteogenic differentiation potential of PDLSCs damaged by 10 ng/ml TNF- α , and the core of this enhancement mechanism might be providing mitochondria to PDLSCs.

The present authors then investigated the mechanism of CB1 affecting mitochondrial function. Mitochondria, the centre of cellular metabolism and energy production, are produced by phagocytosis of α -protein bacillus by eukaryotic progenitor cells.²² When mitochondria are damaged, cells will not regenerate them, but complete the dynamic regulation of the cellular mitochondrial system through a mitochondrial biogenesis process to degrade damaged mitochondria and promote the proliferation of healthy mitochondria.²³ Mitochondrial biogenesis is regulated by a dual genomic program of nuclear coding genes and mitochondrial coding genes, including nuclear coding mitochondrial pro-

teins that control mtDNA transcription and replication. This process requires the induction of mitochondrial DNA polymerase, mitochondrial transcription factor A (TFAM) and TFB2M.^{24,25} Many nuclear coding genes of mitochondrial proteins contain NRF-1 and NRF-2, and PGC-1 α is the central transcription coactivator of NRF-1, NRF-2 and PPAR γ . It can promote the transcription of mitochondrial coding genes such as TFAM and participate in the physiological integration of mitochondrial biosynthesis and oxidative metabolism.^{26,27} When the energy demand of cells increases, the NAD⁺/NADH ratio increases and activates Sirtuin-1 (SIRT1), leading to PGC-1 α deacetylation and activation of NRF-1 and other transcription factors involved in mitochondrial biogenesis, promoting the transcription of target genes and stimulating mitochondrial biogenesis.²⁸ In addition, studies have confirmed that HO-1 also plays an initiating role in mitochondrial biogenesis²⁹; it controls the degradation of free heme and produces CO, iron and biliverdin.³⁰ Elevated endogenous CO levels stimulate the expression of antioxidant enzyme SOD2 and the production of mitochondrial H₂O₂ in Complex III, leading to the activation of Akt/PKB and the inactivation of glycogen synthetase kinase-3. Activation of this signalling pathway greatly stimulates mitochondrial biogenesis by allowing nuclear translocation of NRF-2 and occupying antioxidant response elements (AREs) in the NRF-1 promoter.^{31,32} In the present authors' previous study, the results showed that overexpression of CB1 could significantly increase the expression levels of HO-1, PGC-1 α and NRF-1 in BMSCs compared with the control group.¹¹ This result is consistent with the results of our study conducted in BMSCs. In addition, mtDNA levels were detected to measure intracellular mitochondrial content, and the results showed that the expressions of nicotinamide adenine dinucleotide ND1 and HK2 encoded by mitochondria were significantly higher in HA-CB1 BMSCs. This suggested that CB1 may be associated with mitochondrial biogenesis of BMSCs by activating the HO-1/PGC-1 α /NRF-1 pathway and increase intracellular mitochondrial content.

The present results suggested that supplying mitochondria to damaged cells in an *in vitro* inflammatory microenvironment is an effective way to save the osteoblast ability of cells. Compared with stem cells, the outer membrane of mitochondria lacks surface antigens and has low immunogenicity, and one high-functioning cell can contain hundreds of mitochondria. In addition to directly replacing the damaged mitochondria, some studies have shown that exogenous mitochondria can collocate with the original mitochondria after entering the recipient cells, suggesting that they can fuse with

them,³³ indicating that exogenous mitochondria may also have the ability to rescue the damaged mitochondria in the recipient cells to promote the recovery of cell function. Thus, mitochondria replacement therapy has a wider range of sources, and autogenous, allogenic and even xenogeneic tissues are expected to become donor sources for mitochondrial replacement therapy. However, further studies are required on the acquisition of mitochondria with high purity concentration, the realisation of mitochondrial transfer in the *vivo* model of periodontitis, and the changes and effects of the mitochondrial energy metabolism system after mitochondria enter recipient cells.

Conclusion

In summary, the authors conclude that mitochondrial transfer exists between BMSCs and PDLSCs, which can be simulated by the CM indirect co-culture system; in an 10 ng/ml TNF- α simulated inflammatory microenvironment, HA-CB1 BMSC CM could enhance the osteogenic differentiation ability of PDLSCs, and mitochondria in CM played an important role. CB1 was related to the activation of the HO-1/PGC-1 α /NRF-1 mitochondrial biogenesis pathway, and significantly increased the content of mitochondria in BMSCs, which might be why HA-CB1 BMSC CM had stronger osteogenic differentiation ability of PDLSCs than BMSC CM. These findings have identified the role of mitochondria in restoring the osteogenic differentiation function of PDLSCs damaged by 10 ng/ml TNF- α , which established the research basis for the application of mitochondrial therapy in periodontal tissue regeneration.

Conflicts of interest

The authors declare no conflicts of interest related to this study.

Author contribution

Drs Lan LUO, Wan Hao YAN, Feng Qiu ZHANG and Zhi Peng FAN contributed to the research concept; Dr Lan LUO developed the protocol, extracted the data, analysed the findings and drafted and critically revised the manuscript; Drs Wan Hao YAN, Feng Qiu ZHANG, and Zhi Peng FAN reviewed and revised the manuscript. All the authors approved the manuscript.

(Received Oct 01, 2023, accepted Mar 12, 2024)

References

1. Govindaraj P, Khan NA, Gopalakrishna P, et al. Mitochondrial dysfunction and genetic heterogeneity in chronic periodontitis. *Mitochondrion* 2011;11:504–512.
2. Liu J, Wang X, Xue F, Zheng M, Luan Q. Abnormal mitochondrial structure and function are retained in gingival tissues and human gingival fibroblasts from patients with chronic periodontitis. *J Periodontol Res* 2022;57:94–103.
3. Liu J, Wang X, Zheng M, Luan Q. Oxidative stress in human gingival fibroblasts from periodontitis versus healthy counterparts. *Oral Dis* 2023;29:1214–1225.
4. Napa K, Baeder AC, Witt JE, et al. LPS from *P. gingivalis* Negatively Alters Gingival Cell Mitochondrial Bioenergetics. *Int J Dent* 2017;2017:2697210.
5. Hsu YC, Wu YT, Yu TH, Wei YH. Mitochondria in mesenchymal stem cell biology and cell therapy: from cellular differentiation to mitochondrial transfer. *Semin Cell Dev Biol* 2016;52:119–131.
6. Liu CS, Chang JC, Kuo SJ, et al. Delivering healthy mitochondria for the therapy of mitochondrial diseases and beyond. *Int J Biochem Cell Biol* 2014;53:141–146.
7. Cipolat S, Martins de Brito O, Dal Zilio B, Scorrano L. OPA1 requires mitofusin 1 to promote mitochondrial fusion. *Proc Natl Acad Sci USA* 2004;101:15927–15932.
8. Galve-Roperh I, Chiurchiù V, Díaz-Alonso J, Bari M, Guzmán M, Maccarrone M. Cannabinoid receptor signaling in progenitor/stem cell proliferation and differentiation. *Prog Lipid Res* 2013;52:633–650.
9. Tam J, Trembovler V, Di Marzo V, et al. The cannabinoid CB1 receptor regulates bone formation by modulating adrenergic signaling. *FASEB J* 2008;22:285–294.
10. Bénard G, Massa F, Puente N, et al. Mitochondrial CB1 receptors regulate neuronal energy metabolism. *Nat Neurosci* 2012;15:558–564.
11. Yan W, Li L, Ge L, Zhang F, Fan Z, Hu L. The cannabinoid receptor I (CB1) enhanced the osteogenic differentiation of BMSCs by rescue impaired mitochondrial metabolism function under inflammatory condition. *Stem Cell Res Ther* 2022;13:22.
12. Liu D, Wang Y, Jia Z, et al. Demethylation of IGFBP5 by Histone Demethylase KDM6B Promotes Mesenchymal Stem Cell-Mediated Periodontal Tissue Regeneration by Enhancing Osteogenic Differentiation and Anti-Inflammation Potentials. *Stem Cells* 2015;33:2523–2536.
13. Hayakawa K, Esposito E, Wang X, et al. Transfer of mitochondria from astrocytes to neurons after stroke. *Nature* 2016;535:551–555 [erratum 2016;539:123].
14. Yan W, Cao Y, Yang H, et al. CB1 enhanced the osteo/dentogenic differentiation ability of periodontal ligament stem cells via p38 MAPK and JNK in an inflammatory environment. *Cell Prolif* 2019;52:e12691.
15. Hamanaka RB, Chandel NS. Mitochondrial reactive oxygen species regulate cellular signaling and dictate biological outcomes. *Trends Biochem Sci* 2010;35:505–513.
16. Chernorudskiy AL, Zito E. Regulation of Calcium Homeostasis by ER Redox: A Close-Up of the ER/Mitochondria Connection. *J Mol Biol* 2017;429:620–632.
17. Slots J. Periodontitis: facts, fallacies and the future. *Periodontol* 2000 2017;75:7–23.
18. Slots J. Periodontal herpesviruses: prevalence, pathogenicity, systemic risk. *Periodontol* 2000 2015;69:28–45.
19. Wang YJ, Zhao P, Sui BD, et al. Resveratrol enhances the functionality and improves the regeneration of mesenchymal stem cell aggregates. *Exp Mol Med* 2018;50:1–15.
20. Patananan AN, Wu TH, Chiou PY, Teitell MA. Modifying the Mitochondrial Genome. *Cell Metab* 2016;23:785–796.
21. McCully JD, Cowan DB, Emani SM, Del Nido PJ. Mitochondrial transplantation: From animal models to clinical use in humans. *Mitochondrion* 2017;34:127–134.
22. Guariento A, Piekarski BL, Doulamis IP, et al. Autologous mitochondrial transplantation for cardiogenic shock in pediatric patients following ischemia-reperfusion injury. *J Thorac Cardiovasc Surg* 2021;162:992–1001.
23. Davis DM, Sowinski S. Membrane nanotubes: dynamic long-distance connections between animal cells. *Nat Rev Mol Cell Biol* 2008;9:431–436.
24. Kelly DP, Scarpulla RC. Transcriptional regulatory circuits controlling mitochondrial biogenesis and function. *Genes Dev* 2004;18:357–368.
25. Scarpulla RC. Transcriptional paradigms in Mammalian mitochondrial biogenesis and function. *Physiol Rev* 2008;88:611–638.
26. Wu Z, Puigserver P, Andersson U, et al. Mechanisms controlling mitochondrial biogenesis and respiration through the thermogenic coactivator PGC-1. *Cell* 1999;98:115–124.
27. Kozhukhar N, Alexeyev MF. Limited predictive value of TFAM in mitochondrial biogenesis. *Mitochondrion* 2019;49:156–165.
28. Dominy JE Jr, Lee Y, Gerhart-Hines Z, Puigserver P. Nutrient-dependent regulation of PGC-1 α 's acetylation state and metabolic function through the enzymatic activities of Sirt1/GCN5. *Biochim Biophys Acta* 2010;1804:1676–1683.
29. Bossy B, Petrilli A, Klinglmayr E, et al. S-Nitrosylation of DRP1 does not affect enzymatic activity and is not specific to Alzheimer's disease. *J Alzheimers Dis* 2010; 20(suppl 2):S513–S526.
30. Maines MD. Heme oxygenase: function, multiplicity, regulatory mechanisms, and clinical applications. *FASEB J* 1988;2:2557–2568.
31. Ryter SW, Alam J, Choi AM. Heme oxygenase-1/carbon monoxide: from basic science to therapeutic applications. *Physiol Rev* 2006;86:583–650.
32. Piantadosi CA, Carraway MS, Babiker A, Suliman HB. Heme oxygenase-1 regulates cardiac mitochondrial biogenesis via Nrf2-mediated transcriptional control of nuclear respiratory factor-1. *Circ Res* 2008;103:1232–1240.
33. Lu J, Zheng X, Li F, et al. Tunneling nanotubes promote intercellular mitochondria transfer followed by increased invasiveness in bladder cancer cells. *Oncotarget* 2017;8:15539–15552.

Establishment of an Animal Model of Oral Squamous Cell Carcinoma Invading the Mandible

Xiang Long ZHENG¹, Kang Wei ZHOU¹, Wen LI¹, Ya Qi CHEN¹, Cheng Hui LU², Li Song LIN¹

Objective: To establish an animal model of oral squamous cell carcinoma invading the mandible through multi-sample experiments that verified the stability, repeatability, tumorigenicity and mandible destruction rate of the model.

Methods: Oral squamous cell carcinoma cell suspension was injected into the outer side of the mandible through the anterior edge of the masseter muscle of naked mice to observe the tumour-forming process. Then, the anatomical, histological and imaging examinations were carried out to determine whether the tumour had invaded the mandible. By comparing the tumour growth of multiple groups of various squamous cell carcinoma cells (CAL27, HN6 and HN30 cells), the changes in body weight and characteristics of tumour formation were compared, and the experience was summarised to further verify the stability, repeatability, tumour formation rate and arch damage rate of the model.

Results: The subsequent specimens of tumour-bearing nude mice were validated once the model had been established. *In vitro*, tumour tissue wrapped around the mandible's tumour-bearing side, and the local texture was tough with no resistance to acupuncture. Haematoxylin and eosin staining revealed that squamous cells were infiltrating the mandible in both the horizontal and sagittal planes. Microcomputed tomography results showed that the mandible on the tumour-bearing side displayed obvious erosion damage. Cell lines with various passage rates clearly had diverse tumour-bearing life cycles.

Conclusion: This study successfully established an animal model of oral squamous cell carcinoma invasion of the mandible. The model has excellent biological stability, repeatability, tumorigenesis rate and mandible destruction rate.

Keywords: animal model, invade, life cycle, mandible, oral squamous cell carcinoma
Chin J Dent Res 2024;27(3):235–241; doi: 10.3290/j.cjdr.b5698375

Oral squamous cell carcinoma (OSCC) is one of the most common malignant tumours in the head and neck, and surgery is still the main treatment method.^{1,2} With the

development of existing diagnosis and treatment technology, although the survival rate with early-stage OSCC can reach up to 80%, the 5-year survival rate of middle- and late-stage patients is still approximately 50%.^{3,4} The main causes include local recurrence, lymph node metastasis and distant metastasis.⁵ Even if the tumour is completely removed with an appropriate margin of safety during surgery, local recurrence may still occur. Especially when the tumour invades the jawbone, due to high bone density and hard cortical bone, rapid frozen section and other methods cannot be used to detect the operative bone incisal margin without decalcification. In addition, the interface of OSCC infiltrating the jawbone cannot be accurately defined through imaging examination before surgery,^{6,7} so it is difficult to con-

1 Department of Oral and Maxillofacial Surgery, The First Affiliated Hospital, Fujian Medical University, Fuzhou, P.R. China.

2 School and Hospital of Stomatology, Fujian Medical University, Fuzhou, P.R. China.

Corresponding author: Dr Li Song LIN, Department of Oral and Maxillofacial Surgery, The First Affiliated Hospital, Fujian Medical University, No.20 Cha-Zhong Road, Fuzhou 350005, Fujian Province, P.R. China. Tel: 86-13905006502 Email: dr_lls@hotmail.com

This work was supported by Joint Funds for the Innovation of Science and Technology of Fujian province (no. 2019Y9128)



firm whether the bone incisal margin is negative during the procedure. Thus, it is impossible to resect the diseased jaw tissue safely and accurately.⁸

The types of bone invasion include erosion, infiltration and mixed patterns,⁹ but the specific mechanism and mode of invasion have not been defined. Various animal models have developed to study the pathogenesis, genetic background and novel therapeutic development of OSCC.¹⁰ The information obtained from animal models is crucial for the diagnosis and treatment of OSCC; however, no single model can summarise all aspects, and the corresponding animal models need to be constructed for different studies.¹¹ To further study the specific mechanism or means of invasion of the mandible by OSCC, it is necessary to establish a corresponding animal model to better reflect the invasion of mandible by human tumours.

Despite the fact that there are several animal models for oral cancer, only a very small portion of research has so far focused on the animal model of OSCC invading the mandible,¹²⁻¹⁴ and none of these studies have gone into great depth on the modelling approach, tumorigenicity rate or success rate. The objective of the present study was to investigate and summarise the animal models of OSCC invading the mandible. It also aimed to establish a stable and repeatable animal model of OSCC invading the mandible with high tumorigenicity by implementing repeated experiments on multiple samples with comprehensive verification of anatomy, pathology and imaging.

Materials and methods

Reagents and instruments

Dulbecco's modified Eagle's medium (DMEM), 10% foetal bovine serum (FBS) and 0.25% trypsin (Gibco, Billings, MT, USA) were employed, along with a CBCT machine for dentistry (Kawa Group, Biberach, Germany); microcomputed tomography (microCT) machine (SCANCO Medical, Brüttisellen, Switzerland), 4% paraformaldehyde fixative (Guangzhou Saiguo Biotechnology, Guangzhou, China), isothane (Reward Life Sciences, Shenzhen, China and SCANCO Medical), isoflurane (Reward Life Sciences), ethylenediaminetetraacetic acid (EDTA) decalcification solution (Solarbio, Beijing, China), neutral gum (Taipu Biological, Xiamen, China) and haematoxylin-eosin (HE) staining solution (Xiamen Taipu Biological).

Cell culture

Human-derived OSCC cell lines CAL27 cells, HN6 cells, HN30 cells (Shanghai Zhongqiao Xinzhou Biological Company, Shanghai, China) were cultured in DMEM high glucose medium containing 10% FBS in a humidified incubator with an atmosphere containing 5% CO₂ at 37°C, and trypsin digestion was used for passaging when the cells were fused to 80%.

Animal feeding and grouping

Fifteen male BALB/c nude mice aged 3 to 5 weeks old, with a body mass of around 15 g, were purchased from Shanghai Slaughter Laboratory Animal Co, Ltd, China. All of the animal procedures were conducted in accordance with the Guidelines for the Care and Use of Laboratory Animals and were approved by the Institutional Animal Care and Use Committee at Fujian Medical University. Nude mice were acclimatised to the specific pathogen free (SPF) environment for 1 week, and the experiments were started at a body weight of around 20 g. The feeding environment was set at room temperature of 20°C to 22°C, humidity of 40% to 70%, and a light/dark cycle of 12 hours. The mice were supplied with adequate drinking water and feed.

The fifteen nude mice were randomly divided into three groups of five mice each, namely the CAL27 cell group, HN6 cell group and HN30 cell group. After the tumour was planted, the weight of the nude mice was recorded every other day, and the nude mice were sacrificed when the tumour size reached 1 cm³ or the weight decreased by 25% of the original weight, and the mandibular bone and tumour tissues were taken from the tumour-bearing side.

Tumour cell suspension preparation

When the cell confluence reached around 80% to 90% of the whole bottom of the dish, trypsin digestion was complete, and complete medium was added to terminate the digestion, blowing the cells at the bottom of the dish until all the cells at the bottom of the dish were dislodged; the liquid in the dish was transferred into a centrifuge tube, centrifuged (4°C, 1000 rpm, 5 minutes), and then the supernatant was discarded; 2 ml iced PBS was added to fully resuspend the cells, and 20 µl of the liquid was taken into the cell counting plate, and the cells in the same grid were counted in three different fields of view, and the mean was calculated. The total number of cells contained in 2 ml PBS was calculated by centrifugation and the supernatant was discarded, and

the total number of cells was adjusted to a cell density of 1×10^6 cells/0.1 ml by adding an appropriate amount of iced PBS, and then the cell suspensions were transferred into 2 ml Eppendorf (EP) tubes.

Establishment of animal model

After the nude mice were administered anaesthesia by a small animal gas anaesthesia machine, the appropriate concentration of anaesthetics was continuously administered for maintenance; the cell suspension was prepared and was gently blown out with a pipette gun before the cells were aspirated by a syringe, and the insulin injection needle was used to aspirate 0.1 ml of cells; the nude mice were disinfected with iodine violet in the right masseter area, and then the needle was inserted inwards and backwards at the horizontal level of the lower edge of the biting muscle, with the angle of needle insertion (Fig 1a) being parallel to the bone surface of the mandible, and the needle insertion was roughly 6 mm in length. When the tip of the needle was felt on the outer face of the mandible, the cell suspension was injected slowly, and the injection was observed while injecting. The injection was successful if there was localised elevation and no liquid oozing out of the mouth, and the injection needle was quickly withdrawn after the injection was completed to avoid leakage of the cell solution. The nude mice were put back into their cages to be reared after recovering their mobility.

HE staining

Different levels (sagittal and horizontal) of mandibular tissues were taken for HE staining, and the fixed mandibles were paraffin-embedded, prepared into 4- μ m-thick sections from the horizontal and sagittal planes of the mandible, stained with HE, sealed with neutral gum and observed under a microscope.

MicroCT assay

The specimen was removed from the fixative and wrapped in three to four layers with plastic wrap to retain moisture. It was placed in a sample tube with a diameter of 34 mm, stuffed with cotton to fix it to avoid artifacts caused by movement of the specimen during the scanning process and fixed so that the sample rested on the bottom of the tube, and then placed in the scanning instrument (SCANCO Medical, μ CT100) for scanning.

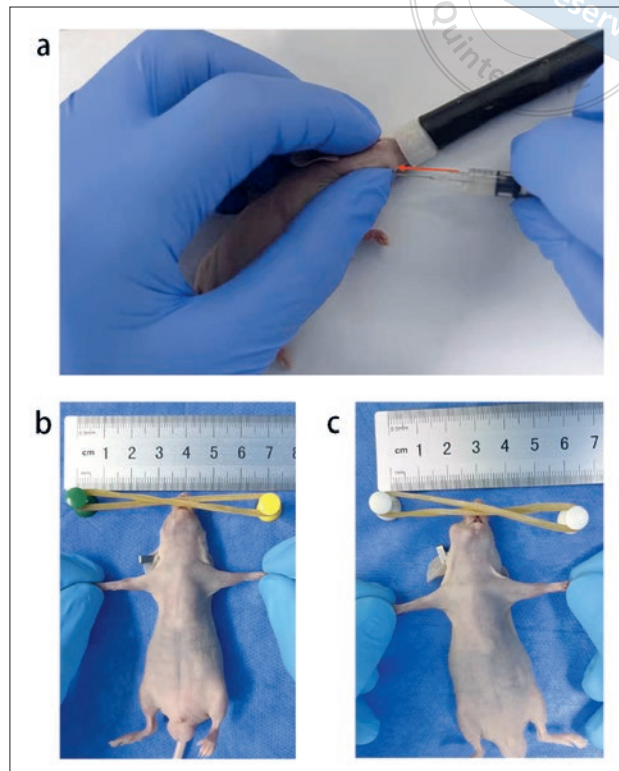


Fig 1a to c Moulding process. The red arrow indicates the needle entry angle (a). The early stage of tumor bearing (b). Later stage of tumour bearing (c).

Statistical analysis

SPSS 25.0 software (IBM, Chicago, IL, USA) was used for statistical analysis. The level of statistical significance was set at $P < 0.05$. One-way ANOVA showed that there was no significant difference in the body weight of nude mice at the time of tumour implantation between the groups ($P > 0.05$), but there was a significant difference in the survival cycle between the groups after tumour implantation ($P < 0.05$).

Results

Anatomical specimen verification

The cranial specimen of nude mice that met the standards for execution (Fig 2a) showed that the lateral occlusal muscle of the jaw on the normal side was not covered by tumour tissue. The normal side of the jaw was entirely peelable and hard when the right and left mandibles were separated, and tumour tissue had attached to the ascending branch of the mandible (Fig 2b). The posterior edge of the jaw was firm and offered little re-

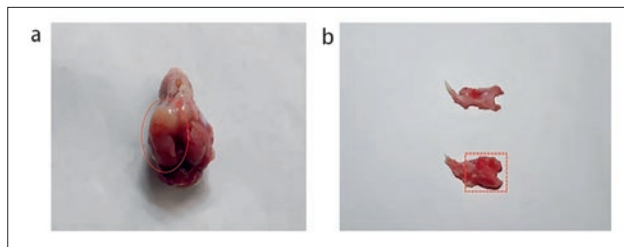


Fig 2a and b Anatomical specimens. Skull specimen; the red dotted area is the lateral mandibular tumour on the tumour-bearing side (a). Mandible specimen; the upper part of the figure is the normal side of the mandible, the mandible anatomical shape is complete and hard; the lower part is the tumour-bearing mandible. The red dotted line shows that the posterior margin of the mandible is wrapped with tumor tissue and is locally tough (b).

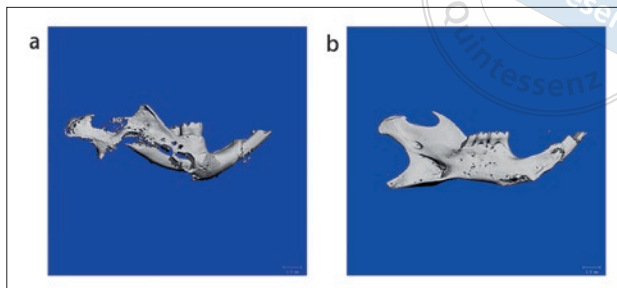


Fig 4a and b MicroCT of the mandible. The tumour-bearing side of the mandible showed that the mandibular bone was clearly damaged (a). Normal lateral mandible; the visible mandible anatomical structure is complete (b).

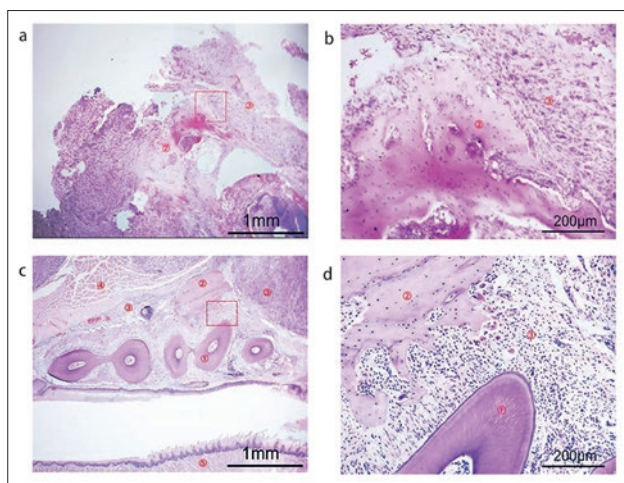


Fig 3a to d HE staining at different levels. Sagittal position of the mandible on the tumour-bearing side (40x); dotted line frame is shown by b (a). Sagittal position of the mandible on the tumour-bearing side (200x) (b). The area shown in (a) and (b) is a certain level of the ascending branches of the mandible from the side view, which show that the ascending branches of the mandible are eroded by tumour tissue. Horizontal position of the mandible on the tumour-bearing side (40x), as shown by dashed line box d (c). The horizontal position of the mandible on the tumour-bearing side (200x) (d). The areas shown in (c) and (d) are a certain level of the posterior teeth and buccal side of the mandible horizontal plane, and the masseter muscle, mandible and around the root of the tooth are all invaded by tumour cells. (Note: 1, teeth; 2, mandible; 3, tumour cells; 4, muscle; 5, tongue.)

sistance to needling, and the tumour profile was milky white.

Pathological verification

The isolated mandibular tissue underwent various levels of histological staining (Fig 3). Section staining from the

lateral side of the mandible revealed that squamous carcinoma cells had infiltrated and extensively destroyed the bone of the ascending mandibular branch at a specific level (Fig 3a and b), whereas section staining from the horizontal plane showed that the homogeneous side of the mandible at the same level had also been extensively destroyed by tumour cells (Fig 3c and d).

Imaging verification

Although the success of the model establishment was essentially verified through a combination of anatomical specimens and histological validation, microCT was performed as a supplement to the anatomical and pathological results to obtain additional 3D validation, as shown in Fig 4. This image demonstrates that, in comparison to the normal side of the mandible, the loaded side of the tumour clearly caused damage to the mandibular bone, and localised erosive destruction was visible.

Clinical manifestations of different oral squamous carcinoma cells invading the mandible

The HN30 and HN6 groups showed faster tumour formation, within just 1 week, whereas the CAL27 group had a noticeably slower tumour formation rate during the growth of the nude mice. The tumour-side samples of three different groups of oral squamous carcinoma cells invading the mandible were photographed and compared after the nude mice were sacrificed (Fig 5). The tumour cycles of the HN30 group were only about 18 days after tumour growth (Fig 5a, c and e), those for the HN6 group were 26 days, and those for the CAL27 group could be up to 52 days (Fig 5b, d and f), but there was no statistically significant difference in the changes in body weight between the groups.

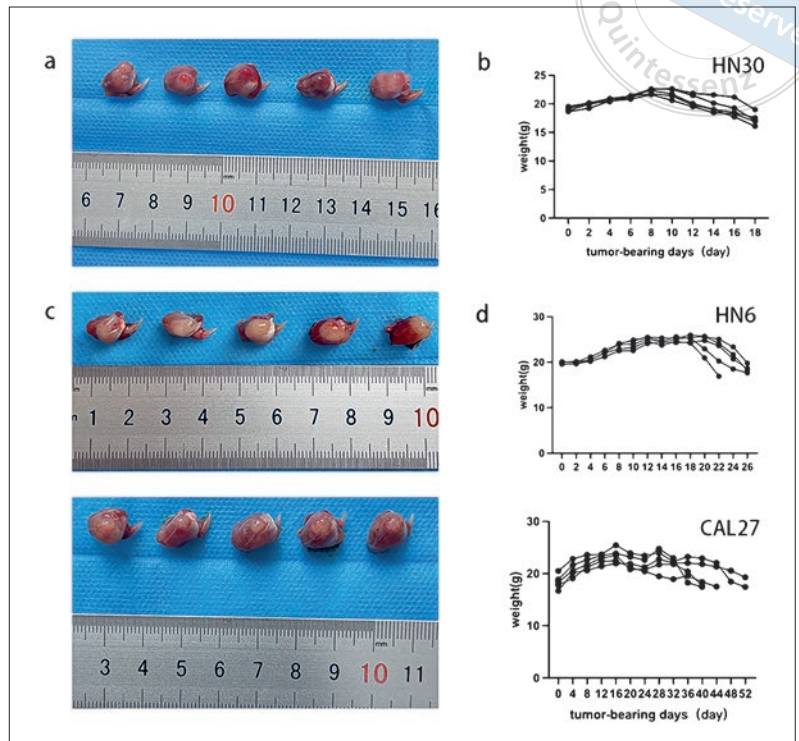


Fig 5a to f Curve of body weight and specimen after tumour formation. The mandibular specimens of the HN30 (a), HN6 (c) and CAL27 groups (e) were obtained after meeting the execution criteria. Body weight change curves of the HN30 (b), HN6 (d) and CAL27 groups (f) during tumour-bearing, respectively.

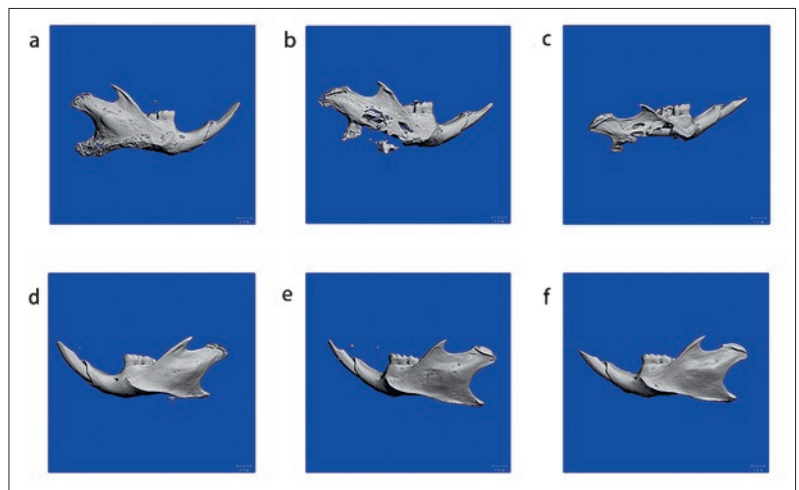


Fig 6 MicroCT of the mandible. The tumour-bearing mandibles in the HN30 (a), HN6 (b) and CAL27 groups (c) showed different degrees of bone destruction of the mandible. Normal lateral mandibles in the HN30 (d), HN6 (e) and CAL27 group (f), indicating complete mandibular anatomy.

Imaging manifestations of mandibular invasion by different OSCC cells

MicroCT examination of three groups of nude mice was performed, and it was found that the HN6 and HN30 group did not cause more obvious destruction to the mandible due to the rapid growth of the tumour. The results of microCT examination between the different groups revealed that, regardless of which OSCC cells were injected at the same injection concentration, the longer the survival cycle of nude mice with tumours,

the more extensive the destruction of the mandible; in contrast, the shorter the survival time of the tumour, the smaller the degree of destruction of the mandible (Fig 6).

Discussion

From 1954, when Salley¹⁵ coated the buccal sac of the golden gopher with dimethylbenzanthracene (DMBA) to make it malignant, to the present, when numerous animal models of oral cancer are frequently utilised,

diverse modelling techniques have been available for various studies. Reviewing the literature on earlier animal models of OSCC invading the mandible, it becomes clear that the modelling techniques used in this animal model were not particularly discussed. To explore the modelling approach further and summarise the modelling experience, the present authors investigated this model through repeated multi-sample experiments in this study.

The present study established the animal model of OSCC invading the mandible through comprehensive verification of anatomical specimens, histology and imaging. Through the processing of anatomical specimens, compared with the mandible on the normal side, the texture of the posterior border of the mandible on the hormonal side became brittle, and the lower border of the mandible could be defective or locally tough, and its bone surroundings were wrapped by tumour tissues to reach the state of no resistance to needling. Through HE staining for histological processing, it was discovered that the bone's surroundings, whether sagittal or horizontal, had been infiltrated by squamous carcinoma cells and had locally displayed infiltrative destruction. MicroCT 3D scans clearly demonstrated that the mandible on the hormonal side showed erosive resorption, which further supported the success of the model.

Some researchers have utilised carcinogenic drugs to apply carcinogenicity to animals' tongues or buccal parts,¹⁶ and there is also the approach involving drinking water carcinogenicity,¹⁷ according to previous experience with the construction of animal models of oral cancer. Although these methods can better simulate the process of tumour growth in the organism, it is questionable whether the tumour tissues they obtain can be the same or similar to the squamous carcinoma cells of human origin after primary culture. Additionally, the operation will be rather difficult and the experimental period of these autologous transplanted tumours, which are subsequently cultivated in primary culture to produce tumours, is significantly longer.

It is well known that the construction of animal models is a relatively long and difficult process, especially the animal model of OSCC invading the mandible; there are problems regarding inexperience in the method of model construction. During the pre-test, the present authors tried to inject the tumour cell suspension into the occlusal muscle, but found that the tumour would grow to the buccal skin in an "exophytic" manner, and its size and shape of the tumour would be different. Secondly, considering that the intraoral injection of the tumour would affect the nude mice's ability to eat and

breathe, the present authors finally chose the injection method mentioned above. Regarding the periosteum as a "natural barrier", they also considered whether it would hinder OSCC from invading the mandible, so designed the intervention periosteum group and the non-intervention periosteum group, and found that squamous carcinomas would damage the mandible regardless of the periosteum treatment; only the time and infiltration depth would be different. However, considering the intervention of the periosteum as an artificial factor, the subsequent experiments did not treat the periosteum.

Based on the experimental process and experience, the present authors concluded that several factors can affect the success of modelling. First, the cells themselves, including cell lineage, cell concentration, cell activity and the survival cycle of various oral squamous carcinoma cells, are significantly different. Second, the feeding environment will also have an impact on the survival cycle of nude mice. Under the SPF environment, the survival cycle of nude mice with tumour-bearing cells (CAL27 cells, injected with 1×10^6 cells/0.1 ml) is generally 1 to 2 months. In contrast, if the nude mice are in the general environment, or are constantly transferred to undergo other operations during this period, this influences the environment, which may lead to the shortening of the survival cycle. Third, for the nude mice tumour model, controlling the age of the mice is the most basic requirement. Thus, it is crucial to choose mice of an appropriate age. In this experiment, nude mice aged 4 to 6 weeks and weighing 20 ± 3 g were used, but their weight fluctuation could not be too great. Fourth, the degree of destruction of the mandible in the mandibular invasion model has a certain relationship with the survival cycle of the tumour-bearing nude mice; in other words, if the experimenter imposes certain changes in the treatment conditions or the operation, which indirectly lead to the prolongation of the survival cycle of the tumour, the degree of destruction of the mandible may also increase accordingly.

Through repeated experiments using numerous samples of various oral squamous carcinoma cells, the present findings demonstrate that, for this model, the method used in the study is straightforward, the experimental period is relatively short and the results satisfy the purpose of the experiment. Although this model is not optimal, it is the most suitable model at present. However, just as one key cannot open all doors, it is important that researchers select the best and most suitable model for their research according to their own experimental purpose, and obtain the results they want in order to cooperate to carry out the related research.

Conclusion

The animal model constructed in the present study not only mimicked the growth pattern of OSCC invading the mandible to a certain extent, but also provided a basis for conducting related research, and at the same time laid the foundation for other scholars to carry out research into the mechanism of OSCC invading the mandible, even though the present study has some shortcomings, such as the fact that the nude mice themselves have a defective immune system, which limits the development of immune-related research.

Acknowledgements

The authors thank all the study participants who contributed to this study.

Conflicts of interest

The authors declare no conflicts of interest related to this study.

Author contribution

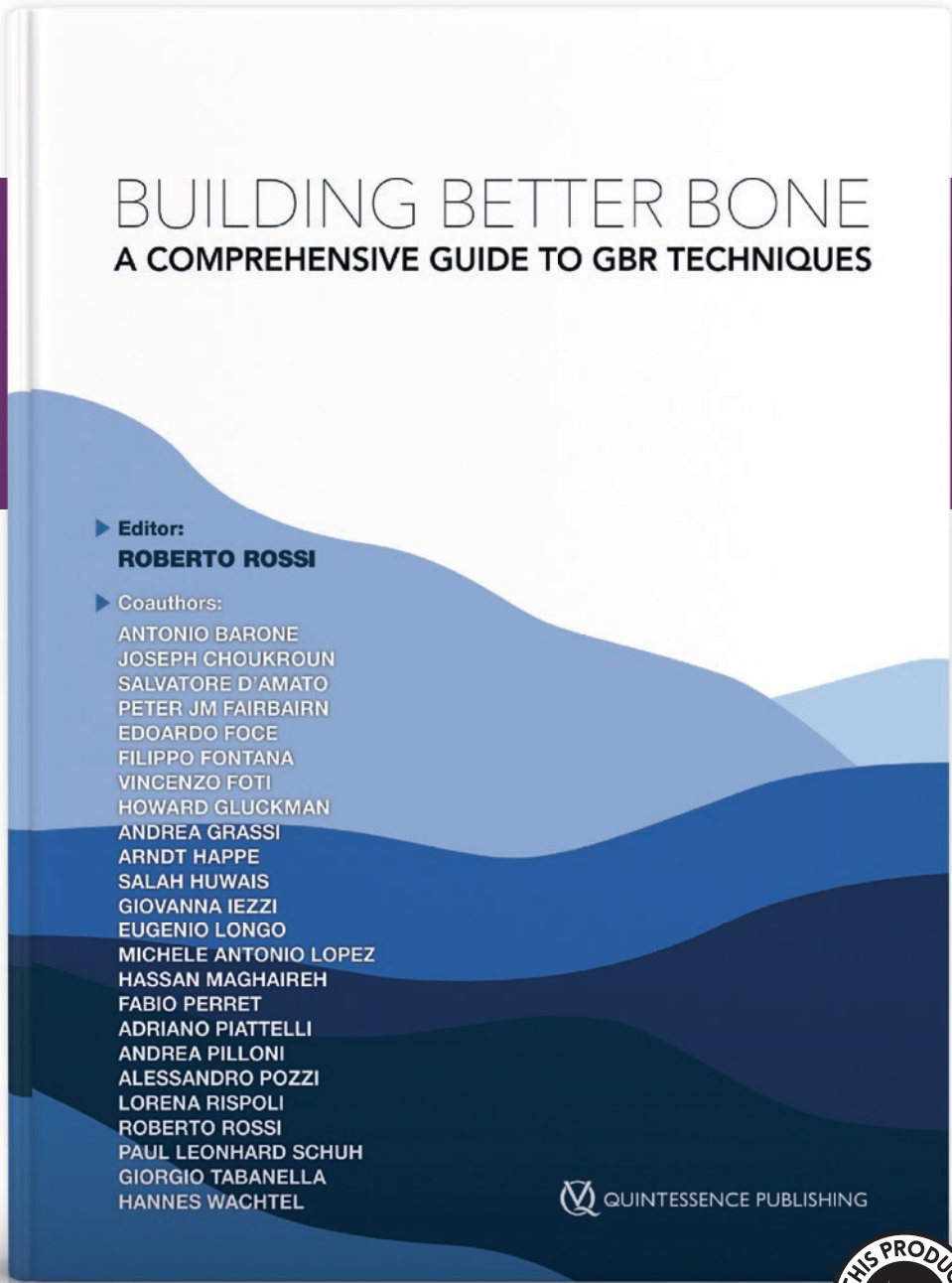
Dr Xiang Long ZHENG performed the experiments, analysed the data and drafted the manuscript; Drs Ya Qi CHEN and Cheng Hui LU contributed to the analysis and interpretation of the data; Drs Wen LL, Kang Wei ZHOU and Li Song LIN designed the study, analysed the data and critically revised the manuscript.

(Received Sep 09, 2023, accepted Mar 12, 2024)

References

1. Botticelli A, Mezi S, Pomati G, et al. The 5-Wh of immunotherapy in head and neck cancer. *Crit Rev Oncol Hematol* 2020;153:103041.
2. Miao L, Lv X, Huang C, Li P, Sun Y, Jiang H. Long-term oncological outcomes after oral cancer surgery using propofol-based total intravenous anesthesia versus sevoflurane-based inhalation anesthesia: A retrospective cohort study. *PLoS One* 2022;17:e0268473.
3. Silva LC, Faustino ISP, Ramos JC, et al. The importance of early treatment of oral squamous cell carcinoma: Case report. *Oral Oncol* 2023;144:106442.
4. Fan H, Tian H, Cheng X, et al. Aberrant Kank1 expression regulates YAP to promote apoptosis and inhibit proliferation in OSCC. *J Cell Physiol* 2020;235:1850–1865.
5. Fukumoto C, Uchida D, Kawamata H. Diversity of the Origin of Cancer Stem Cells in Oral Squamous Cell Carcinoma and Its Clinical Implications. *Cancers (Basel)* 2022;14:3588.
6. Hinni ML, Ferlito A, Brandwein-Gensler MS, et al. Surgical margins in head and neck cancer: a contemporary review. *Head Neck* 2013;35:1362–1370.
7. Goldschmidt S. Surgical Margins for Ameloblastoma in Dogs: A Review With an Emphasis on the Future. *Frontiers in Veterinary Science* 2022;9:830258.
8. Moratin J, Horn D, Metzger K, et al. Squamous cell carcinoma of the mandible – Patterns of metastasis and disease recurrence in dependence of localization and therapy. *J Cranio-maxillofac Surg* 2020;48:1158–1163.
9. Michalek J, Brychtova S, Pink R, Dvorak Z. Prognostic and predictive markers for perineural and bone invasion of oral squamous cell carcinoma. *Biomed Pap Med Fac Univ Palacky Olomouc Czech Repub* 2019;163:302–308.
10. Supsavhad W, Dirksen WP, Martin CK, Rosol TJ. Animal models of head and neck squamous cell carcinoma. *Vet J* 2016;210:7–16.
11. van der Worp HB, Howells DW, Sena ES, et al. Can Animal Models of Disease Reliably Inform Human Studies? *PLoS Med* 2010;7:e1000245.
12. Nomura T, Shibahara T, Katakura A, Matsubara S, Takano N. Establishment of a murine model of bone invasion by oral squamous cell carcinoma. *Oral Oncol* 2007;43:257–262.
13. Lee JK, Lim SC, Kim HD, et al. KITENIN represents a more aggressive phenotype in a murine model of oral cavity squamous carcinoma. *Otolaryngol Head Neck Surg* 2010;142:747–752.e741-742.
14. Furuta H, Osawa K, Shin M, et al. Selective inhibition of NF- κ B suppresses bone invasion by oral squamous cell carcinoma in vivo. *Int J Cancer* 2012;131:E625–E635.
15. Salley JJ. Experimental carcinogenesis in the cheek pouch of the Syrian hamster. *J Dent Res* 1954;33:253–262.
16. Tanaka T, Kawabata K, Kakumoto M, et al. Chemoprevention of 4-nitroquinoline 1-oxide-induced oral carcinogenesis by citrus auraptene in rats. *Carcinogenesis* 1998;19:425–431.
17. Yu L, Liu XQ, Chen YH, Chen X, Nie MH. Study on expression of LIM domain only protein 1 in SD rat oral buccal mucosa carcinogenesis induced by 4-nitro-quinoline N-oxide [in Chinese]. *Hua Xi Kou Qiang Yi Xue Za Zhi* 2020;38:133–138.

EXPERT "RECIPE MANUAL"



Roberto Rossi (Ed)

Building Better Bone

A Comprehensive Guide to GBR techniques

1st Edition 2024

Hardcover; incl 14 Videos, 408 pages, 1,360 illus.

ISBN 978-88-7492-096-9

€218

This book analyzes all aspects of a common problem in implant dentistry: the loss of one or more teeth, and the subsequent physiologic resorption of both hard and soft tissue. Defects resulting from tooth loss can be treated in several different ways, with similar but different surgical techniques, materials, and methods. GBR is a well-established approach with both advantages and disadvantages. Understanding how to select the optimal GBR technique ensures reduced risks for patients and clinicians alike. This book is intended to be a "recipe manual" for how to help build better bone, and includes varied protocols representing the state of the art in modern dentistry, without commercial bias. The book is also enriched by 14 videos that provide detailed explanations of the techniques adopted, and each chapter illustrates expert recommendations for optimizing the techniques presented.



Role of Antioxidant Enzymes in Pathogenesis of Oral Squamous Cell Carcinoma: a Systematic Review and Meta-analysis

Zainab NIAZI¹, Farah FARHAN², Sadia MUNEEER³, Hasan MUJTABA⁴, Nurul IBRAHIM⁵, Norhayati YUSOP¹

Objective: To investigate the antioxidant enzyme status in biological samples of patients with oral squamous cell carcinoma (OSCC) and compare them with biological samples of healthy people through a systematic review and meta-analysis.

Methods: Antioxidant enzymes of catalase (CAT), sodium dismutase (SOD) and glutathione peroxidase (GPx) were included in the analysis. A literature search was conducted of the PubMed, Science Direct, Scopus, Web of Science and Wiley Online Library databases for studies published between January 1999 and December 2022. A total of 831 articles were selected, of which 131 were found to be relevant. Finally, the full texts of 12 studies were screened and included. Studies that evaluated other antioxidant enzymes were excluded. Standardised mean difference (SMD) was derived to conduct a meta-analysis using comprehensive meta-analysis v3 (Biostat, Englewood, NJ, USA). A random effects model with 95% confidence interval (CI) was used to estimate the effect size. $P < 0.05$ was considered significant.

Results: CAT levels were measured in eight studies ($n = 567$) and the mean values for the OSCC and control groups were 4.81 ± 2.57 and 10.02 ± 1.81 , respectively (SMD 3.18, 95% CI 1.01 to 1.42; $P = 0.001$). SOD level was evaluated in 11 studies ($n = 762$) and the values for the OSCC and control groups were 3.78 ± 1.45 and 7.34 ± 1.79 , respectively (SMD 3.66, 95% CI 1.51 to 1.94; $P = 0.001$). GPx level was evaluated in 10 studies ($n = 697$) and the values for the OSCC and control groups were 13.33 ± 1.42 and 16.54 ± 2.9 , respectively (SMD 1.91, 95% CI 1.34 to 1.77; $P = 0.001$). The heterogeneity between the studies was severe ($I^2 \geq 90\%$). The risk of bias between studies was low to moderate.

Conclusion: Analysis revealed that the levels of antioxidant enzymes decreased in biological samples of patients with OSCC as compared to healthy controls. Understanding the pathological progress of OSCC by analysing the level of antioxidant enzymes is beneficial in formulating a personalised, targeted pro-oxidant therapy for cancer treatment.

Keywords: antioxidant enzymes, oral squamous cell carcinoma, pathogenesis

Chin J Dent Res 2024;27(3):243–251; doi: 10.3290/j.cjdr.b5698337

1 Universiti Sains Malaysia School of Dental Sciences, Kelantan, Malaysia.

2 Rawal Institute of Health Sciences, Islamabad, Pakistan.

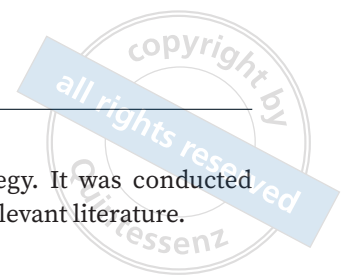
3 National University of Medical Sciences, Islamabad, Pakistan.

4 Shaheed Zulfiqar Ali Bhutto Medical University, Islamabad, Pakistan.

5 International Islamic University Malaysia, Pahang, Malaysia.

Corresponding author: Dr Norhayati YUSOP, Basic Sciences and Medical Unit, School of Dental Sciences, Universiti Sains Malaysia, Kelantan, 16150, Malaysia. Tel: 60- 97671185. Email: norhayatiyusop@usm.my

Antioxidant enzymes are proteins that play a critical role in protecting the body from the harmful effects of free radicals.^{1,2} Reactive oxygen species (ROS) are chemically reactive molecules that are generated as a byproduct of various cellular processes, including mitochondrial oxidative metabolism.³ Excessive levels of ROS can cause damage to cells. Hydroxyl radical (OH), hydrogen peroxide (H₂O₂) and superoxide (O²⁻) are some of the most common ROS generated in cells.⁴



The cellular antioxidant system in mammalian cells is composed of various enzymes that work together to protect cells from the harmful effects of oxidative stress. These enzymes include catalase (CAT), copper/zinc-containing superoxide dismutase (CuZn-SOD), manganese-containing superoxide dismutase (Mn-SOD) and glutathione peroxidase (GPx).⁵ Oxidative stress occurs when there is an imbalance between the production of ROS and the ability of cells to detoxify them.⁶ There is growing evidence to suggest that oxidative stress and ROS can contribute to the development of cancer.⁷

Cancer is a group of diseases characterised by the abnormal growth and division of cells that can invade and destroy surrounding tissues.⁸ Oral cancer is a serious disease that affects a significant number of people worldwide. It is estimated that around 3% of the world's population is affected by oral cancer.⁹ It is responsible for a high mortality rate and predominantly occurs in men.¹⁰ Smoking, tobacco use, areca nut chewing and alcohol consumption are among the well-known risk factors for oral cancers. In the context of oral carcinoma, studies have suggested that ROS play a role in the development and progression of the disease. For example, ROS levels have been shown to be higher in oral cancer cells compared to normal oral cells.¹¹⁻¹³

However, many studies have suggested that the activity levels of SOD, GPx and catalase are associated with the prognosis of cancer, including oral cancer.^{14,15} Reactive nitrogen species (RNS) are produced by the body's immune system in response to infection or inflammation. The levels of RNS and nitrosamines are increased in patients with oral squamous cell carcinoma (OSCC), a type of oral cancer.¹⁶ Hence, this analysis is focused on gathering the existing information on the expression status of relevant antioxidant enzymes of CAT, SOD and GPx in the tissues of OSCC. It was hypothesised that antioxidant enzymes play a role in pathogenesis samples of OSCC as compared to healthy tissue. By analysing the gathered data, the present authors aimed to investigate the potential association between antioxidant enzyme expression and OSCC development and progression. This study is expected to be useful in providing key information for future treatment and management of oral cancer.

Materials and methods

This systematic review and meta-analysis was conducted according to the population (samples with OSSC positive patients), intervention/exposure (enzymes CAT, SOD and GPx), controls (samples from normal tissue from the same patients) and outcomes (levels of anti-

oxidant enzymes (PIECO) strategy. It was conducted through the assessment of the relevant literature.

Databases and search engine

The study protocol was performed strictly adhered to the Preferred Reporting Items for Systematic reviews and Meta-Analysis (PRISMA) guidelines.¹⁷ The PubMed, Science Direct, Scopus, Web of Science and Wiley Online Library databases were searched for literature published between January 1999 and December 2022. A total of 12 case-controlled and cohort studies were included to investigate the status of antioxidant enzyme levels in patients with OSCC. Including studies that compare OSCC patients with healthy controls is also important to establish potential differences in antioxidant enzyme levels that may be associated with the development or progression of OSCC. The MeSH terms used in the literature search included "carcinoma, squamous cell", "mouth neoplasms", "squamous cell carcinoma of head and neck", "antioxidants enzymes and "pathology, oral". All studies discussing the role of antioxidant enzymes in OSCC and the control group were shortlisted and identified based on abstract and title screening. The relevant studies and abstracts were saved in Mendeley Web to have a proper reference.

Eligibility criteria

The inclusion criteria were case-control and cohort studies that evaluate the association between antioxidants and OSCC. Additionally, the criterion for including studies with sufficient data for calculating 95% confidence interval (CI) is important to ensure that the analysis was based on robust and reliable data. The following characteristics were extracted from each study: main author, publication year, sample size, level of antioxidant enzymes (catalase, sodium dismutase, glutathione peroxidase) and measurements in biological samples of OSCC patients and the control group. Articles not published in English or on unrelated topics, cadaveric studies and reviews, studies that did not include the three antioxidant enzymes CAT, SOD or GPx and measurement standards that were not the same were all excluded.

Antioxidant enzyme levels were assessed by polymerase chain reaction (PCR), DNA analysis and immunohistochemistry. These tests are extremely reliable.^{9,11} All the studies were analysed fully, including the methodology and variables to be measured. After evaluating all the features, the authors reviewed them against the search criteria. All the shortcomings of studies were

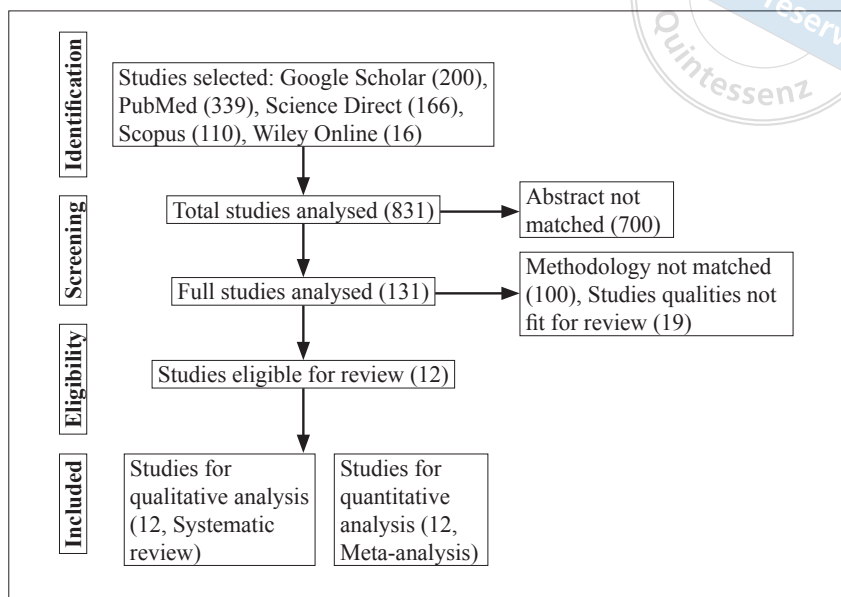


Fig 1 Study selection: PRISMA flowchart.

evaluated by entering values in the Newcastle-Ottawa quality assessment scale (NOS). The data were collected and tabulated separately in the specified format.

Data extraction and outcomes

Levels of antioxidant enzymes and their mean analysis were the outcomes, whereas study design, age range, sex, sampling technique, sample size and their *P* values were extracted from articles and tabulated in a separate table for detailed analysis.

Data collection and assessment

Two independent reviewers (ZN and FF) were involved in the literature review process. They independently reviewed the full texts of studies that passed the initial screening process, extracting relevant data from each one. Any disagreement between these two investigators was resolved through discussion with a third author. Duplicate references were eliminated using manual reference management software Mendeley to save time and reduce the risk of errors. The NOS was used to assess the quality of the studies.¹⁸ The NOS is divided into three sections, which assess the quality of a study's selection, comparability and outcome investigation. It assigns points or stars for each question in each section of the scale. For cohort studies, a score of up to 3 is categorised as high risk of bias, a score between 4 and 6 is classed as moderate risk of bias, and a score between 7 and 9 is categorised as low risk of bias. For cross-sectional studies, a score of up to 4 is categorised as high risk

of bias, a score between 5 and 6 is classed as moderate risk of bias, a score between 7 and 8 is deemed low risk of bias, and a score between 9 and 10 is categorised as very low risk of bias.

Data synthesis

The standardised mean difference (SMD) was used in the meta-analysis to pool the results of studies that had reported outcomes using different measurement scales or units. It was calculated by dividing the difference in means of the two groups by the pooled standard deviation. For SMD, statistical software Comprehensive Meta-Analysis v 3.0 (Biostat, Englewood, NJ, USA) was used.¹⁹ SMD was employed to compare the levels of CAT, SOD and GPx biomarkers between patients with OSCC and a control group with an effect size of 95% CI. A random-effects model was used to account for significant heterogeneity with I^2 , *Q* test and *T*-squared values among the studies in this analysis. Prediction intervals with forest plots and publication bias with funnel plots was used. Studies with the same values of CAT, SOD and GPx in similar units were included.

Results

A total of 831 studies were gathered using the search strategy, including 339 from PubMed, 166 from Science Direct, 200 from Google Scholar, 110 from Scopus and 16 from Wiley Online Library. After screening of abstracts and titles, 700 studies that did not meet the inclusion criteria were excluded. The full texts of all the remain-



Table 1 Study characteristics and level of CAT, SOD and GPx in different biological samples.

Study	Country	Study design	Sex	Age range (y)	Sample size	Sample type	Unit	OSCC, mean ± SD	Healthy, mean ± SD	P value
Subapriya et al ²⁰	India	Cohort	M 8, F4	45–60	12	Erythrocyte-lysate	µmole/s/mg Hb	CAT 1.89 ± 0.12; SOD 1.53 ± 0.22; GPx 8.62 ± 0.08	CAT 2.77 ± 0.26; SOD 3.63 ± 0.35; GPx 11.63 ± 1.12	≤ 0.05
Beevi et al ²¹	India	Cohort	M 12, F 3	33–72	15	Erythrocyte	µmole/mg/Hb	CAT 14.44 ± 1.63; SOD 10.07 ± 2.93; GPx 33.4 ± 1.38	CAT 33.63 ± 2.59; SOD 21.35 ± 2.80; GPx 13.80 ± 1.22	0.0001
Manoharan et al ²³	India	Case control	M 48, F 0	40–60	48	Erythrocyte-lysate	µmole/mg/Hb	CAT 1.22 ± 0.07; SOD 1.73 ± 0.09; GPx 15.24 ± 1.3	CAT 1.76 ± 0.12; SOD 2.29 ± 0.17; GPx 22.32 ± 1.86	≤ 0.01
Kalayci et al ²²	Turkey	Case control	M 14, F 6	40–76	20	Tissue	U/mg protein	SOD 0.76 ± 0.02; GPx 1.89 ± 1.71	SOD 0.86 ± 0.02; GPx 0.17 ± 0.11	≥ 0.05
Sharma et al ²⁴	India	Cohort	M 102, F 18	40–60	120	Blood	U/ml	SOD 3.92 ± 1.75; GPx 0.03 ± 0.62	SOD 3.11 ± 1.95; GPx 0.02 ± 0.02	0.001
Srivastava et al ²⁵	India	Case control	M 27, F 13	38–85	40	Blood	u/g Hb	CAT 1.30 ± 0.02; SOD 1.45 ± 0.11; GPx 0.03 ± 0.62	CAT 1.95 ± 0.49; SOD 2.28 ± 0.30; GPx 0.02 ± 0.02	≤ 0.001
Shilpasree et al ²⁶	India	Case control	M 15, F 15	40–70	30	Tissue	nmol/min/mg	CAT 0.22 ± 0.31; SOD 1.57 ± 0.14; GPx 7.72 ± 3.96	CAT 0.59 ± 0.04; SOD 2.91 ± 0.35; GPx 19.70 ± 1.49	≤ 0.0001
Sehitogullari et al ²⁷	Turkey	Case control	M 23, F 42	50–70	65	Serum	U/ml	SOD 7.39 ± 2.62; GPx 22.05 ± 2.73	SOD 25.01 ± 2.83; GPx 47.32 ± 3.75	0.05
Banerjee et al ²⁸	India	Case control	M 25, F 5	25–50	30	Tissue	mg/min	CAT 2.00 ± 2.09	CAT 6.40 ± 0.29	0.0001
Babiuch et al ²⁹	Poland	Case control	M 20, F 20	25–70	40	Saliva	U/ml	SOD 7.07 ± 5.30; GPx 20.53 ± 0.73	SOD 2.36 ± 2.42; GPx 15.00 ± 17.00	0.001
Shahi et al ³⁰	India	Case control	M 86, F 34	26–68	120	Blood	U/min/ml	CAT 14.70 ± 9.80; SOD 4.60 ± 2.24	CAT 29.00 ± 9.20; SOD 10.80 ± 7.40	≤ 0.005
Sushma et al ³¹	India	Case control	M 125, F 75	26–70	200	Serum	U/100 mg protein	CAT 2.71 ± 6.51; SOD 1.49 ± 0.49; GPx 10.70 ± 0.73	CAT 4.03 ± 1.48; SOD 6.10 ± 1.12; GPx 13.80 ± 1.25	≤ 0.005

The Granularity-Related Inconsistency of Means (GRIM) test is used to identify potential errors or inconsistencies in the reporting of means of CAT, SOD and GPx markers in the selected studies.

CAT level was measured in eight studies. In five studies,^{21,26,28,30,31} the statistical means were inconsistent. SOD level was measured in 11 studies (Table 1). The GRIM statistical test showed that three studies^{24,27,29} and the five abovementioned studies of CAT levels are inconsistent due to the differences in biological sample collection method and sample sizes.

GPx level was measured in 10 studies. The GRIM statistical test showed that statistical means were inconsistent in all studies.

Thus, there is the possibility of publication bias between studies in which statistical means were inconsistent.

ing 131 studies relevant to the present studies were screened. Finally, only 12 studies had data compatible with a meta-analysis (Fig 1).

All study characteristics and the levels of CAT, SOD and GPx in various biological samples are presented in Table 1.²⁰⁻³¹ The NOS was used to assess the quality of the studies (Table 2).²⁰⁻³¹

The biological samples of CAT levels in eight studies (n = 567) were reported. The mean values for the OSCC and control groups were 4.81 ± 2.57 and 10.02 ± 1.81, respectively. The overall SMD in the random model was 3.18 (Z = 4.92, 95% CI 1.01 to 1.42; P = 0.0001). There was

severe heterogeneity between the studies (I² = 96.3%, Q = 188.47, τ² = 3.01, variance 5.41; P = 0.0001). There was an increase in CAT level in all studies with respect to CAT activity (Fig 2). The study publication bias was measured in a funnel plot (Fig 3).

The level of SOD was evaluated in 11 studies (n = 762). The mean values for the OSCC and control groups were 3.78 ± 1.45 and 7.34 ± 1.79, respectively. The overall level of SOD in biological samples showed an SMD in the random model of 3.66 (Z = 4.10, 95% CI 1.51 to 1.94; P = 0.001). There was severe heterogeneity between the studies (I² = 98.2%, Q = 556.37; τ² = 8.42, variance 28.11;

Table 2 Quality of studies assessed using the NOS.

Selection					Comparability		Exposure				
Study	Case definition	Case represents	Control selection	Control definition	Known cont. factor	Potential cont. factor	Secure patient	Interviewer blinded to case and control	Similarity case and control	No response	Total
Subapriya et al ²⁰	1	1	1	1	NA	NA	1	NA	1	NA	6
Beevi et al ²¹	1	1	1	NA	1	NA	1	NA	NA	NA	5
Kalayci et al ²²	1	1	1	1	NA	NA	1	NA	1	NA	6
Monohara et al ²³	1	1	1	NA	NA	NA	1	NA	1	1	6
Sharma et al ²⁴	1	1	1	1	1	NA	1	NA	1	1	8
Srivastava et al ²⁵	1	1	1	1	NA	1	1	NA	1	1	8
Shilpasree et al ²⁶	1	1	1	1	NA	NA	1	NA	1	1	7
Sehitogullari et al ²⁷	1	1	1	1	1	1	1	NA	NA	1	8
Banerjee et al ²⁸	1	1	1	1	NA	NA	1	NA	1	1	7
Babiuch et al ²⁹	1	1	1	1	NA	NA	1	NA	NA	1	6
Shahi et al ³⁰	1	1	1	1	NA	NA	1	NA	1	1	7
Sushma et al ³¹	1	1	1	1	NA	NA	1	NA	1	NA	6

Note: For cohort studies, the NOS classes a score of up to 3 as high risk of bias, a score between 4 and 6 as moderate risk of bias, and a score between 7 and 9 as low risk of bias. For cross-sectional studies, the NOS classes a score of up to 4 as high risk, a score between 5 and 6 as moderate risk of bias, a score between 7 and 8 as low risk of bias, and a score between 9 and 10 as very low risk of bias. NA, not available.

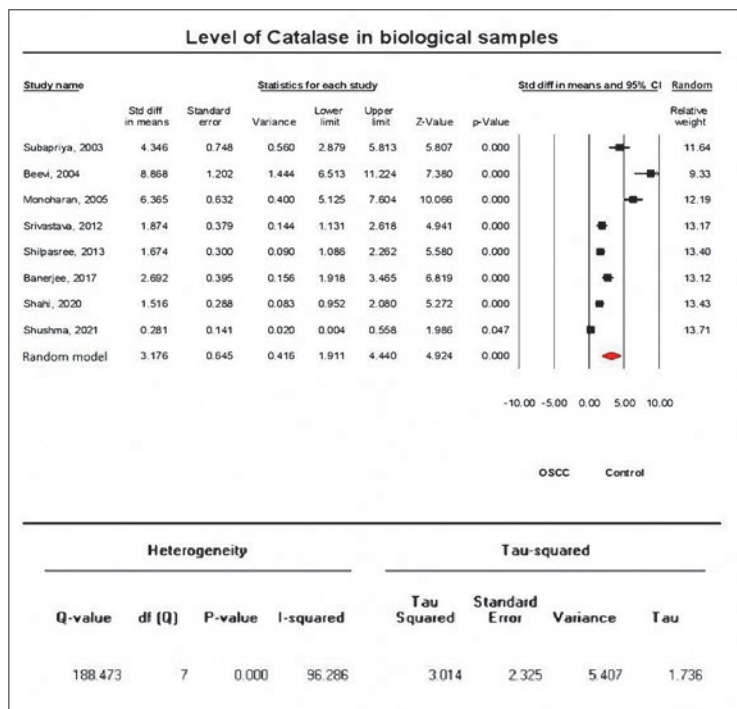


Fig 2 Forest plot showing weighted mean/relative weight (random) and SMD estimates with 95% CI for the differences in CAT levels between the OSCC group and the healthy control group. To estimate the variance of true effect size between the studies, τ^2 was applied (value: 3.01).

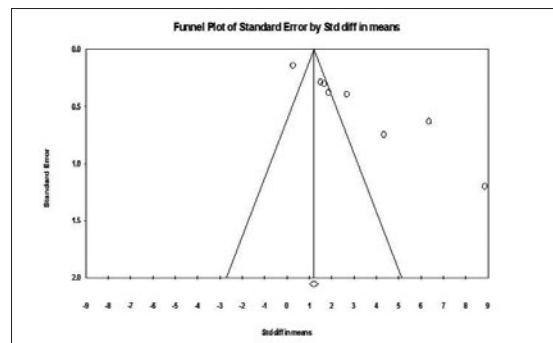


Fig 3 Publication bias between the studies. The funnel plot shows that only three studies were significant, perhaps due to the inconsistencies between the biological sample types and means of the studies. The margin of error was 10% between the studies' level of publication bias.

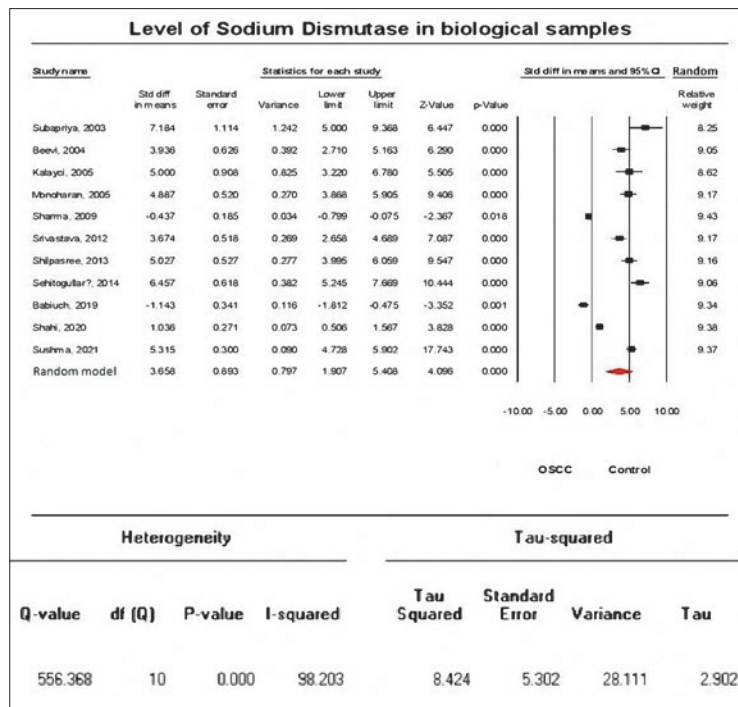
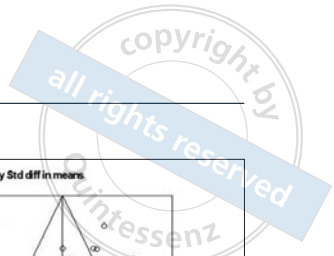


Fig 4 Forest plot showing weighted mean/relative weight (random) and SMD estimates with 95% CI for the differences in SOD levels between the OSCC group and the healthy control group. To estimate the variance of true effect size between studies, τ^2 was applied (value: 8.42).

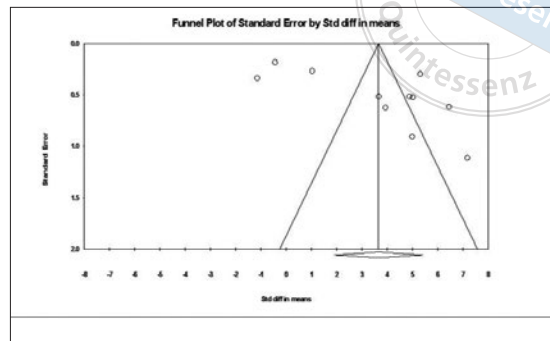


Fig 5 Publication bias between the studies. The funnel plot shows that only three studies were significant, perhaps due to the inconsistencies between the means of the studies. The margin of error was 10% between the studies' level of publication bias.

$P = 0.0001$). The level of SOD was significantly decreased in biological samples with OSCC compared to healthy ones (Fig 4). The study publication bias was measured in a funnel plot (Fig 5).

The GPx level was calculated in 10 studies ($n = 697$). The mean for the OSCC and control groups was 13.33 ± 1.42 and 16.54 ± 2.90 , respectively. There was a significant decrease in GPx levels in biological samples with OSCC. The overall SMD in GPx level in the random model was 1.91 ($Z = 2.13$, 95% CI 1.34 to 1.77; $P = 0.03$). There was severe heterogeneity between the studies ($I^2 = 98.1\%$, $Q = 471.57$, $\tau^2 = 7.50$, variance 29.96, $P = 0.0001$); however, the GPx level was significantly decreased in biological samples with OSCC compared to healthy ones (Fig 6). The study publication bias was measured in a funnel plot (Fig 7).

The high heterogeneity in this meta-analysis showed I^2 values of CAT 96.3, SOD 98.2 and GPx 98.1 (Figs 2, 4 and 6). The different methods used in reporting studies to measure antioxidant enzyme levels could be the reason for high heterogeneity. When meta-regression analysis was performed on sample size and types, insignificant R^2 (9%, $P = 0.211$) was recorded.

The R^2 value was very low and insignificant in the meta-regression model, and indicates that the sample

size and types of samples were also potential reasons for heterogeneity.

Discussion

This study investigated the role of antioxidant enzymes in OSCC. A total of 12 studies were included in the analysis. Most of the studies reported that the statistical means of CAT, SOD and GPx levels in biological sample were inconsistent. The combined analysis of the studies of antioxidant enzymes is considered severely heterogeneous. The overall quality of the evidence is "average to good".

Oxidative stress occurs when there is an imbalance between the production of ROS and the body's ability to counteract or repair the damage caused by them.³² Prolonged exposure to oxidative stress and sustained inflammation can lead to the accumulation of genetic damage, which can increase the risk of cancer development. This is because oxidative stress can cause damage to DNA and other cellular components, and if the damage is not repaired or removed, it can accumulate over time and lead to genetic mutations and other changes that contribute to cancer initiation.³³ ROS are associated with high free radicals and reactivity that are

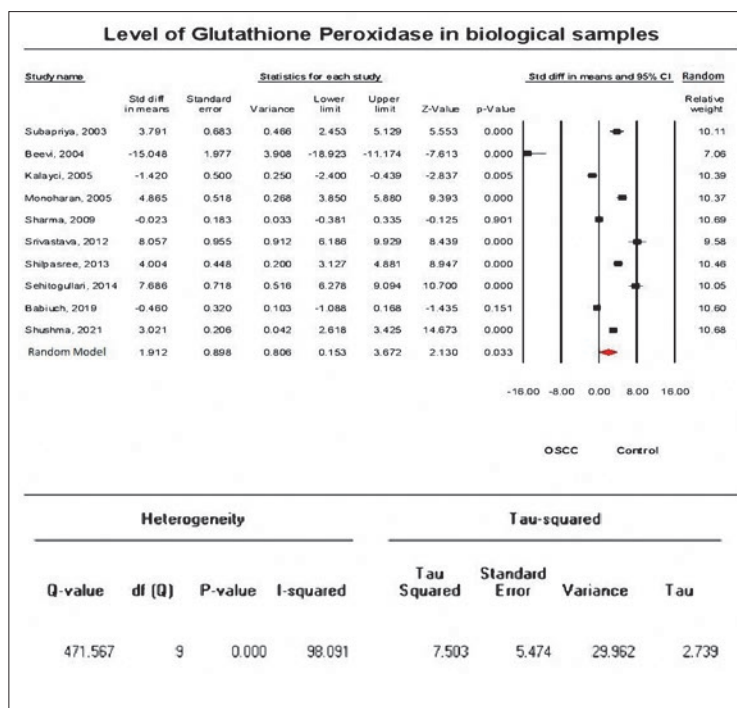


Fig 6 Forest plot showing weighted mean/relative weight (random) and SMD estimates with 95% CI for the differences in GPx levels between the OSCC group and the healthy control group. To estimate the variance of true effect size between studies, τ^2 was applied (value: 7.50).

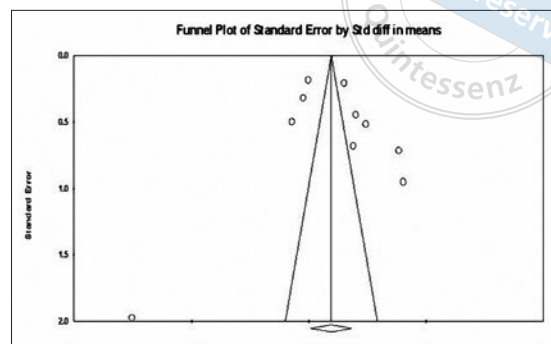


Fig 7 Publication bias between the studies. The funnel plot shows that no studies were significant, perhaps due to the inconsistencies between the mean data of the studies. The margin of error was 10% between the studies' level of publication bias.

involved in different processes, especially in the initiation and promotion of OSCC.³⁴ A network of antioxidant enzymes controls the cellular maintenance of the redox system. Amongst the enzymes, the most common are CAT, SOD and GPx.³⁵ Despite the existence of diverse protection mechanisms against oxidant injuries, redox homeostasis is altered within tumour cells. Excessive ROS production is associated with alteration of gene expression and genetic instability, favouring cancer cell proliferation.³⁶

In the present study, levels of CAT, SOD and GPx were analysed in different biological samples taken from patients with OSCC and healthy patients. In a study performed by Subapriya et al,²⁰ the activity of CAT, SOD and GPx was decreased by 58%, 33% and 59%, respectively, in preoperative OSCC patients as compared to normal subjects. The findings showed that an imbalance in the redox status of patients with oral cancers may be due to the compromised antioxidant levels. Decreased levels of CAT, GPx and SOD in erythrocyte lysate of oral cancer patients as compared to healthy patients has also been reported.^{21,23} Furthermore, GSH-Px levels were reported to increase significantly in cancerous patients' tissue as compared with cancer-free tissues ($P \leq 0.05$), whereas an insignificant

difference was reported between SOD activities ($P \geq 0.05$).^{22,23}

Overall, a decline in the enzymatic and non-enzymatic antioxidant enzyme level in oral cancer patients has been a common finding in various studies.²¹⁻²⁴ Antioxidant levels decreased gradually in oral cancer patients from stage II to stage IV.²⁵ Further experimental evidence also demonstrated a significantly low level ($P = 0.001$) of SOD and GPx in cancer patients compared to healthy patients.²⁶ Similarly, the mean levels of antioxidant enzymes CAT, SOD and GPx were lower in study cases, and the difference was highly statistically significant.^{27,28} These findings suggest the presence of oxidative stress in oral cancer patients; however, analysis of correlation (r) showed a significantly negative correlation between antioxidant and pro-oxidant levels in patients ($P \leq 0.05$).²⁷ Hence, it is postulated that OSCC is closely associated with a marked increase in oxidative stress and a decrease in antioxidant enzyme activities.²⁸ On a similar note, a decrease in antioxidant level was reported in the blood of patients diagnosed with OSCC as compared with healthy controls ($P \leq 0.001$).²⁶ Meanwhile, GSH showed a significant positive correlation with SOD ($P \leq 0.001$), GPx and CAT ($P \leq 0.01$).²⁶ Likewise, oral cancer

patients demonstrated significantly reduced levels of SOD and GPX ($P \leq 0.005$), with no significant difference observed with regard to catalase level.³¹ The findings further suggested the role of superoxide dismutase and glutathione peroxidases in the progression and development of oral carcinogenesis.³¹

However, in a different study performed on OSCC samples, post-hoc analysis showed that patients with OSCC had a markedly increased level of SOD compared with the control groups.³⁰ Different approaches have been used by researchers to evaluate the amount of SOD, GPX and catalase in diverse biological samples, which may have different results. The majority of the OSCC group patients in those studies were categorised using various clinical staging methods and histological grading systems. Future research intending to evaluate the impact of oxidative stress on tumours should consider these details in the OSCC group's antioxidant enzymes assessment.

Limitations

This analysis has several limitations. The Begg test failed to find a statistically significant publishing bias. It was also challenging to compare the research to determine the relationship between the results due to the wide variety of sample sizes in the different studies. Further analysis of the effect of antioxidant enzymes on tumour tissue should be carried out to better understand the relationship between the different treatments and outcomes. Biological samples should be preferred as they experience the greatest enzymatic changes in patients with tumours compared to normal samples.

Conclusion

The majority of investigations showed that individuals with OSCC had significantly lower antioxidant levels than healthy controls. Antioxidant enzymes are possible biomarkers for oxidative stress and a reliable prognostic predictor of OSCC.

Conflicts of interest

The authors declare no conflicts of interest related to this study.

Author contribution

Drs Zainab NIAZI and Norhayati YUSOP contributed to the research design and data collection; Drs Farah FARHAN and Sadia MUNEER contributed to the stat-

istical analysis and manuscript draft; Drs Hasan MUJ-TABA and Zainab NIAZI contributed to project management and manuscript revision; Dr Nurul IBRAHIM contributed to the critical revision of the manuscript.

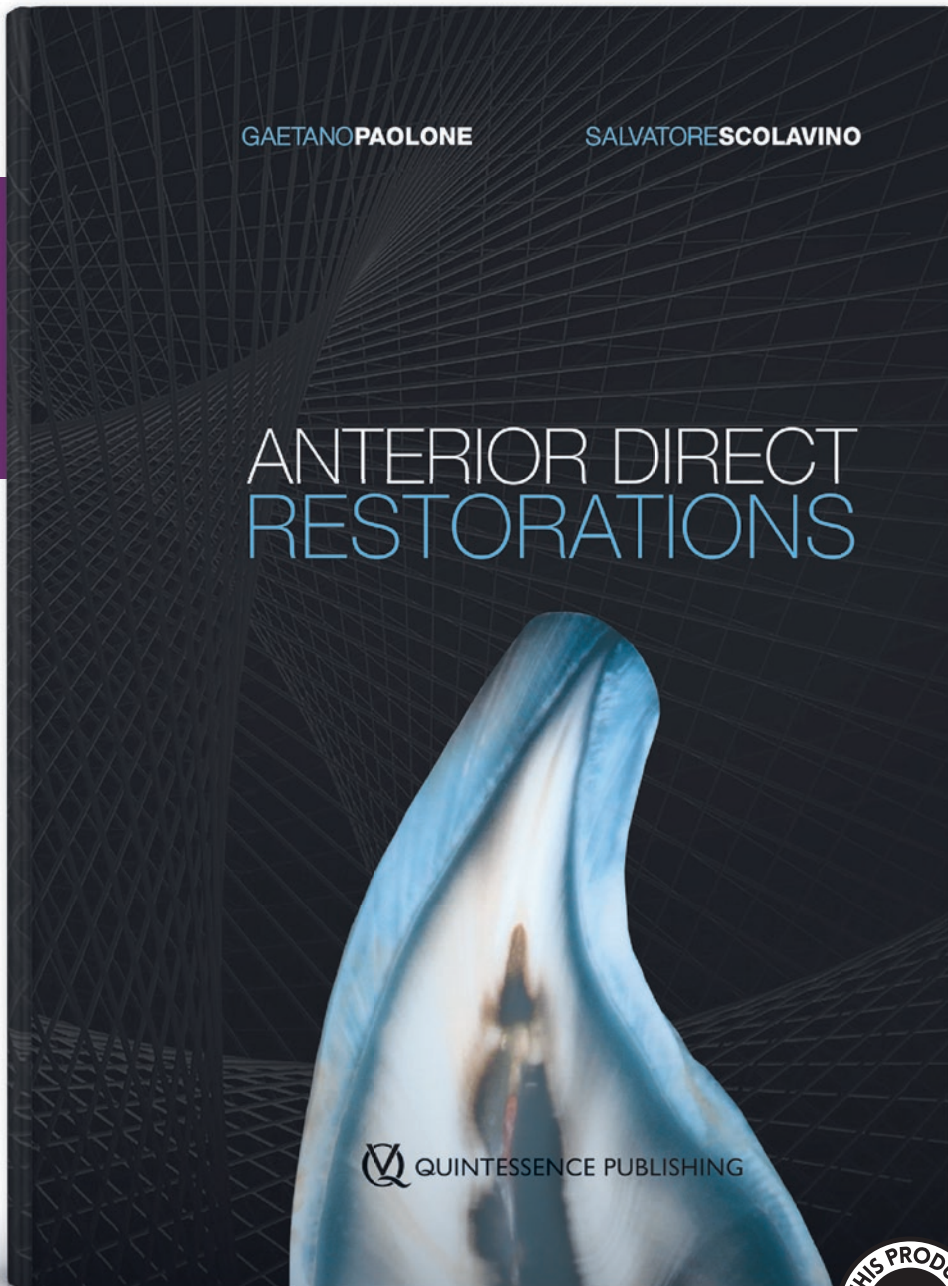
(Received June 20, 2023; accepted May 30, 2024)

References

1. Young IS, Woodside JV. Antioxidants in health and disease. *J Clin Pathol* 2001;54:176–186.
2. Roy Z, Bansal R, Siddiqui L, Chaudhary N. Understanding the role of free radicals and antioxidant enzymes in human diseases. *Curr Pharm Biotechnol* 2023;24:1265–1276.
3. Rogers NM, Seeger F, Garcin ED, Roberts DD, Isenberg JS. Regulation of soluble guanylate cyclase by matricellular thrombospondins: implications for blood flow. *Front Physiol* 2014;5:134.
4. Zuo L, Zhou T, Pannell BK, Ziegler AC, Best TM. Biological and physiological role of reactive oxygen species--the good, the bad and the ugly. *Acta Physiol (Oxf)* 2015;214:329–348.
5. Ighodaro OM, Akinloye OA. First line defence antioxidants-superoxide dismutase (SOD), catalase (CAT) and glutathione peroxidase (GPX): Their fundamental role in the entire antioxidant defence grid. *Alexandria J Med* 2018;54:287–293.
6. He L, He T, Farrar S, Ji L, Liu T, Ma X. Antioxidants maintain cellular redox homeostasis by elimination of reactive oxygen species. *Cell Physiol Biochem* 2017;44:532–553.
7. Hayes JD, Dinkova-Kostova AT, Tew KD. Oxidative stress in cancer. *Cancer Cell* 2020;38:167–197.
8. Jiang WG, Sanders AJ, Katoh M, et al. Tissue invasion and metastasis: Molecular, biological and clinical perspectives. *Semin Cancer Biol* 2015;35(suppl):S244–S275.
9. Bugshan A, Farooq I. Oral squamous cell carcinoma: metastasis, potentially associated malignant disorders, etiology and recent advancements in diagnosis. *F1000Res* 2020;9:229.
10. Abati S, Bramati C, Bondi S, Lissoni A, Trimarchi M. Oral cancer and precancer: a narrative review on the relevance of early diagnosis. *Int J Environ Res Public Health* 2020;17:9160.
11. Kumar SA, Indu S, Gautami D, VarRuchi S. Oral squamous cell carcinoma (OSCC) in humans: Etiological factors, diagnostic and therapeutic relevance. *Res J Biotechnol* 2020;15:141–151.
12. Pastushenko I, Blanpain C. EMT transition states during tumor progression and metastasis. *Trends Cell Biol* 2019;29:212–226.
13. Vo TT, Wu CZ, Lee IT. Potential effects of noxious chemical-containing fine particulate matter on oral health through reactive oxygen species-mediated oxidative stress: Promising clues. *Biochem Pharmacol* 2020;182:114286.
14. Weydert CJ, Cullen JJ. Measurement of superoxide dismutase, catalase and glutathione peroxidase in cultured cells and tissue. *Nat Protoc* 2010;5:51–66.
15. Jablonska E, Gromadzinska J, Peplonska B, et al. Lipid peroxidation and glutathione peroxidase activity relationship in breast cancer depends on functional polymorphism of GPX1. *BMC Cancer* 2015;15:657.
16. Scher RL. Role of nitric oxide in the development of distant metastasis from squamous cell carcinoma. *Laryngoscope* 2007;117:199–209.
17. Page MJ, McKenzie JE, Bossuyt PM, et al. The PRISMA 2020 statement: an updated guideline for reporting systematic reviews. *Int J Surg* 2021;88:105906.

18. Andrade C. Mean Difference, Standardized Mean Difference (SMD), and Their Use in Meta-Analysis: As Simple as It Gets. *J Clin Psychiatry* 2020;81:20f13681.
19. Bae JM. A suggestion for quality assessment in systematic reviews of observational studies in nutritional epidemiology. *Epidemiol Health* 2016;38:e2016014.
20. Subapriya R, Kumaraguruparan R, Nagini S, Thangavelu A. Oxidant-antioxidant status in oral precancer and oral cancer patients. *Toxicol Mech Methods* 2003;13:77–81.
21. Beevi SS, Rasheed AM, Geetha A. Evaluation of oxidative stress and nitric oxide levels in patients with oral cavity cancer. *Jpn J Clin Oncol* 2004;34:379–385.
22. Kalayci A, Ozturk A, Ozturk K, Karagozoglu E, Dolanmaz D. Superoxide dismutase and glutathione peroxidase enzyme activities in larynx carcinoma. *Acta Otolaryngol* 2005;125:312–315.
23. Manoharan S, Kolanjiappan K, Suresh K, Panjamurthy K. Lipid peroxidation & antioxidants status in patients with oral squamous cell carcinoma. *Indian J Med Res* 2005;122:529–534.
24. Sharma M, Rajappa M, Kumar G, Sharma A. Oxidant-antioxidant status in Indian patients with carcinoma of posterior one-third of tongue. *Cancer Biomark* 2009;5:253–260.
25. Srivastava KC, Austin RD, Shrivastava D, Sethupathy S, Rajesh S. A case control study to evaluate oxidative stress in plasma samples of oral malignancy. *Contemp Clin Dent* 2012;3:271–276.
26. Shilpasree AS, Kumar K, Itagappa M, Ramesh G. Study of oxidative stress and antioxidant status in oral cancer patients. *Int J Oral Maxillofac Surg* 2013;4:2–6.
27. Sehitogullari A, Aslan M, Sayir F, Kahraman A, Demir H. Serum paraoxonase-1 enzyme activities and oxidative stress levels in patients with esophageal squamous cell carcinoma. *Redox Rep* 2014;19:199–205.
28. Banerjee S, Mukherjee S, Mitra S, Singhal P. Altered expression of mitochondrial antioxidants in oral squamous cell carcinoma. *J Oral Sci* 2017;59:439–446.
29. Babiuch K, Bednarczyk A, Gawlik K, et al. Evaluation of enzymatic and non-enzymatic antioxidant status and biomarkers of oxidative stress in saliva of patients with oral squamous cell carcinoma and oral leukoplakia: a pilot study. *Acta Odontol Scand*. 2019;77:408–418.
30. Shahi Y, Samadi FM, Mukherjee S. Plasma lipid peroxidation and antioxidant status in patients with oral precancerous lesions and oral cancer. *Oral Sci Int* 2020;17:86–93.
31. Sushma PS, Jamil K, Udaykumar P, et al. Analysis of CCND1 protein and circulatory antioxidant enzyme activity association in oral squamous cell carcinoma. *Saudi J Biol Sci* 2021;28:6987–6991.
32. Pizzino G, Irrera N, Cucinotta M, et al. Oxidative stress: harms and benefits for human health. *Oxid Med Cell Longev* 2017;2017:8416763.
33. George S, Abrahamse H. Redox potential of antioxidants in cancer progression and prevention. *Antioxidants (Basel)* 2020;9:1156.
34. Menegon S, Columbano A, Giordano S. The dual roles of NRF2 in cancer. *Trends Mol Med* 2016;22:578–593.
35. Juneja S, Rathore AS, Sharma K, Shetty D, Jain A. Antioxidant-oxidant index as a biomarker in oral potentially malignant disorders and oral squamous cell carcinoma: a biochemical study. *J Clin Diagn Res* 2017;11:ZC05–ZC08.
36. Flohé L. Looking back at the early stages of redox biology. *Antioxidants (Basel)* 2020;9:1254.

COMPREHENSIVE CLINICAL GUIDE



Gaetano Paolone | Salvatore Scolavino

Anterior Direct Restorations

1st Edition 2024; 462 pages, 2,450 illus.

ISBN 978-88-7492-055-6

€210

This book about direct adhesive restorations of the anterior teeth is enriched with diagrams and drawings as teaching aids to simplify the clinical techniques described and guide the reader in applying them. The book explores the concepts essential for understanding shape, emphasizing its fundamental role in achieving esthetic success. Also covered are concepts related to color, including materials with color adjustment potential, and the necessary tools and instruments such as shade guides, methods of isolating the surgical field, and photographic equipment, to ensure the predictable execution of esthetic restorations. In addition, the diagnosis and treatment of white lesions (white spots), fragment reattachment procedures, anterior interproximal lesions, cervical lesions, and direct restorations on endodontically treated teeth (including whitening techniques) are included.



www.quint.link/anterior-teeth



books@quintessenz.de



+49 (0)30 761 80 667

 **QUINTESSENZ PUBLISHING**

Application of Chairside CAD/CAM and Its Influencing Factors among Chinese Dental Practitioners: a Cross-sectional Study

Aihemaiti MUHETAER^{1,2}, Hong Ye YANG^{1,2}, Cui HUANG,^{1,2}

Objective: To examine the increased use of chairside CAD/CAM among Chinese dental practitioners, and to explore the existing barriers influencing its further application and satisfaction levels.

Methods: A semi-structured questionnaire was developed to gather respondents' demographic information, as well as their experiences and behaviours regarding the implementation of chairside CAD/CAM. A specialised web-based survey system and WeChat were used to display and distribute the final questionnaire. Then, the data were analysed with Chi-square tests and regression analyses to determine the effects of various demographic variables on chairside CAD/CAM applications.

Results: A total of 1,969 questionnaire responses were included in the analyses. Chairside CAD/CAM systems were used by 36.9% of participants, with a higher usage rate observed among prosthodontists (60.0%) and dental practitioners holding a PhD degree (57.7%). Chairside CAD/CAM-fabricated prostheses were most commonly used in the posterior maxilla (83.3%) and mandible (86.0%), followed by the anterior maxilla and mandible (63.8% and 48.6%, respectively). Major barriers to further application included high initial investment, frequent updates of equipment and software programs, and a lack of expertise in chairside CAD/CAM usage.

Conclusion: Most dental practitioners did not use chairside CAD/CAM systems. The application rate was significantly influenced by sex, location, educational background, department and type of healthcare facility. Chairside CAD/CAM users showed limited satisfaction with the aesthetic performance of the fabricated prostheses. To improve the popularity of chairside CAD/CAM systems, especially among dental practitioners lacking advanced academic degrees, it is highly advisable to optimise CAD software programs and offer comprehensive training opportunities.

Keywords: chairside CAD/CAM restoration, cross-sectional study, dental practitioners, survey
Chin J Dent Res 2024;27(3):253–262; doi: 10.3290/j.cjdr.b5698327

1 State Key Laboratory of Oral & Maxillofacial Reconstruction and Regeneration, Key Laboratory of Oral Biomedicine Ministry of Education, Hubei Key Laboratory of Stomatology, School and Hospital of Stomatology, Wuhan University, Wuhan, P.R. China.

2 Department of Prosthodontics, School and Hospital of Stomatology, Wuhan University, Wuhan, P.R. China.

Corresponding author: Drs Hong Ye YANG and Cui HUANG, Department of Prosthodontics, School and Hospital of Stomatology, Wuhan University, No. 237 Luoyu Road, Wuhan 430079, P.R. China. Tel: 86-27-87686056. Email: yanghongye@whu.edu.cn; huangcui@whu.edu.cn

This study was supported by grants from the Technology Innovation Major Special Project of Hubei Province (2019ACA139) and the Natural Science Foundation of Hubei Province (2022CFB068).

The development of dental materials and technologies has progressed significantly over the past century.¹ Traditional dental laboratory procedures, including lost wax precision casting of gold alloys, dough modelling and curing of acrylic resins, and powder sintering of dental porcelains, have been widely used for fabricating crowns, bridges and dentures^{2,3}; however, since the 1970s, computer-assisted technology has revolutionised dentistry through the development of dental CAD/CAM systems.⁴ A computer-controlled milling machine was introduced in 1971, which facilitated crown fabrication following an optical impression. This innovation, known as the Duret system, was developed by Dr Duret



and rapidly gained global recognition for transforming dental CAD/CAM systems.⁵ In the 1990s, after achieving success in creating crowns and three-unit bridges, a CAD/CAM system was employed for the production of implant-supported abutments and frameworks.⁶

With the growth of social economy and the increased preference for metal-free materials, CAD/CAM techniques have entered a period of rapid development.⁷ Based on the fabrication processes used, the CAD/CAM system can be classified into two major categories: laboratory and chairside manufacturing systems.⁸ Both systems consist of optical impressions, digital design software programs and milling machines.^{9,10} In the laboratory production approach, the dental technician is given full responsibility for fabricating the prostheses, which requires at least two visits. In contrast, chairside CAD/CAM enables dental practitioners to manage the whole procedure, from the digital impression and design to digital fabrication.¹¹ This approach allows for the completion of the definitive prostheses in a single appointment, which is attractive to both patients and dental practitioners.⁷ Chairside CAD/CAM systems also boast the benefit of virtual simulation and digital design, allowing for multiple treatment steps using CAD software programs without direct contact with patients.¹² Furthermore, the utilisation of intraoral optical impressions substantially reduces the risk of infection, improves the gag reflex and alleviates patient discomfort, especially in elderly individuals with respiratory or oral mucosa diseases.¹³

To the best of the present authors' knowledge, research on the application of chairside CAD/CAM systems among dental practitioners worldwide remains scarce. The status of CAD/CAM technology in dental practices in the UK and Ireland was reported in 2016.^{14,15} As yet, there are no published studies regarding dental practitioners' attitudes towards the quality of chairside CAD/CAM-fabricated prostheses and potential limitations in their further application.

Thus, the present authors explored the potential factors impacting the adoption of chairside CAD/CAM by using a semi-structured questionnaire. The research objectives were to determine the current status of chairside CAD/CAM in Chinese dental practices, to explore potential correlations between the application of chairside CAD/CAM and respondents' sociodemographic characteristics, and to identify the existing barriers influencing its further infiltration and levels of user satisfaction. The null hypothesis was that dental practitioners' demographic characteristics would not significantly affect the adoption of chairside CAD/CAM technology.

Materials and methods

Ethical approval

This study was conducted following the Strengthening the Reporting of Observational Studies in Epidemiology (STROBE) guidelines (Table S1, provided on request).¹⁶ Approval of the study protocol was obtained from the Medical Ethics Committee of the School and Hospital of Stomatology, Wuhan University (no. 2021-B21). Every participant was provided with a short introduction detailing the objectives of the study, the estimated time for questionnaire completion, and the researcher's contact information. To ensure completeness and accuracy of responses, the data collector provided clarity on any queries raised by participants. All respondents were informed that submitting the survey was seen as providing implicit consent to participate. The acquired data was kept strictly confidential and anonymous.

Survey design and participant recruitment

Using the sample size calculation formulae for cross-sectional studies, the sample size was calculated. A recent study reported that CAD/CAM application rate in Hubei province was 24.8%.¹⁷ The sample size was 1,164 with a 5% margin of error and 95% confidence interval when the sample proportion was 0.248. Given that 10% of the samples dropped out, the original sample size should be at least 1,280.

The questionnaire was developed with modifications based on previous studies^{14,15,18} and optimised with the collaboration of the Department of Prosthodontics. It was pilot tested with 15 general dental practitioners and 15 prosthodontists, and the feedback was used to improve the quality of the final questionnaire. Employing a specialised web-based survey system (www.wjx.cn), the final questionnaire was prepared and then disseminated through the Chinese Stomatological Association (CSA) membership group on WeChat, the most widely used social media platform in China. Respondents could only submit the questionnaire after responding to all the questions. The survey was only accessible via WeChat, and each account could only complete it once. Once the questionnaires had been submitted, the respondents were unable to change their answers. As planned, surveys containing contradictory responses and anomalous completion times (less than 1 minute or more than 30 minutes) were excluded.

The questionnaire (supplementary material, provided on request) consisted of four parts containing 25

questions, and the primary language was Chinese. The first section (questions #1 to #11) focused on dental practitioners' demographic and clinical data. The next eleven questions (#12 to #22) surveyed attitudes and experiences related to chairside CAD/CAM application. Using Likert scale questions, chairside CAD/CAM users were asked to rate their actual feelings and behaviours, then evaluate the overall quality of chairside CAD/CAM-fabricated prostheses. Factors for evaluation included marginal fitness, contact points, aesthetics, occlusion and long-term outcomes. Two questions (#23 and #24) were designed to evaluate the perspectives of respondents who had never used a chairside CAD/CAM system before. The final question (#25) asked all respondents to evaluate their perspectives on the potential use of CAD/CAM technology. The Likert scale questions were rated on a scale from 1 to 5, with 1 indicating "completely disagree" and 5 indicating "completely agree". To ensure a representative sample, the questionnaire was distributed across seven geographic regions in China.

Statistical analysis

The original data were obtained from the specialised web-based survey system and entered into a database using SPSS (SPSS 18.0, IBM, Chicago, IL, USA). For the semi-open questions, on sources of CAD/CAM knowledge (#14) and types of chairside CAD/CAM-fabricated prosthesis (#18), three authors independently collected and coded the themes, with any inconsistencies resolved through discussion. Respondents' attitudes towards chairside CAD/CAM-fabricated prostheses were evaluated by calculating the mean of the Likert scale item scores (#21). Descriptive statistics and frequency tables were used to summarise respondents' background information. A Pearson chi-square test was conducted to investigate the differences in the application status of chairside CAD/CAM among respondents with various demographic characteristics. A one-way analysis of variance (ANOVA) with a Tukey adjustment was conducted to evaluate the perspectives of chairside CAD/CAM users on both the technology and the overall quality of prostheses.

The decision to use the chairside CAD/CAM system was explored using generalised estimating equations (GEE) regression analyses. Based on a predetermined criterion, all variables (#1 to #10) presented in the first section of the survey were regarded as independent variables, including age, sex, department, academic degree, monthly income, occupational title, years of practice, location, hospital level and type of healthcare facility. In this analysis, the present authors initially

performed univariate analysis, and then added all significant variables to a multivariate analysis.

Results

General information

A total of 1,975 questionnaires were downloaded from the online survey system, and 1,969 valid responses were included in the further analyses. All participants completed the survey within 10 minutes. Respondents' sociodemographic data are presented in Table 1. Of 1,969 dental practitioners, there were 928 men (47.1%) and 1,041 women (52.9%), and dental practitioners from eastern areas constituted the highest proportion (33.7%). The age group of 26 to 35 years was significantly represented, with 671 participants (34.1%) falling within this range. More than half of the surveyed dental practitioners (986, 50.1%) worked in general dentistry, followed by prosthodontics (558, 28.3%) and implantology (158, 8.1%). Almost one quarter of them (485, 24.6%) had fewer than 5 years of work experience. Regarding participants' educational backgrounds, the majority held a bachelor's degree (823, 41.8%), followed by those with a master's degree (711, 36.1%), and 267 (13.6%) dental practitioners held a PhD. Respondents who worked in public hospitals were predominant (1409, 71.6%, including general and dental hospitals), followed by private services (514, 26.1%).

Basic characteristics of chairside CAD/CAM users

The study indicated that 36.9% of participants used chairside CAD/CAM systems. Based on the geographical distribution, individuals from the northwest and northern areas exhibited higher application rates than the national average, at 54.1% and 52.0%, respectively, whereas the central region reported the lowest rate at 29.1%. The regional difference in application rate was statistically significant ($P < 0.001$). In addition, over half of dental practitioners (51.9%) in public dental hospitals used chairside CAD/CAM, followed by those in private healthcare facilities (31.5%) and public general hospitals (26.9%). According to the level of healthcare facilities, respondents from tertiary hospitals had the highest application rate (40.1%), whereas private dental clinics/unspecified settings had the lowest application rate (26.9%); this difference was statistically significant ($P < 0.001$). Furthermore, 72.3% of users started using CAD/CAM within the last 5 years, and 64.0% of dental practitioners only used it once to twice a week.

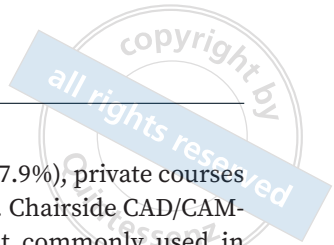


Table 1 Demographic information of respondents.

Characteristic		n	Percent- age (%)
Sex	Male	928	47.1
	Female	1,041	52.9
Location	East	663	33.7
	Central	351	17.8
	South	204	10.4
	North	98	5.0
	Northeast	291	14.8
	Northwest	205	10.4
	Southwest	157	8.0
Age (years)	≤ 25	150	7.6
	26~35	671	34.1
	36~45	600	30.5
	46~55	449	22.8
	> 55	99	5.0
Academic degree	Junior college or below	168	8.5
	Bachelor's	823	41.8
	Master's	711	36.1
	PhD	267	13.6
Occupational title (from lowest to highest)	Associate doctor	121	6.1
	Resident doctor	478	24.3
	Attending doctor	693	35.2
	Associate professor	451	22.9
	Professor	226	11.5
Years of dental practice	≤ 5	485	24.6
	5-10	354	18.0
	11-15	321	16.3
	16-20	235	11.9
	> 20	574	29.2
Monthly income (Chinese Yuan)	≤ 5,000	314	15.9
	5,001-10,000	427	21.7
	10,001-15,000	418	21.2
	15,001-20,000	331	16.8
	> 20,000	479	24.3
Type of healthcare facility	Public dental hospital	695	35.3
	Public general hospital	714	36.3
	Private services	514	26.1
	Other	46	2.3
Hospital rank in scale (from highest to lowest)	Tertiary hospital	1,151	58.5
	Secondary hospital	351	17.8
	Primary hospital	58	2.9
	Private clinic and unclassified	409	20.8
Department	General dentistry	986	50.1
	Prosthodontics	558	28.3
	Endodontics	98	5.0
	Implantology	159	8.1
	Other	168	8.5
Total		1,969	100.0

As illustrated in Fig 1a, manufacturers' technical support (74.7%) and medical journals (66.9%) were the leading sources of CAD/CAM-related knowledge, fol-

lowed by continuing education (47.9%), private courses (45.5%) and social media (34.4%). Chairside CAD/CAM-fabricated prostheses were most commonly used in the posterior mandible (86.0%) and maxilla (83.3%), followed by the anterior maxilla (63.8%) and mandible (48.6%), and this difference in preferred location was statistically significant ($P < 0.001$) (Fig 1b). In terms of educational background, participants with a PhD degree (57.7%) display a tendency to employ the chairside CAD/CAM system at a frequency more than double that of respondents with a junior college degree or below (23.2%). Nearly two-thirds of the dental practitioners in the department of prosthodontics (60.0%) integrate chairside CAD/CAM into their practice, whereas doctors specialising in other disciplines have an application rate of lower than half (Table S2, provided on request); however, the application of chairside CAD/CAM by respondents with different numbers of years of dental experience was not statistically significant ($P > 0.05$).

In terms of the application of chairside CAD/CAM materials, glass-ceramics were found to exhibit the highest application rate (85.7%), followed by resin-matrix ceramics (39.8%) and polycrystalline ceramics (35.1%), and this preference in material selection was statistically significant ($P < 0.001$) (Fig S1, provided on request). Furthermore, inlays/onlays were the most commonly fabricated prostheses (86.2%), followed by all-ceramic crowns (79.3%), whereas other prostheses were adopted by fewer than 40% of respondents (Fig S2, provided on request). The GEE regression analysis results are presented in Table 2. According to the multivariate analysis, the application of chairside CAD/CAM was significantly associated with sex, location, academic degree, department and type of healthcare facility; however, no statistically significant differences were observed in relation to age, occupational title, years of dental practice or rank in scale of hospitals where they worked. The application rates demonstrated a marked increase among respondents from the north ($P = 0.011$) and northwest ($P < 0.001$). This trend was also mirrored in respondents who held an advanced degree, such as a Master's ($P = 0.015$) or PhD ($P < 0.003$). Additionally, professionals serving within the departments of prosthodontics ($P < 0.001$), implantology ($P < 0.012$) or endodontics ($P < 0.006$) also reported a significantly higher application rate.

Respondents' attitudes towards chairside CAD/CAM

CAD/CAM-fabricated prostheses were evaluated based on five primary criteria: marginal fitness, contact

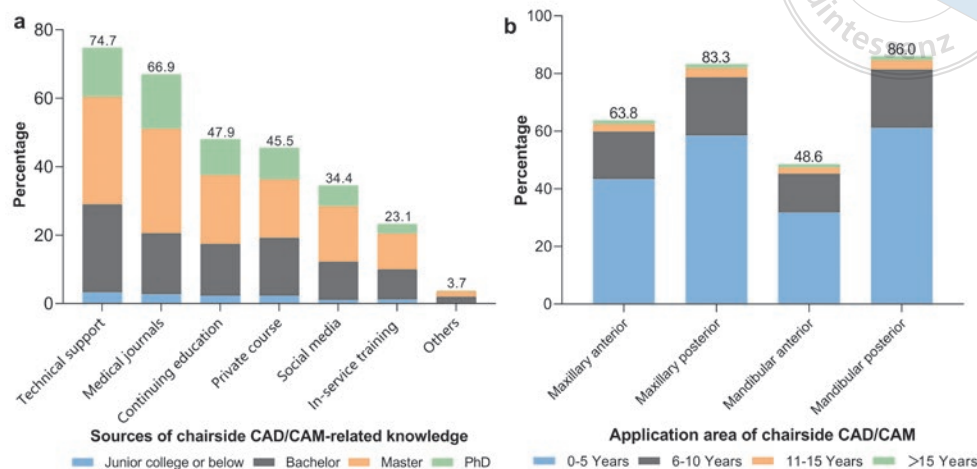


Fig 1a and b Sources of chairside CAD/CAM-related knowledge among respondents (a). Application area of chairside CAD/CAM-fabricated prostheses (b).

points, aesthetics, occlusion and long-term outcome. The results indicated that respondents expressed the highest level of satisfaction regarding marginal fitness (4.02 ± 1.06), with 75.2% of them rating it as excellent or very good, followed by contact points (74.1%) and occlusion (73.7%); however, satisfaction with aesthetics was the lowest (3.72 ± 1.08), with only 28.0% of doctors believing that CAD/CAM-fabricated prostheses delivered excellent aesthetic performance (Fig 2). Interestingly, the satisfaction levels of respondents with varying weekly usage frequencies were statistically significant in terms of marginal fitness, contact points, aesthetics, occlusion and long-term outcome ($P < 0.05$) (Table 3).

Figure 3 illustrates the perspectives of chairside CAD/CAM users in relation to their clinical experience, whereas Fig 4 presents the perspectives of non-users based on their subjective comprehension. The Cronbach alpha values for Q16 and Q23 were 0.832 and 0.989, respectively, suggesting a high level of internal consistency.¹⁹ The majority of chairside CAD/CAM users believed that it decreased fabrication costs and improved quality and productivity. More than half of respondents believed that chairside CAD/CAM techniques increased work efficiency, shortened operative time and decreased the number of visits required. Nearly two-thirds of chairside CAD/CAM users (66.1%) felt that their clinical decisions were influenced by the system, and the vast majority (94.4%) said they would recommend it to their colleagues. With regard to non-users, approximately 46.0% stated that the initial cost of equipment was high. Moreover, they felt that technology upgrades occurred too frequently. Around 47.8% of non-users lacked knowledge on how to use CAD/CAM equipment correctly. Surprisingly, the major-

ity of non-users (91.6%) were interested in integrating chairside CAD/CAM techniques into their dental practice. In the last section of the survey, 1,817 individuals (92.3%) expressed confidence in the future importance of chairside CAD/CAM.

Discussion

This study provided information about the implementation of chairside CAD/CAM in Chinese dental practices and potential factors that could influence its continued adoption. Based on the results, the application rate was significantly influenced by sex, location, educational background, department and type of healthcare facility. Accordingly, the null hypothesis was rejected. The present study found that 36.9% of respondents used chairside CAD/CAM systems in clinical workflows. Among these dental practitioners, 72.3% had begun adopting this technology within the last 5 years, with 64.0% of them using it once to twice per week. A study conducted in Switzerland documented an application rate of 23% among surveyed dental practitioners.²⁰ Dental practitioners in the United Kingdom were surveyed to examine the infiltration of CAD/CAM technology in dental clinics, and the findings revealed that the majority of dental practitioners surveyed did not employ any component of the CAD/CAM system.¹⁴ Based on a study carried out in dental clinics and laboratories of the United States Navy, it was discovered that by June 2017, a substantial proportion of indirect prostheses were manufactured using CAD/CAM systems (38.1%), and that there has been consistent growth in the adoption of CAD/CAM-fabricated prosthesis over the past 5 years.²¹ In an in vivo study, Vogler et al²² evaluated the

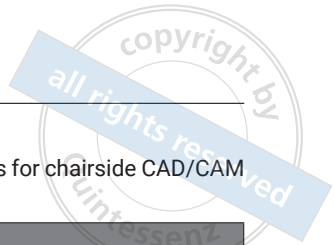


Table 2 Results of univariate and multivariate generalised estimating equations (GEE) regression analyses for chairside CAD/CAM application.

Variable		Univariate analysis			Multivariate analysis		
		Odds ratio	95% confidence interval	P value	Odds ratio	95% confidence interval	P value
Sex				0.268			0.019*
	Male	Reference			Reference		
	Female	0.902	(0.751, 1.083)	0.268	0.763	(0.609, 0.957)	0.019*
Location				< 0.001*			< 0.001*
	East	Reference			Reference		
	Central	0.746	(0.564, 0.987)	0.040*	0.805	(0.589, 1.101)	0.175
	South	0.795	(0.567, 1.115)	0.184	0.815	(0.555, 1.197)	0.296
	North	1.976	(1.289, 3.029)	0.002*	1.904	(1.160, 3.126)	0.011*
	Northeast	0.954	(0.714, 1.274)	0.747	0.733	(0.518, 1.037)	0.079
	Northwest	2.151	(1.566, 2.954)	< 0.001*	2.310	(1.572, 3.396)	< 0.001*
	Southwest	1.287	(0.902, 1.836)	0.164	0.665	(0.436, 1.012)	0.057
Age			0.152			0.631	
Highest degree				< 0.001*			0.002*
	Junior college or below	Reference			Reference		
	Bachelor's	1.298	(0.880, 1.916)	0.188	1.225	(0.778, 1.931)	0.381
	Master's	2.428	(1.648, 3.579)	< 0.001*	1.891	(1.130, 3.165)	0.015*
	PhD	4.508	(2.925, 6.948)	< 0.001*	2.442	(1.359, 4.386)	0.003*
Occupational title			0.117				
Years of dental practice			0.342				
Monthly income (Chinese Yuan)				< 0.001*			0.033*
	≥ 5,000	Reference			Reference		
	5,001–10,000	0.699	(0.489, 0.914)	0.011*	0.887	(0.572, 1.374)	0.591
	10,001–15,000	1.052	(0.777, 1.424)	0.745	1.430	(0.909, 2.250)	0.122
	15,001–20,000	1.064	(0.773, 1.464)	0.705	1.237	(0.768, 1.993)	0.382
	> 20,000	1.328	(0.992, 1.779)	0.057	1.504	(0.912, 2.483)	0.110
Type of healthcare facility				< 0.001*			< 0.001*
	Public dental hospital	Reference			Reference		
	Public general hospital	0.340	(0.272, 0.425)	< 0.001*	0.528	(0.399, 0.700)	< 0.001*
	Private services	0.426	(0.336, 0.540)	< 0.001*	1.193	(0.722, 1.972)	0.491
	Other	0.291	(0.145, 0.582)	< 0.001*	0.520	(0.240, 1.126)	0.097
Hospital level				< 0.001*			0.269
	Tertiary hospital	Reference			Reference		
	Secondary hospital	0.932	(0.729, 1.191)	0.574	1.013	(0.733, 1.401)	0.938
	Primary hospital	0.727	(0.415, 1.273)	0.264	0.894	(0.471, 1.696)	0.731
	Private clinic and unclassified	0.549	(0.428, 0.703)	< 0.001*	0.620	(0.352, 1.092)	0.098
Department				< 0.001*			< 0.001*
	General dentistry	Reference			Reference		
	Prosthodontics	4.618	(3.695, 5.772)	< 0.001*	3.737	(2.798, 4.991)	< 0.001*
	Implantology	2.404	(1.572, 3.675)	< 0.001*	1.797	(1.137, 2.839)	0.012*
	Endodontics	2.480	(1.757, 3.501)	< 0.001*	1.721	(1.164, 2.545)	0.006*
	Other	0.809	(0.543, 1.206)	0.299	0.740	(0.464, 1.180)	0.206

*Statistically significant ($P < 0.05$).

impression quality and accuracy of CAD/CAM-fabricated posts and cores in comparison to conventionally cast posts and cores. They found that the application of a fully digital chairside workflow achieved better accuracy of fit of posts and cores and higher feasibility of

impression taking than the conventional workflow.²² Ming et al²³ compared CAD/CAM-fabricated glass fibre posts and cores with traditional casting titanium posts and cores, posts and cores fabricated using the selective laser melting (SLM) technique, and prefabricated

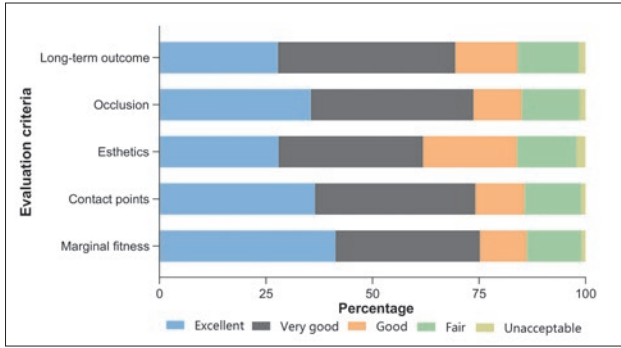


Fig 2 Evaluation of chairside CAD/CAM-fabricated prostheses.

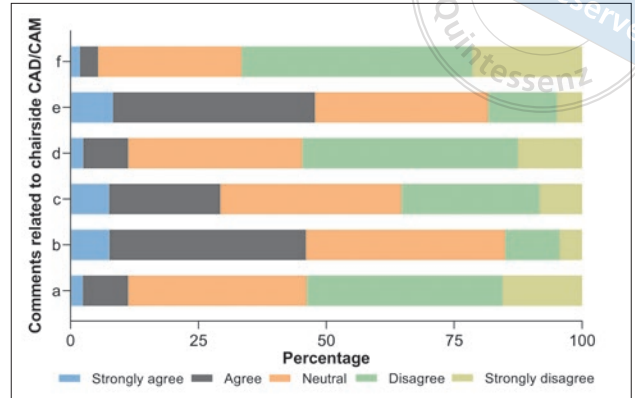


Fig 4 Attitudes of non-users of chairside CAD/CAM based on self-perceived knowledge. a, The quality of CAD/CAM-fabricated prostheses was inferior to that of traditional methods; b, The initial investment in chairside CAD/CAM equipment was high, and upgrades were needed too frequently; c, The conventional impression was more accurate and convenient; d, I did not perceive any advantages over conventional procedures, and I am unable to change my working habits; e, I am not familiar with chairside CAD/CAM systems, or none were available; f, I prefer traditional techniques over digital dentistry.

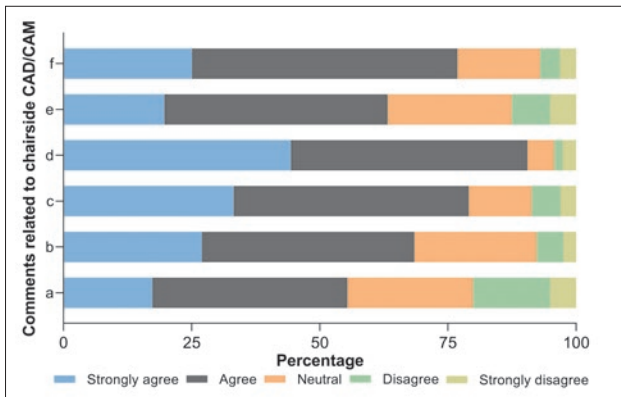


Fig 3 Attitudes of chairside CAD/CAM users based on clinical experience. a, It decreased the cost of fabricating prostheses; b, It improved the overall quality of prostheses; c, It increased productivity; d, It reduced operative time and frequency of visits; e, It was a marketing tool for patient recruitment; f, It makes it possible to keep up with the development of digital dentistry.

Table 3 Relationship between satisfaction levels and weekly use frequency based on five criteria.

Variable	Weekly use frequency (mean ± standard deviation)					F	P value
	1~2 (n = 465)	3~4 (n = 126)	5~6 (n = 34)	7~8 (n = 27)	> 8 (n = 74)		
Marginal fitness	3.89 ± 1.06	4.11 ± 1.05	4.18 ± 0.94	4.48 ± 0.98	4.42 ± 0.98	6.230	< 0.001*
Contact points	3.86 ± 1.05	3.98 ± 1.10	4.18 ± 0.90	4.37 ± 1.01	4.24 ± 1.00	3.930	0.004*
Aesthetics	3.62 ± 1.07	3.75 ± 1.12	3.91 ± 0.87	4.15 ± 1.03	4.01 ± 1.09	3.783	0.005*
Occlusion	3.83 ± 1.05	3.94 ± 1.10	4.26 ± 0.96	4.37 ± 1.01	4.23 ± 1.05	4.670	< 0.001*
Long-term outcome	3.68 ± 1.03	3.79 ± 1.09	4.15 ± 0.93	4.30 ± 0.99	4.23 ± 0.96	7.395	< 0.001*

*Statistically significant ($P < 0.05$).

glass fibre posts and composite resin cores. The internal adaptation and mechanical properties were evaluated. The results demonstrated that CAD/CAM-fabricated glass fibre posts and cores exhibited excellent internal adaptation and high fracture resistance, similar to traditional casting titanium posts and cores and 3D-printed posts and cores, and the fracture pattern was mostly restorable.²³ These findings provide valuable insights into the current landscape of chairside CAD/CAM in

dental practice and offer a positive outlook on its incorporation into clinical workflows.

Interestingly, the present survey reflected broad satisfaction and a positive attitude towards chairside CAD/CAM systems. Chairside CAD/CAM users reported that it increased work efficiency, shortened operative time, and improved quality and productivity. Thus, it was unsurprising that a significant proportion of dental practitioners who participated in the study said they

would recommend chairside CAD/CAM techniques to their colleagues. At the same time, most non-users believed that the initial investment required was one of the major obstacles. Economically, dental practitioners could face challenges in recouping their investment due to the high cost involved in procuring equipment. Consequently, it seems that dental professionals might encounter pressure to use materials that are not supported by clinical evidence but are instead chosen based on economic factors such as production costs, efficiency and the desire for all-ceramic restorations.¹⁵

According to geographical distribution, respondents from the northwest and north used chairside CAD/CAM at a higher rate than the average. Chairside CAD/CAM equipment enables dental practitioners in underdeveloped regions to maintain a relatively high level of prosthetic quality despite the absence or uneven geographic distribution of dental laboratories. Additionally, dental professionals working in public dental hospitals and tertiary hospitals exhibited a greater tendency to use chairside CAD/CAM systems. In contrast, dental practitioners working in other facilities showed a stronger preference for traditional fabrication methods. The preference for chairside CAD/CAM systems in public dental hospitals and tertiary hospitals might stem from the frequent encounters with complex clinical cases that require careful handling of occlusal reconstruction and material selection. Valuable tools like virtual articulators and occlusion detectors offered by some CAD/CAM systems enhance these processes.^{24,25}

Another interesting finding was that dental professionals were more likely to use chairside CAD/CAM-fabricated prostheses in the posterior maxilla and mandible. In the anterior area, achieving a successful dental restoration requires more than a high survival rate; it also demands long-term aesthetic stability that is dependent on several variables, such as material selection, prosthesis design and cementation methods.^{26,27} Differences in saturation, hue and transparency between restorations and natural teeth can lead to aesthetic complications.²⁸ The survey used in the present study revealed that only 28.0% of dental practitioners agreed that CAD/CAM-fabricated prostheses could deliver an excellent aesthetic result. Thus, aesthetics may be a crucial factor influencing the popularity of chairside CAD/CAM. However, treatment outcomes depend greatly on the level of consideration given to selecting the distinct characteristics and attributes of the different CAD/CAM materials. In terms of material selection, glass-ceramics were found to be the most commonly used, with an application rate of more than twice that of other materials. One specific type of glass-

ceramic, the lithium disilicate block, is provided in a pre-crystallised state and has a flexural strength of 130 ± 30 MPa. This initial state makes it easier to mill the material. After undergoing heat treatment in a ceramic oven at 850°C for 20 to 25 minutes, its strength can be significantly increased, meeting the requirements for crown and inlay/onlay restorations.^{29,30} On the other hand, polycrystalline ceramic is relatively opaque and high in strength and takes longer to fabricate, which may limit its use in chairside and aesthetic zone restorations.^{31,32} It is worth noting that the industry has implemented polychromatic blocks and ultra-translucent zirconia materials for CAD/CAM applications with the aim of enhancing the aesthetics of full contour monolithic restorations over the past few years.³³

The present study showed that the main sources of knowledge about chairside CAD/CAM were manufacturers' technical support and medical journals, followed by continuing education. Dental practitioners with a higher level of academic qualification demonstrated a great inclination towards incorporating chairside CAD/CAM technology into their workflows. Meanwhile, respondents with a PhD degree expressed a preference for acquiring knowledge by reading medical journals. In contrast, dental practitioners with a junior college degree showed a greater willingness to accept technical support. This might be due to the fact that PhD students have a strong interest in new technologies and have developed problem-solving skills from reading medical journals.³⁴ Previous research has demonstrated the significant role that continuing education plays in enhancing clinicians' diagnostic and treatment skills.³⁵ Continuing education programmes provide healthcare professionals with opportunities to update their knowledge, learn new techniques and keep pace with the latest advancements in their respective fields. Furthermore, the present study demonstrated a positive correlation between dental practitioners who use CAD/CAM more frequently and higher levels of satisfaction with the marginal fitness, contact points, aesthetics, occlusion and long-term outcomes achieved using prostheses. Considering all of these factors, it is clear that chairside CAD/CAM-related training programmes are vital for dental practitioners, particularly those without high academic degrees or occupational titles.

Using a semi-structured questionnaire is an effective strategy for collecting data on the perspectives and experiences of a diverse group of respondents.³⁶ However, a limitation of the present study is the fact that although the CSA holds the highest authority in the field, there remains the potential for sample bias. To reduce the risk of bias and ensure clarity, the pres-

ent authors developed the survey questions with the help of specialists and conducted a pilot study. In future research, a qualitative study will still be necessary to conduct a more comprehensive analysis of the experience and attitudes of Chinese dental practitioners towards the CAD/CAM system. By including semi-open and open questions, researchers can collect a broader range of personalised opinions from both users and non-users of this technology. This method can provide a profound understanding of the current limitations of CAD/CAM systems and respondents' expectations for their future development. Considering that dental practitioners were the primary providers of information, further investigation is still required to better reflect the perspectives not only of dental practitioners but also of patients, dental technicians and manufacturers throughout the treatment procedure. By incorporating data from multiple sources, researchers can gather unique insights into the factors influencing the slow adoption of chairside CAD/CAM techniques and identify potential areas for improvement. This topic can be explored in future research.

Conclusion

Within the limitations of this study, several conclusions could be drawn. First, most participants did not employ any part of the chairside CAD/CAM system, but expressed strong belief in its future significance and an interest in incorporating it into their workflows. Second, CAD/CAM-fabricated prostheses were more frequently used to treat posterior teeth. Glass-ceramic was the material of choice, followed by resin-matrix ceramics and polycrystalline ceramics. The chairside CAD/CAM application rate showed a significant association with sex, department, location, educational background and healthcare facility. Third, dental practitioners with high academic degrees showed a significant interest in incorporating chairside CAD/CAM into their workflows, with a preference for obtaining relevant knowledge from medical journals. In contrast, those with a bachelor's degree or below showed a greater willingness to seek technical support. Finally, the major barriers to wider adoption of chairside CAD/CAM included the high initial investment, frequent updates of hardware and software programs, a lack of perceived aesthetic benefits, and a lack of expertise in operating these systems.

Conflicts of interest

The authors declare no conflicts of interest related to this study.

Author contribution

Dr Aihemaiti MUHETAER contributed to the conception, method, data collection, investigation, analysis and manuscript draft; Dr Hong Ye YANG contributed to the visualisation, writing, review and editing of the manuscript; Dr Cui HUANG contributed to the conception, funding support, research supervision and manuscript revision.

(Received Nov 05, 2023, accepted Mar 12, 2024)

References

1. Li RW, Chow TW, Matinlinna JP. Ceramic dental biomaterials and CAD/CAM technology: State of the art. *J Prosthodont Res* 2014;58:208–216.
2. Yang J, Li H, Xu L, Wang Y. Selective laser sintering versus conventional lost-wax casting for single metal copings: A systematic review and meta-analysis. *J Prosthet Dent* 2022;128:897–904.
3. Saeed F, Muhammad N, Khan AS, et al. Prosthodontics dental materials: From conventional to unconventional. *Mater Sci Eng C Mater Biol Appl* 2020;106:110167.
4. Miyazaki T, Hotta Y, Kunii J, Kuriyama S, Tamaki Y. A review of dental CAD/CAM: Current status and future perspectives from 20 years of experience. *Dent Mater J* 2009;28:44–56.
5. Davidowitz G, Kotick PG. The use of CAD/CAM in dentistry. *Dent Clin North Am* 2011;55:559–570, ix.
6. Alfarsi MA, Okutan HM, Bickel M. CAD/CAM to fabricate ceramic implant abutments and crowns: A preliminary in vitro study. *Aust Dent J* 2009;54:12–16.
7. Spitznagel FA, Boldt J, Gierthmuehlen PC. CAD/CAM ceramic restorative materials for natural teeth. *J Dent Res* 2018;97:1082–1091.
8. Alghazzawi TF. Advancements in CAD/CAM technology: Options for practical implementation. *J Prosthodont Res* 2016;60:72–84.
9. Zaruba M, Mehl A. Chairside systems: A current review. *Int J Comput Dent* 2017;20:123–149.
10. Aziz A, El-Mowafy O, Tenenbaum HC, Lawrence HP, Shokati B. Clinical performance of chairside monolithic lithium disilicate glass-ceramic CAD-CAM crowns. *J Esthet Restor Dent* 2019;31:613–619.
11. Lambert H, Durand JC, Jacquot B, Fages M. Dental biomaterials for chairside CAD/CAM: State of the art. *J Adv Prosthodont* 2017;9:486–495.
12. Barenghi L, Barenghi A, Garagiola U, Di Blasio A, Gianni AB, Spadari F. Pros and cons of CAD/CAM technology for infection prevention in dental settings during COVID-19 outbreak. *Sensors (Basel)* 2021;22:49.
13. Siqueira R, Galli M, Chen Z, et al. Intraoral scanning reduces procedure time and improves patient comfort in fixed prosthodontics and implant dentistry: A systematic review. *Clin Oral Investig* 2021;25:6517–6531.
14. Tran D, Nesbit M, Petridis H. Survey of UK dentists regarding the use of CAD/CAM technology. *Br Dent J* 2016;221:639–644.
15. Blackwell E, Nesbit M, Petridis H. Survey on the use of CAD-CAM technology by UK and Irish dental technicians. *Br Dent J* 2017;222:689–693.

16. von Elm E, Altman DG, Egger M, et al. The strengthening the reporting of observational studies in epidemiology (STROBE) statement: guidelines for reporting observational studies. *Int J Surg* 2014;12:1495–1499.
17. Muhetaer A, Yang H, Zhao Y, Huang C. A survey of application of digital technology in Hubei dental practice [in Chinese]. *Kou Qiang Yi Xue Yan Jiu* 2021;37:1084–1088.
18. Nassani MZ, Ibraheem S, Shamsy E, Darwish M, Faden A, Kujan O. A survey of dentists' perception of chair-side CAD/CAM technology. *Healthcare (Basel)* 2021;9:68.
19. Eisinga R, Grotenhuis Mt, Pelzer B. The reliability of a two-item scale: Pearson, Cronbach, or Spearman-Brown? *Int J Public Health* 2013;58:637–642.
20. Mühlemann S, Sandrini G, Ioannidis A, Jung RE, Hämmerle CHF. The use of digital technologies in dental practices in Switzerland: A cross-sectional survey. *Swiss Dent J* 2019;129:700–707.
21. Walker S, Kosaraju A, Lien W, Vandewalle KS. A survey of US air force general dentists regarding computer-aided design/computer-aided manufacturing usage. *J Contemp Dent Pract* 2020;21:249–252.
22. Vogler JAH, Billen L, Walther KA, Wöstmann B. Conventional cast vs. CAD/CAM post and core in a fully digital chairside workflow - An in vivo comparative study of accuracy of fit and feasibility of impression taking. *J Dent* 2023;136:104638.
23. Ming X, Zhang Z, Xie W, Zhang Y, Li Y, Zhang W. Internal adaptation and mechanical properties of CAD/CAM glass fiber post-cores in molars: An in vitro study. *J Dent* 2023;138:104685.
24. Lepidi L, Galli M, Mastrangelo F, et al. Virtual articulators and virtual mounting procedures: Where do we stand? *J Prosthodont* 2021;30:24–35.
25. Joda T, Zarone F, Ferrari M. The complete digital workflow in fixed prosthodontics: A systematic review. *BMC Oral Health* 2017;17:124.
26. Kurbad A. A new milling machine for computer-aided, in-office restorations. *Int J Comput Dent* 2017;20:201–213.
27. Edelhoff D, Prandtner O, Saeidi Pour R, Liebermann A, Stimelmayr M, Güth JF. Anterior restorations: The performance of ceramic veneers. *Quintessence Int* 2018;49:89–101.
28. Ishikawa-Nagai S, Yoshida A, Sakai M, Kristiansen J, Da Silva JD. Clinical evaluation of perceptibility of color differences between natural teeth and all-ceramic crowns. *J Dent* 2009;37 suppl 1:e57–e63.
29. Zarone F, Di Mauro MI, Ausiello P, Ruggiero G, Sorrentino R. Current status on lithium disilicate and zirconia: A narrative review. *BMC Oral Health* 2019;19:134.
30. Chen Y, Yeung AWK, Pow EHN, Tsoi JKH. Current status and research trends of lithium disilicate in dentistry: A bibliometric analysis. *J Prosthet Dent* 2021;126:512–522.
31. Tabatabaian F. Color in zirconia-based restorations and related factors: A literature review. *J Prosthodont* 2018;27:201–211.
32. Miyazaki T, Nakamura T, Matsumura H, Ban S, Kobayashi T. Current status of zirconia restoration. *J Prosthodont Res* 2013;57:236–261.
33. Mao L, Kaizer MR, Zhao M, Guo B, Song YF, Zhang Y. Graded ultra-translucent zirconia (5Y-PSZ) for strength and functionalities. *J Dent Res* 2018;97:1222–1228.
34. Wang W. Medical education in China: Progress in the past 70 years and a vision for the future. *BMC Med Educ* 2021;21:453.
35. McAdams CD, McNally MM. Continuing medical education and lifelong learning. *Surg Clin North Am* 2021;101:703–715.
36. Edwards P. Questionnaires in clinical trials: Guidelines for optimal design and administration. *Trials* 2010;11:2.

GET A HANDLE ON EVERYTHING

Perfect training with Quintessence e-books:
compact, portable, always available

Copyright by
all rights reserved
Quintessenz



We offer our e-books on numerous platforms (including Apple Books, Google Play Books and Amazon Kindle Store), so you can read them on the device of your choice: smartphone, tablet, e-reader, laptop, or PC. You can find all our e-books here: www.quint.link/e-books.

